Chapter 1

Introduction

Non-Hodgkin Lymphoma (NHL) is a very common type of cancer in the United States, accounting for about 4% of total cancers each year. These cancers can arise in either T or B lymphocytes, the white blood cells that make up the principal cellular component of the adaptive immune system, but the majority (85%) originate in B cells (American Cancer Society). A number of B cell NHLs develop from and are characterized by specific, recurring translocations between genetic loci found on two different chromosomes. One of the frequent targets of these recurrent translocations in B cells is the immunoglobulin heavy chain locus (IgH), which encodes for the large polypeptide chain of the vertebrate antibody. Examples of malignancies that are characterized by translocations to IgH include human Burkitt Lymphoma and mouse plasmacytomas, which harbor translocations between IgH and the oncogene c-Myc (Myc), human mantle zone lymphoma (translocation between IgH and Bcl-1), and human follicular lymphoma (translocation between IgH and Bcl-2) [1, 2]. The reason that IgH is targeted so often for translocation is still an area of active investigation, but what is clear is that when an oncogene is translocated to IgH, it is put under the control of the IgH promoter, which is strongly and ubiquitously expressed in B cells. This seems to provide cells with the growth advantage they need to become cancerous.

Although this thesis will focus on translocations to the IgH locus, there are a variety of other hematopoietic as well as a limited number of solid tumors that are caused by recurring translocations. In fact, more than 50% of leukemias and lymphomas that reappear in multiple patients and are highly associated with different cancer subtypes are caused by translocations [3]. For a translocation to occur, two chromosomes must be broken, repositioned, and joined together. Thus, translocations are likely to be the result of faulty DNA double-strand break (DSB) repair.

DNA double strand breaks and the DNA damage response

Maintenance of genomic stability is of utmost importance for the survival of both cells and organisms. DSBs are among the lesions that are most toxic to cells, in that they can lead to initiation of senescent or apoptotic pathways. In the instance that the cell does not die from the lesion, it will most likely accumulate genetic aberrations, such as chromosomal translocations, that can lead to diseases like cancer. DSBs are caused by processes endogenous to the cell such as meiotic recombination, replication fork collapse, or during immune development. They are also caused by exogenous sources such as ionizing radiation and reactive oxygen species. Regardless of the cause, it is estimated that each cell suffers from ten DSBs each day [4]. The cell has evolved sophisticated mechanisms with which to identify and repair DSBs, known collectively as the DNA damage response (DDR).

The DDR includes numerous proteins that function in concert to sense the break, stop the cell from continuing to cycle, and recruit repair machinery. These proteins are broken up into categories known as sensors, transducers, and effectors. Sensors are a group of proteins that

function to recognize and bind to a DSB, transducers work to augment and diversify the signal, and effectors regulate numerous elements of cellular function such as the cell cycle, apoptosis, and DNA repair (Fig. 1.1). Numerous layers of regulation exist to guarantee that the cell responds to DSBs in the most appropriate manner possible, using the most precise repair pathway for the given cellular context.

There are two prominent pathways for DSB repair, homologous recombination (HR) and non-homologous end joining (NHEJ). Homologous recombination can utilize an existing sister chromatid to serve as a template for repair, and thus predominates in the S/G2 phases of the cell cycle. Non-homologous end joining, on the other hand, does not require homology to join broken ends of DNA and instead ligates ends together regardless of the loss of nucleotides and cell cycle phase. It is obvious that these repair pathways each function in unique cellular circumstances, however, there are times in which a cell must chose between competing DSB repair pathways. In these cases, the phase of the cell cycle and the nature of the broken DNA ends are important in determining the DSB repair pathway chosen, however exactly how the cell chooses its repair pathway is still an area of investigation [5].

Homologous Recombination

Homologous Recombination is a genetic process in which nucleotide sequences are exchanged between homologous molecules of DNA. HR is initiated by resection of the broken ends of DNA by the nucleases Exo1 and CtIP (Sae2 in yeast), in conjunction with the Mre11/Rad50/Nbs1 (MRN) complex, leaving 3' single stranded DNA overhangs [6]. The single-stranded DNA (ssDNA) then attracts the recombinase Rad51, which assembles itself into nucleoprotein filaments that surround the ssDNA, and allows for strand invasion into a

homologous chromosome, which can then be used as a template for repair [7]. A displacement loop (D-loop) is formed during strand invasion between the invading strand and the homologous chromosome, allowing polymerases to elongate and synthesize the invading broken strand. During extension of the invading strand, the 5' end of the broken DNA is captured by annealing to the extended D loop, leading to the formation of two Holliday junctions (HJs). Depending on how these HJs are cut by endonucleases, the chromosomes will be resolved into either crossover or non-crossover products [7]. Alternately, the break can be resolved by synthesis-dependent strand annealing (SDSA), in which elongation of the invading strand occurs in a single HJ, which slides along the DNA until the elongated strand is displaced. This displaced strand forms a 3' overhang in the original double-stranded break duplex, and is then annealed to the opposite end of the break. DNA synthesis fills in gaps left over from annealing, and extends both ends of the still present single stranded DNA break, ligating all remaining gaps to produce recombinant non-crossover DNA[8].

Besides being a prominent pathway for DSB repair, HR has crucial roles in meiosis and mitosis, as demonstrated by the fact that mouse knockouts of essential HR genes cause early embryonic lethality [9-12]. HR generates diversity among progeny from shared parents by mediating the exchange of information between the maternal and paternal alleles. Additionally, it guarantees proper segregation of homologous chromosome pairs at the first meiotic division through the formation of crossovers [13].

Non Homologous End joining

In the absence of homologous genetic material, cells are still able to repair DSBs via non-homologous end joining pathways (Fig. 1.2). While HR requires a 3' overhang, NHEJ can

accept a wide variety of ends as substrates for ligation. When a double-strand break occurs in the DNA, Ku is one of the first proteins to respond and bind to the ends. In eukaryotes, Ku consists of a heterodimer of two subunits, Ku70 and Ku80, which binds to the broken ends of the DNA and serves as a docking station for and increases the affinity of the nuclease complex (Artemis: DNA-PKcs), polymerases (pol μ and pol λ) and the ligase complex (Xrcc4:DNA LigaseIV:XLF) required to complete NHEJ [14].

Upon binding of Ku to the DNA, it recruits the serine/threonine kinase DNA- PK as its catalytic subunit (termed DNA-PKcs), which then activates downstream repair and signaling pathways [15]. DNA-PKcs also complexes with the nuclease Artemis to process DNA ends, which is essential for NHEJ, particularly in the immune system. This complex contains both 5' and 3' endonucleolytic activity as well as hairpin opening functions, while Artemis alone also contains 5' exonucleolytic functions [16]. The polymerases pol μ and pol λ bind to Ku and are suited for NHEJ due to their flexibility. Pol μ is capable of template-independent synthesis, while pol λ can use template-primers with limited homology and fill gaps in DNA at low dNTP concentrations [17, 18]. The ligase complex Xrcc4 and DNA LigaseIV (Lig 4) binds Ku and is activated by the protein XLF [19]. Xrcc4:Lig 4 is particularly suited for NHEJ because it can ligate incompatible DNA end configurations in the absence of homology, as well as ligating across short gaps [20].

The proteins mentioned above have been shown to be indispensible for the canonical, or classical NHEJ pathway (C-NHEJ) (Fig. 1.2). It has been shown, however, that cell lines deficient in Ku and Xrcc4 are still able to repair linear plasmid substrates lacking a homologous partner [21, 22]. This backup pathway or set of pathways for end joining has been termed alternative NHEJ (A-NHEJ). Although the details of A-NHEJ remain elusive, studies implicate

A-NHEJ to depend on the X-ray repair cross-complementing protein 1 (Xrcc1) and DNA Ligase III (Lig 3). Sequencing of DNA junctions formed in the absence of C-NHEJ factors reveals that A-NHEJ relies heavily on small areas of homology between broken DNA ends for repair, termed microhomology. It is increasingly thought that A-NHEJ is the pathway responsible for oncogenic translocations. Studies in which translocation joins were sequenced predominantly display microhomology both in the presence and absence of C-NHEJ factors [23, 24].

NHEJ in B lymphocyte development

Although DNA DSBs can be detrimental to the viability of a cell, there are certain cellular conditions that require programmed DSBs for cellular development. One of these circumstances is during receptor and antibody development in B lymphocytes. In order for the immune system to respond to the vast variety of antigens that can be encountered by an organism, it must be able to produce a diverse population of B cells, each of which has the ability to express a unique B cell receptor (BCR) and antibody. Antibodies are comprised of two immunoglobulin heavy (IgH) and two light (IgL) chains, each of which contain a constant region, which defines the effector function of the antibody, and a variable region, which is responsible for antigen recognition. The variable region of both chains is assembled in a process called V(D)J recombination. The appropriate effector function of the antibody is chosen through a process known as class switch recombination. Both of these processes involve double-strand break intermediates that require repair via the NHEJ pathways [25].

V(D)J recombination

During V(D)J recombination, variable (V), diversity (D), and joining (J) region gene segments are recombined to form a single exon that is expressed as the variable region of the immunoglobulin heavy chain (IgH). The immunoglobulin light chain rearranges in a similar way, but lacks the diversity segment. In B lymphocytes, V(D)J occurs in the bone marrow during the pre-B stage of development, and must be completed in order for the lymphocytes to migrate to the peripheral lymph.

During V(D)J recombination, the recombination activating gene (RAG) endonuclease, comprised of the RAG1 and RAG2 proteins, recognizes specific DNA sequences called recombination signal sequences (RSSs) that flank each of the numerous V, D, and J segments [26]. RAG cleaves DNA at the RSSs, resulting in four broken DNA ends, two signal ends and two coding ends, which require proteins from the classical NHEJ pathway for processing and joining [27]. The importance of V(D)J in immune development is underscored by the fact that human patients and mouse knockouts deficient in members of the C-NHEJ are severely immunodeficient [16, 28-33].

Class switch recombination (CSR)

Upon the successful completion of V(D)J, naïve B cells express their IgH and IgL variable region exons as cell surface receptors with an IgM constant region. They are then free to migrate to peripheral lymph, such as the spleen and lymph nodes. In the peripheral lymph, they can then undergo an antigen dependent developmental process, class switch recombination, which also requires DSB intermediates. The goal of CSR is to switch the IgH constant region to an isotype that is most effective for the antigen presented to the B cell [34].

In mice, the heavy chain loci contain eight constant region exons (Cμ, Cδ, Cγ3, Cγ1, Cγ2b, Cγ2a, Cε and Cα), which are downstream of the V(D)J exon and each encode for a different antibody isotype. During CSR, DSBs are generated in switch (S) regions, highly repetitive, G rich, 1-12 kb sequences of DNA, which precede each C_H exon. This process is initiated by the enzyme activation induced cytosine deaminase (AID), which deaminates cytosines in the S regions. AID preferentially deaminates cytosines contained in the consensus sequence WRCY, where W= adenine or thymine, R= purine, C= cytosine, and Y= pyrimidine [35]. The resulting uracils are then excised by the uracil DNA glycosylase (UNG), leaving single-strand breaks (SSBs) in the DNA. It is thought that two SSBs in close proximity on complementary strands are then converted to a DSB, although the exact mechanism remains unclear [36]. The joining of these two DSBs results in the placement of the appropriate downstream C exon near the IgH promoter, and the expression of a new immunoglobulin isotype (Fig. 1.3).

C-NHEJ has been shown to play a major role in repairing DSBs between S regions in CSR. Genetic knockouts of C-NHEJ factors such as Ku, Lig4 and Xrcc4 show significant decreases in CSR [37, 38]. Unlike V(D)J recombination, however, knockouts of C-NHEJ factors do not abrogate all class switching. B cells can still undergo CSR at levels up to 50% of wild type by means of A-NHEJ [38].

Somatic Hypermutation

There is one more process of note in the development of the BCR that involves programmed DNA damage. This process, somatic hypermutation (SHM), is important for the diversity of the antibody repertoire and the production of antibodies with increased affinity for

antigen. SHM is also initiated by AID, which targets cytosines in DNA surrounding the V(D)J exon and Sμ.[39]. The subsequent uracils are then either replicated to produce C/G to T/A transition mutations, or are removed by UNG to leave an abasic site that can either be excised or resynthesized by error prone polymerases, resulting in point mutations. The B cells with the greatest affinity for foreign antigen are then selected to differentiate into antibody producing plasma cells [40]. Although SHM consists mostly of single nucleotide substitutions, there is both indirect and direct evidence that DSBs are formed as an accidental byproduct in SHM. Sequencing studies show that 5-10% of mutations are small insertions/deletions [41], while mouse knock-ins and PCR assays reveal high numbers of DSBs in germinal center B cells [42, 43]. Although the formation of DSB intermediates implicates a role for NHEJ in SHM, it seems that hypermutation can proceed in the absence of C-NHEJ factors such as DNA-PKcs [44].

The MRN complex

The protein of interest in this dissertation is Mre11, a member of the MRN complex. The complex is composed of meiotic recombination 11 (Mre11), Rad50, and Nijmegen breakage syndrome 1 (Nbs1, also known as nibrin) and is a global player in DNA damage responses. It senses and physically relocates to areas of DNA damage rapidly following the insult, tethers and bridges broken DNA ends over long and short distances, and is responsible for activating pathways of repair and cell cycle checkpoint [45]. One of the first known functions for MRN is its requirement in the ataxia telangiectasia mutated (ATM) signaling pathway. ATM is a serine/ threonine kinase that is activated when DSBs are generated. ATM phosphorylates a variety of proteins involved in cell cycle checkpoint control, DNA repair, and apopototic responses.

Activation of these proteins is extremely important for the G1/S, intra S and G2/M cell cycle checkpoints as well as the initiation of DNA repair [46].

Mre11, Rad50, and Nbs1

Mre11 is a nuclear protein that contains 3' to 5' double-stranded DNA exonuclease activities, as well as single stranded DNA endonucleolytic activities [47-50]. The N terminus of Mre11 contains a phosphodiesterase domain as well as four highly conserved nuclease domains (Fig. 1.3) [51]. The third nuclease domain contains a highly conserved histidine residue (H129) that has been shown by both biochemical and structural studies to be responsible for nucleolytic catalysis by stabilizing the sugar-phosphate moiety of the scissile bond during nucleolysis [52, 53]. In yeast, a point mutation of this residue caused a mild radiation sensitivity phenotype[54]. The C-terminus of Mre11 is disordered and less conserved, and contains the DNA binding domain in budding yeast [55]. Mre11 functions as a dimer to bind both sides of a DSB and stabilize them in close proximity [53]. The nucleolytic activities of Mre11 can then serve to process the bound ends once inside the dimer.

The second member of the complex, Rad50, has ATPase and adenylate kinase functions. The protein contains ATPase domains at both the N- and C-termini, which have the ability to fold onto each other to form a globular domain, near which Mre11 associates and DNA is bound and processed. The folding of the two termini of Rad50 is facilitated by the interaction of its two large, flexible coiled-coil domains (Fig. 1.4-1.5). Together, Mre11 and Rad50 form a heterotetramer that functions as the DNA binding and processing core of the complex, whose importance is underscored by the fact that both proteins are conserved from bacteria and archaea up to humans [56].

The third member of the complex, Nbs1, is less conserved but has a yeast homolog called Xrs2 [51]. The N-terminus of Nbs1 contains several phospho-peptide binding domains that are commonly found in DDR proteins; a forkhead binding (FHA) and a BRCA1 C-terminal (BRCT) domain which are adaptably attached to a Mre11-binding domain at the C-terminus by a sequence that creates a flexible tether (Fig. 1.4) [57, 58]. Nbs1 provides the MRN complex with its signaling role by interacting with and activating ATM in response to DSBs, or ATM- and Rad3-related (ATR) protein kinases in response to replication fork stalling [59]. Nbs1 is also critical for the nuclear localization of MRN and functions together with Rad50 ATP binding and hydrolysis to enhance Mre11 nucleolytic activities [60].

MRN functions in DSB repair

Upon the occurrence of a DSB, the Mre11/Rad50 heterotetramer senses and binds to the broken DNA ends. Structural data of Mre11 bound to DNA shows that Mre11 dimerization is critical for binding, and it binds DNA ends with 2 to 3 nucleotide overhangs or branched structures [53]. The Mre11 DNA binding domain can accommodate ssDNA, but prefers dsDNA and branched substrates [46]. Once bound to DNA, the Mre11/Rad50 heterotetramer functions to bridge DNA ends in two ways. It can bridge DSBs at short range (within 100 Ångstrom) by simultaneously binding more than one DNA end within one heterotetramer (Fig. 1.5) [61]. Furthermore, when the coiled-coil domains of Rad50 fold back on themselves they assemble a zinc hook that allows multiple heterotetramers to tether DNA chains at distances up to 1200 Ångstrom (Fig. 1.5) [62].

Once bound to DNA, the nucleolytic activities of Mre11 can then function to process the broken ends for resection. As mentioned, Mre11 contains 3’ to 5’ double- stranded DNA

exonuclease activities, as well as single-stranded DNA endonucleolytic activities. Studies suggest that Mre11 works with other nucleases such as CtIP to facilitate the 3' to 5' resection that initiates HR [45]. Studies, including one presented in this thesis, also show that nucleolytic activities of Mre11 are important for the processing of at least a subset of DSBs during NHEJ [63-65]. Since there are a variety of end substrates that need to be repaired during NHEJ, it seems that Mre11 is able to handle a subset of these, and the MRN complex is then able to hand the break off to either the C- or A-NHEJ pathways for repair [63].

MRN in human disease and mouse knockouts

The importance of the MRN complex and its role in ATM mediated signaling is underscored by the identification of mutations to members of the MRN complex in inherited genetic syndromes. Inherited mutations of the ATM kinase lead to a syndrome called ataxia telangiectasia (A-T), while humans harboring mutations in Mre11 manifest in a similar disorder labeled ataxia telangiectasia-like disorder (ATLD) [66]. Hypomorphic mutations in Nbs1 lead to Nijmegen breakage syndrome (NBS), while mutations in Rad50 lead to NBS-like disorder (NBSLD) [67]. The clinical and cellular features of these disorders emphasize the importance of MRN's roles in the DDR.

Clinically, patients with A-T or ATLD present with ataxia, neurodegeneration, and immunodeficiency [66]. A-T patients are also predisposed to cancer, while only 2 of the known cases of ATLD have developed tumors [68]. NBS and NBSLD patients, alternately, present with microcephaly, "bird-like" facial features, immunodeficiency, and severe predisposition to cancer [67, 69]. Despite these clinical differences, however, cells from these patients exhibit similar phenotypes including widespread genomic instability in metaphase spreads, sensitivity to

ionizing radiation (IR) and other DNA damaging agents, and defects in cell cycle checkpoints [67, 69].

In corroboration with disease alleles in humans, mouse knockouts of MRN complex members reveal its importance in the DDR. Unlike ATM knockouts, which are viable, but show growth and immune defects as well as infertility and tumor development, knockouts of Mre11, Rad50, and Nbs1 are early embryonic lethal [70-73]. Additional mouse models containing disease alleles that mimic A-T, ATLD, NBS and NBSLD have been created, and the phenotypes of these cells correlate with those of cells from human patients, again stressing the importance of this complex in mammalian development and cellular response to DNA damage.

Translocations to IgH

As mentioned earlier, a number of tumors result from translocations between the immunoglobulin heavy chain locus (IgH) and a proto-oncogene. There is much evidence that these translocations result from faulty repair during V(D)J and class switch recombination. For example, the human t(14:18) that translocates Bcl-2 to IgH in patients with follicular lymphoma clearly joins Bcl-2 to the RSS segment of either J_H or D_HJ_H, indicating that the B cell was attempting to join J_H to D_H or V_H to D_HJ_H [74]. There are also many translocations in mature B cells that involve joining of the proto-oncogene and the S region of C_H. These include the IgH:Myc translocation in human Burkitt's lymphoma and mouse plasmacytoma [1, 75], Bcl-3:IgH in B cell chronic lymphocytic leukemia [76], and Pax-5:IgH in lymphoplasmacytoid lymphoma [77], among others. Involvement of the S region indicates faulty repair during CSR,

after the breaks are introduced. Additionally, has been shown that like CSR, the formation of these translocations is dependent upon AID [78].

The multistep model of carcinogenesis states that several genetic events are necessary for a cell to turn cancerous [79]. Indeed, translocations to the IgH locus are found in normal mice and humans at about 1 in 10^4 to 10^6 cells, while the development of lymphoma is a rare event in the healthy population [2]. In agreement with this model are data from transgenic mouse studies that demonstrate that the overexpression of a proto-oncogene such as Myc is not sufficient to produce tumors [80]. However, it is likely that these translocations are often the driving genetic event of the tumors due to the fact that these translocations are readily detectable in precancerous conditions. This begs the question: What is it about the IgH locus that gives its translocation partner the growth advantage in so many cancers? There must be some mechanism of control contained either within or around the IgH locus that contributes to it being favored for translocations as well as deregulation of oncogenes.

There are several regulatory features of IgH that have been studied to determine if they are important for the translocation to and subsequent deregulation of oncogenes. These features include a 5' intronic enhancer (Eμ), a strong promoter, and a 3' regulatory region (3'RR) that contains five elements that act as potent enhancers of transcription. The 5' intronic enhancer and the promoter are almost always lost during translocation, however, making it unlikely that they are crucial for oncogenic deregulation. On the other hand, translocations to Sμ often put the oncogene under the control of the IgH 3' enhancer region [2]. Indeed, studies have shown that genetic deletion of the 3'RR protects mice from B cell lymphomas with CSR associated translocations [81]. However, the possibility that there are cis-acting elements located outside of

the IgH locus exist that impact translocation to and deregulation of oncogenes has not been investigated.

Overview of Thesis

The studies presented in this thesis investigate roles for the MRN complex, as well as potential cis-acting elements located outside of the IgH locus, on CSR and oncogenic translocation in B lymphocytes using two distinct mouse models. MRN has been shown to function in many cellular contexts including HR, V(D)J recombination, telomere maintenance, and at replication forks. However, roles for the MRN complex in NHEJ, CSR, and the formation of translocations have yet to be elucidated. The hypothesis that drives the first two chapters of this thesis is that loss of the MRN complex will lead to end joining defects that lead to decreased levels of CSR and increased levels of translocations in B cells. The results of these studies show that indeed, MRN as well as Mre11 nucleolytic activities are involved in CSR, and that the MRN complex acts upstream of both classical and alternative NHEJ pathways. However, the end joining defects that accompany the loss of the MRN complex in B cells do not result in mouse mortality from B cell lymphomas. The fourth chapter of this thesis investigates the stage of tumor formation that follows translocation, examining possible roles for elements outside of IgH in oncogene deregulation. The results show that IgH is able to undergo translocations to an oncogene in multiple places in the genome and in multiple orientations in relation to the centromere, and that these translocations are able to lead to malignancy. Thus, it is clear that the MRN complex plays complex but crucial roles in mammalian NHEJ and tumor development,

while translocations to the IgH locus that may be enhanced by NHEJ defects are controlled by elements contained within the locus itself.

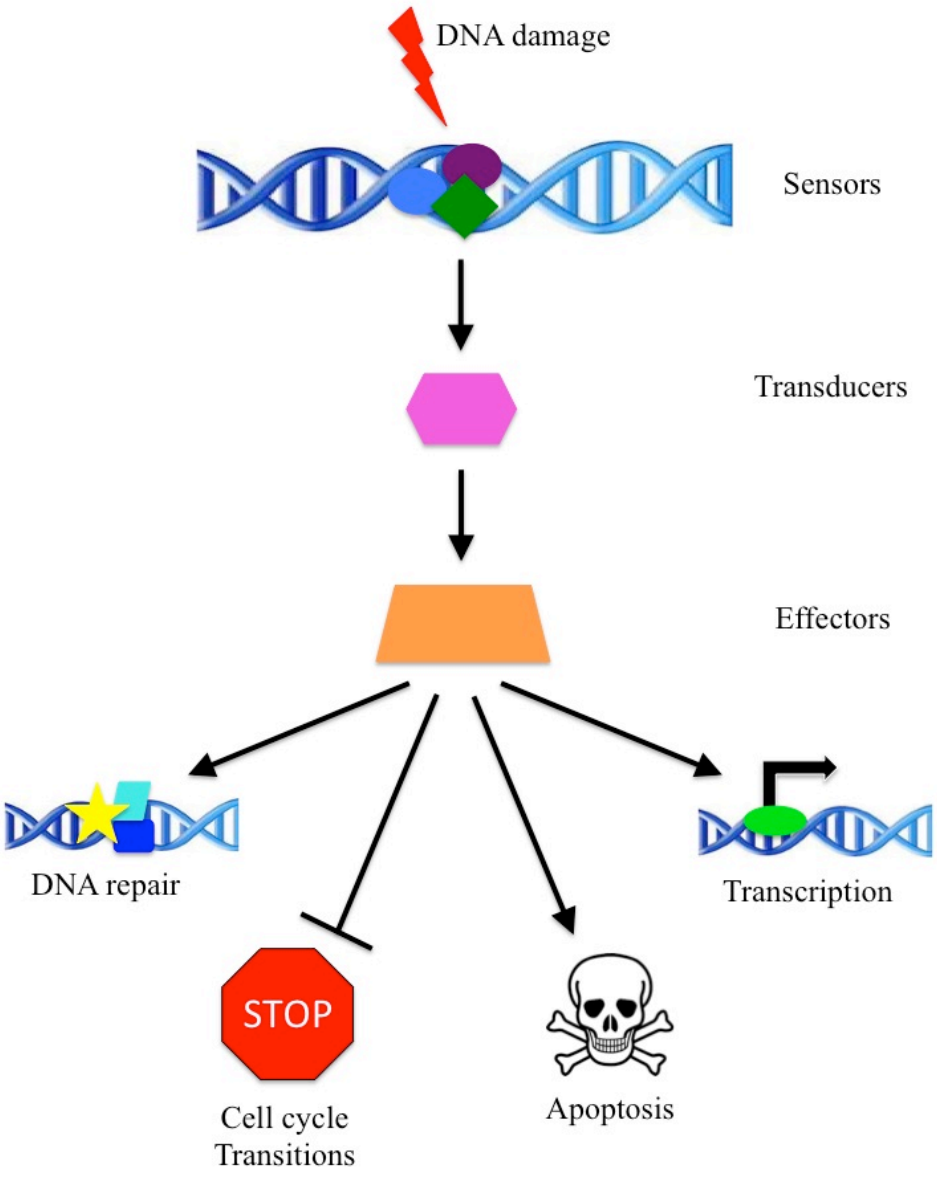

Figure 1.1: The DNA damage response (DDR). The DNA damage response is the sophisticated mechanism that the cell has evolved for the recognition and repair of damage to its DNA. It consists of sensor, transducer, and effector proteins, each of which plays a unique and crucial role in the DDR.

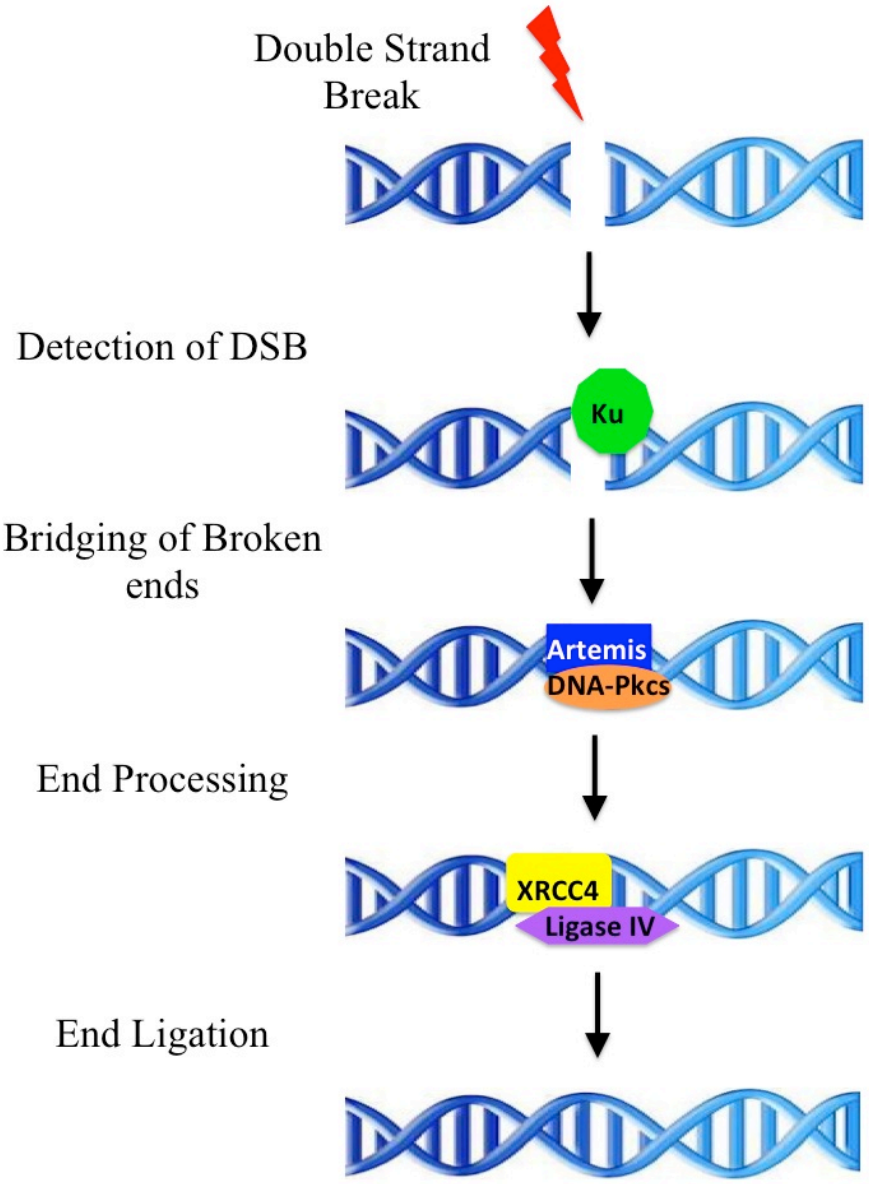

Figure 1.2: The classical non-homologous end joining (NHEJ) pathway. Following a double strand break, Ku binds the broken ends of the DNA, recruiting nucleases such as Artemis and DNA-PKcs for end processing, polymerases, and finally the ligation complex Xrcc4/Ligase IV for break resolution.

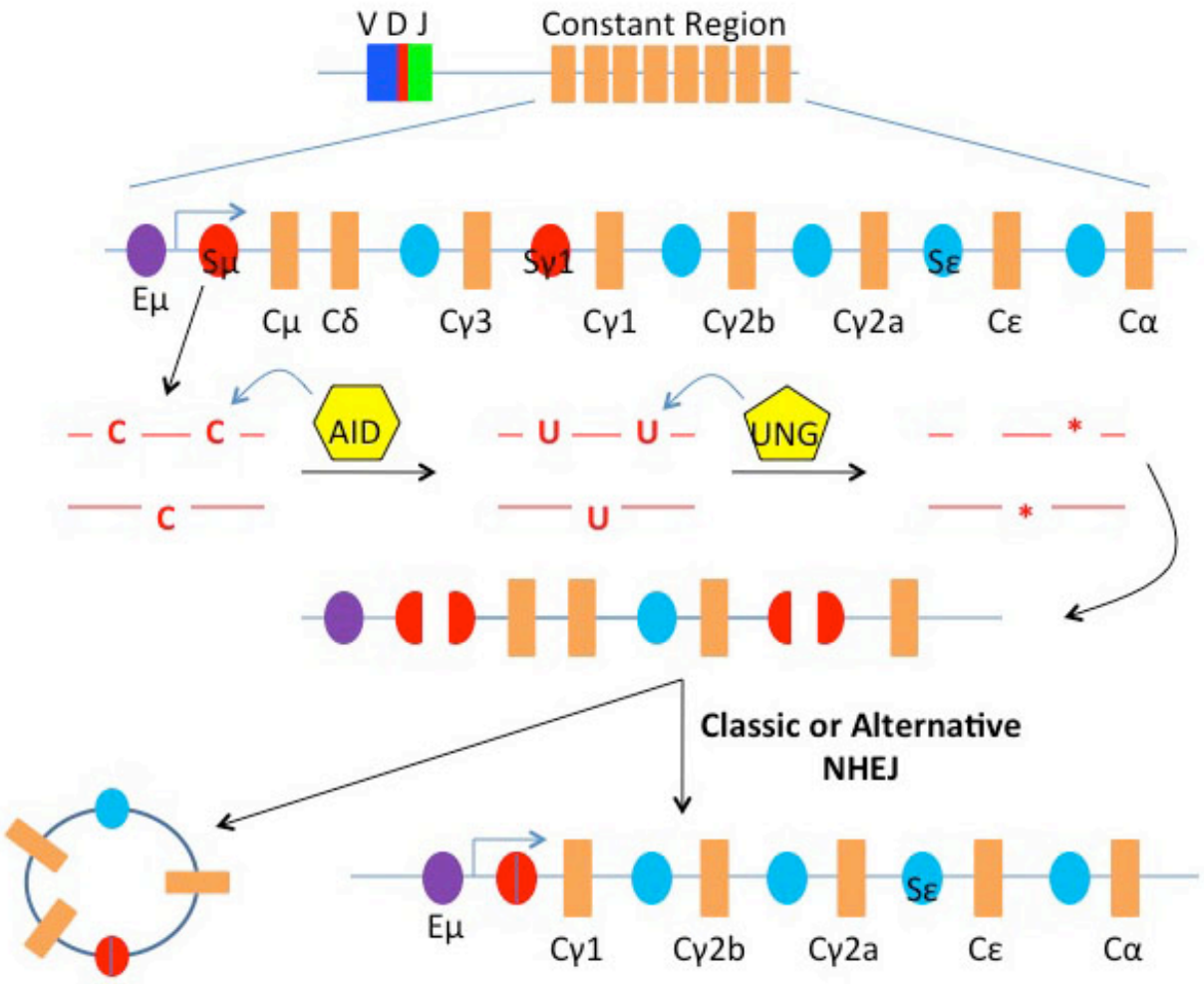

Figure 1.3: Schematic of class switch recombination (CSR). During CSR, AID deaminates cytosines in S regions that precede each C region exon. The resulting uracils are removed by UNG, resulting in abasic sites that are converted into DNA DSBs. The broken ends are then handed off to the classical or alternative NHEJ pathway for repair.

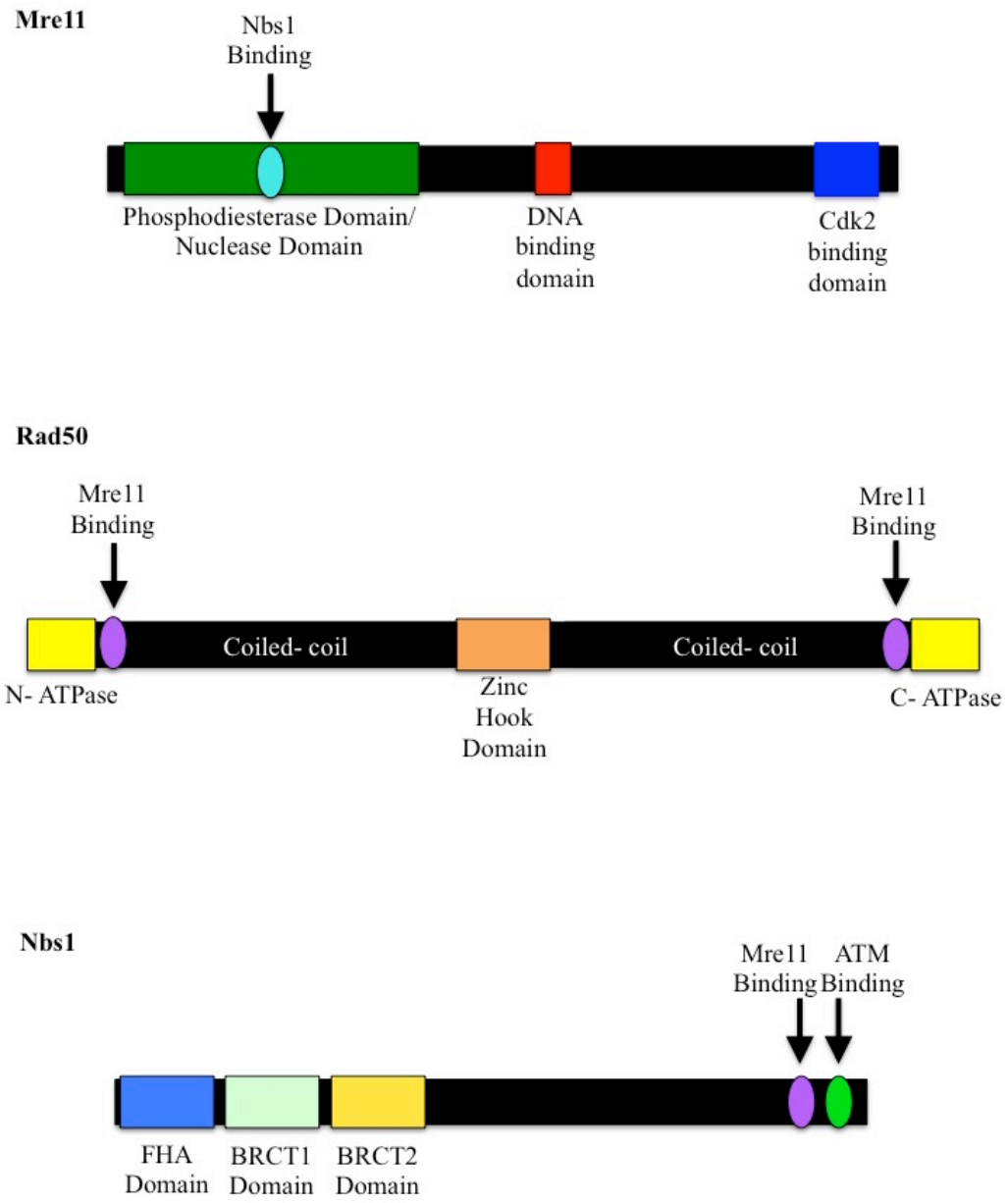

Figure 1.4: Schematic of the Mre11/Rad50/Nbs1 (MRN) complex members. The MRN complex consists of Mre11, Rad50 and Nbs1. Mre11 contains an N-terminal phosphodiesterase domain, as well as a nuclease domain that has 3' to 5' double- stranded DNA exonuclease and single-stranded DNA endonucleolytic activities. Rad50 has N- and C-terminal ATPase domains as well as two coiled-coil domains that meet at a zinc hook. Nbs1 contains a forkhead binding (FHA) and two BRCA1 binding (BRCT) domains.

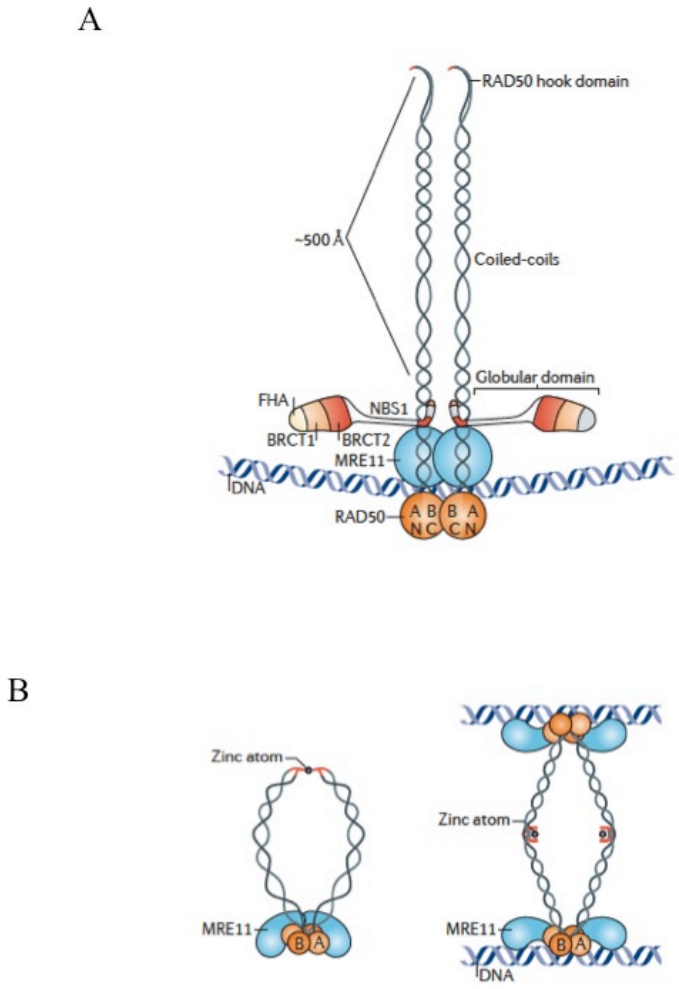

Figure 1.5: The MRN complex bridging and tethering functions. (A) A single Mre11/Rad50 heterotetramer bridges broken DNA ends in short range. Nbs1 and Mre11 interact with the ATPase domains of Rad50, while the coiled-coil domains fold back on themselves to form a zinc hook. (B) The Mre11/Rad50 heterotetramer can interact with other heterotetramers through the zinc hook to tether broken DNA at a longer distance. Figure was taken and adapted from Stracker et al., 2011 [45].

Chapter 2

Multiple functions of MRN in end-joining pathways during isotype class switching

Abstract

The Mre11-Rad50-Nbs1 (MRN) complex has many roles in response to DNA double-strand breaks, but its functions in repair by non-homologous end joining (NHEJ) pathways are poorly understood. We have investigated requirements for MRN in class switch recombination (CSR), a programmed DNA rearrangement in B lymphocytes that requires NHEJ. To this end, we have engineered mice that lack the entire MRN complex in B lymphocytes or that possess an intact complex that harbors mutant Mre11 lacking DNA nuclease activities. MRN deficiency confers a strong defect in CSR, affecting both the classic and alternative NHEJ pathways. In contrast, absence of Mre11 nuclease activities causes a milder phenotype, revealing a separation of function within the complex. We propose a model in which MRN stabilizes distant breaks and processes DNA termini to facilitate repair by both the classical and alternative NHEJ pathways.

Modified from Dinkelmann M*, Spehalski E*, Stoneham T, Buis J, Wu Y, Sekiguchi JM, Ferguson DO. Multiple functions of MRN in end-joining pathways during isotype class switching. Nature Structural and Molecular Biology, 2009 Aug 16; (8):808-13.
(*co-first authorship)

Introduction

DNA double-strand breaks (DSBs) are highly toxic lesions that can lead to instability of the genome. Chromosomal rearrangements resulting from incorrectly repaired breaks can cause cancer, birth defects and other diseases [82]. DSBs can be induced by exogenous sources such as ionizing radiation or certain chemicals, but many arise from endogenous sources such as collapsed replication forks and oxidative DNA damage. Despite the risks, in some circumstances organisms intentionally induce DSBs in their own DNA as part of a developmental program. In mammals, this occurs in lymphocytes to facilitate formation of the adaptive immune system and in developing gametes during meiosis. Regardless of the cause of DSBs, they are rapidly sensed and acted upon by one of several pathways of DSB repair [83].

In mammals, two primary mechanisms of DSB repair have been characterized, homologous recombination (HR) and non homologous end joining (NHEJ) [83]. Homologous recombination facilitates repair by using intact homologous sequences elsewhere in the genome as a template to replace missing sequences at the DSB and is the pathway that generates crossovers during meiotic recombination. Non-homologous end joining facilitates repair by directly ligating the two sides of a DSB and is required for programmed rearrangements in developing lymphocytes. Recently, it has become clear that NHEJ is actually comprised of two pathways; classic NHEJ (C-NHEJ) which is defined by dependence on DNA Ligase IV (Lig 4) complexed with the DNA repair protein Xrcc4; and alternative NHEJ (A-NHEJ) which is independent of Lig 4/Xrcc4 and might require DNA Ligase III (Lig 3) and Xrcc1 [38, 84-87].

The two programmed recombination reactions in developing B lymphocytes serve to illustrate the strong influence of context on the choice of repair pathway. V(D)J recombination

generates much of the vast diversity of the antibody repertoire and is initiated via site specific DNA cleavage by the RAG endonuclease. Completion of this reaction depends almost entirely on the C-NHEJ pathway [85]. Once V(D)J recombination has occurred, the initial secreted antibodies and surface receptors all possess heavy chains of the IgM class (or IgD formed via alternative splicing). Upon stimulation of these B lymphocytes by antigen, the original IgM (or IgD) class heavy chain gene undergoes class switch recombination (CSR). CSR causes the original V(D)J exon to be brought into proximity to a DNA region encoding heavy chains of IgG, IgE, or IgA classes, each of which imparts distinct effector functions. In contrast to V(D)J recombination, approximately 50% of CSR events require A-NHEJ [38, 88, 89].

The Mre11/Rad50/Nbs1 (MRN) complex plays a central role in cellular responses to DSBs. Attesting to the importance of this complex, mouse knockouts of any component causes early embryonic lethality [71-73], and subtle partial-loss-of-function alleles cause inherited human syndromes featuring developmental delay, neurodegeneration, cancer predisposition, and immunodeficiency [82]. The complex localizes rapidly to DSBs [90-92], where Mre11/Rad50 heterotetramer(s) bind DNA on one or both sides of the break, and Mre11 utilizes single strand endonuclease activity to initiate repair by the HR pathway [60, 71]. Upon recognition of a DSB by the complex, the NBS1 component interacts with and activates the ataxia-telangiectasia mutated (ATM) kinase, which phosphorylates numerous downstream proteins that control responses such as cell cycle checkpoints and chromatin modification [93-95].

Although MRN's roles in DSB detection and repair by HR are fairly well understood, far less is known about its roles in end joining. Therefore, we endeavored to uncover and elucidate roles of the MRN complex in CSR, as this process involves both NHEJ pathways. CSR is facilitated by two DSBs generated in a multistep process initiated by activation- induced cytosine

deaminase (AID) [35]. The DSBs occur in highly repetitive 1 to 12 kilobase (kb) long switch regions (S), located upstream of each heavy chain constant region (C) [96]. One DSB occurs upstream of Cμ (encoding IgM), while the second occurs upstream of the particular C region destined to encode the new heavy chain class. The DSBs are typically more than 100 kb apart, and the large intervening region is deleted from the genome upon ligation of the two distant breaks. Action by the two end joining pathways can be distinguished by sequencing cloned joins. Sequences that arose from blunt ends are generated by C-NHEJ (Lig 4/Xrcc4 dependent) while those that arose from overhangs and feature microhomologies are generated by A-NHEJ (Lig 4/XRCC4 independent)[38, 86, 97].

Through the use of engineered germline Mre11 mutations and a *Cre/LoxP* conditional allele, we have bypassed embryonic lethality and generated mice with Mre11 deficiencies restricted to the B lymphocyte lineage. The mutations include a null allele of Mre11 that causes deficiency of the entire MRN complex, and a single amino acid change that eliminates Mre11 nuclease activities but maintains stability of the MRN complex. The impact of these alleles on CSR makes it clear that the MRN complex has multiple roles in both C- and A-NHEJ.

Materials and Methods

Generation of mice

$Mre11^{cond/+}$, $Mre11^{cond/-}$, and $Mre11^{cond/H129N}$ mice have been described previously. Mice are a mixed background of C57BL/6 and 129X1/SvJ. $Mre11^{cond/+}$, $Mre11^{cond/-}$, and $Mre11^{cond/H129N}$ mice were crossed with CD19-cre or CD21-cre expressing mice (129X1/SvJ) (Jackson Labs). Bone marrow analysis was performed on 3 - 5 week old mice, and Class Switch Recombination experiments were preformed on 6 - 12 week old mice.

Mouse Genotyping

Mre11 genotyping was preformed as previously described [71]. Cre genotyping was performed using thermocycling conditions of 36 cycles of 94°C for 30sec, 51.7°C for 1min, 72°C 1min with the following PCR primers: *cre-up1*: 5'- CTA GGC CAC AGA ATT GAA AGA TCT -3', *cre-dn1*: 5'- GTA GGT GGA AAT TCT AGC ATC ATC C -3', *IL-2 up*: 5'- GCG GTC TGG CAG TAA AAA CCT ATC -3', and *IL-2 dn*: 5'- GTG AAA CAG CAT TGC TGT CAC TT -3'.

Western Blots

Western blots were preformed for MRN components as previously described [71]. αGAPDH was used at 1:3000 (Santa Cruz) as a protein loading control. Rabbit polyclonal αAID was used at 1:1000 and was a generous gift from Jayanta Chaudhuri (Sloan-Kettering Institute) [98].

B lymphocyte enrichment and cell culture

Mature B lymphocytes were isolated from mouse spleens using a B Lymphocyte Enrichment Kit (BD IMag) and cultured B cells in RPMI media supplemented with 10% (v/v) FBS and 1% (v/v) Pen/Strep (10,000 U ml^{-1} Pen + 10,000 ug ml^{-1} Strep) with or without the following cytokines: 1 μg ml^{-1} αCD40 (BD Bioscience) plus 25 ng ml^{-1} IL-4 (R&D Systems). For cell tracking experiments, cells were incubated in RPMI media containing 10 μM CFDA SE dye (Vybrant CFDA SE Cell Tracer Kit, Invitrogen) at 37°C for 10 min and washed with PBS prior to plating. B lymphocytes were plated at $1x10^6$ cells ml^{-1} and cultured for 4 days.

Flow Cytometry

Cell surface markers were analyzed on a Beckman Coulter FC500 Flow Cytometer using Cytomics RXP software. Cells were washed with PBS + 10% (v/v) FBS, and incubated on ice in the dark for 30 - 60 min using various combinations of the following antibodies: αB220 (1:200, eBioscience), αIgG1 (1:100, BD Pharmingen), αIgE (1:100, Southern Biotech), αIgM (1:200, Southern Biotech), αCD25 (1:100, eBioscience). Data was analyzed using FlowJo software.

2- color FISH

B lymphocytes were incubated in colcemid (KaryoMAX) for 3 hours, washed twice with PBS, and incubated in 75 mM KCl for 15 min at 37°C. Cells were then fixed with 3:1 methanol/acetic acid and dropped onto glass slides, which were dried on a 42°C hot plate. 2-color FISH labeling was done as described using BAC 199 (aka 199M11, Invitrogen) and BAC 207 (aka RP22-207123, BAC PAC Resources). Slides were stained with DAPI (Invitrogen) according to manufacturer's instructions. FISH images were acquired on an Olympus BX61 microscope using a 60x objective, DAPI, FITC, and Texas Red filters, a CCD camera, and FISHview software (Applied Spectral Imaging).

ELISA assays

Microtiter plates were coated with IgM and IgG1 antibodies (Southern Biotech) in a humid chamber overnight. Plates were washed 4x with PBS + 0.05% (v/v) Tween 20, blocked with PBS + 10% (v/v) FCS for 2 - 5 h, and washed 4x with PBS + 0.05% (v/v) Tween 20. Serial dilutions (IgG1: 0 - 10^{-1}, and IgM: 0 - 10^{-2}) of stimulated B lymphocyte culture supernatants were added to coated wells. Concentrations of standards were as follows: IgM (0 - 0.1 μg ml^{-1}, Southern Biotech); IgG1 (0 - 0.25 μg ml^{-1}, Southern Biotech). Supernatant and standards were

incubated on plates in a humid chamber at RT for 2 - 5 h. Plates were washed 4x with PBS + 0.05% (v/v) Tween 20, and Alkaline Phosphate reagent (Southern Biotech) was diluted 1:4000 in ELISA Tris Buffer [17.8 g L^{-1} Trizma HCl + 10.6 g L^{-1} Trizma Base + 10 g L^{-1} BSA + 0.2 g L^{-1} Magnesium Chloride pH = 8.0], added to the microtiter plates, and incubated overnight. Plates were washed 4x with PBS + 0.05% (v/v) Tween 20. 100 μl of 1 mg ml^{-1} phosphatase substrate in ELISA Carbonate Buffer [2.33 g L^{-1} Sodium carbonate + 2.86 g L^{-1} sodium bicarbonate + 0.2 g L^{-1} Magnesium Chloride pH = 9.8] was added to each well and incubated for 30 - 60 min. Readings were taken on an EL808 machine (Biotek Instruments, Inc.) using 405 nm wavelength.

CSR join sequence

CSR joins were amplified by nested PCR using genomic DNA prepared from day 4 stimulated B lymphocyte cultures. PCR conditions have been described [99]. Sμ primers for Sμ - Sγ1 and Sμ - Sε joins were: SμOut, 5'- AAG TTG AGG ATT CAG CCG AAA CTG GAG AGG -3'; and SμIn, 5'- TTC TTC CCT CTG ATT ATT GGT CTC C -3'. Sγ1 primers for Sμ - Sγ1 joins were: Sγ1Out, 5'- CTG CTC TTC TGT GGT TTT TGA CTG GGT TCC -3'; and Sγ1In, 5'-AAC TAC TAA ACT TGT ACC TGT CCT GGC ACC -3'. Sε primers for Sμ - Sε joins (Sε1 and Sε2) have been described [38]. We cloned PCR products using Topo-TA cloning kit (Invitrogen) and analyzed sequences using Seqbuilder 7.0 software (DNAstar).

Immunofluorescent foci

For immunofluorescence, MEFs were grown on 4 chamber glass slides, and treated with 10 Gy of IR (^{137}Cs source). MEFs were washed with 20 mM HEPES, 50 mM NaCl, 3 mM $MgCl_2$, 300 mM sucrose, 1% (w/v) triton X-100 and fixed in 4% (w/v) paraformaldehyde. Cells were blocked in PBS with 10% (v/v) fetal bovine serum, incubated overnight at 4°C with

polyclonal MDC1 antibody (1:100, Abcam, ab41951), or 53BP1 antibody (gift of Xiaochun Yu, University of Michigan) then incubated 1 h with the secondary goat anti-rabbit AlexaFlour 555 antibody (1:1000, Molecular Probes).

Results

Generation of mice with B lymphocyte Mre11 deficiencies

Our lab has utilized an engineered mouse allele of Mre11 that functions as wild type until it is conditionally inactivated via the Cre recombinase (Fig. 2.1A). Work in our lab, done by former post-doctoral fellow Dr. Jeffrey Buis, has shown that conversion of conditional ($Mre11^{cond/-}$) to null ($Mre11^{-/-}$) causes depletion of not only Mre11 but the entire MRN complex, probably owing to instability of the other components [71]. In addition, we have utilized an allele containing a targeted single amino acid change (Mre11 H129N) that eliminates the endo- and exonuclease activities of Mre11 without disrupting the MRN complex, or its ability to sense DSBs and activate ATM (Fig. 2.1A-B) [71]. Studies of the Mre11 H129N allele performed by Dr. Buis revealed that the nuclease activities of Mre11 are required for DSB repair via the HR pathway [71].

Homozygosity for the Mre11 null allele ($Mre11^{-/-}$) or nuclease deficient allele ($Mre11^{H129N/H129N}$) causes early embryonic lethality, necessitating use of the $Mre11^{cond}$ allele and tissue- specific expression of the cre recombinase [71]. CD19-cre initiates expression in bone marrow B lymphocyte progenitors [100]. Through breeding, former post-doctoral fellow Dr. Maria Dinkelmann generated the following experimental mice: $Mre11^{cond/+}$, $Mre11^{cond/-}$, and $Mre11^{cond/H129N}$, each containing one allele of CD19-cre. Therefore, these mice contain B

lymphocytes with the following genotypes; Mre11$^{-/+}$, Mre11$^{-/-}$, and Mre11$^{-/H129N}$. PCR was used to confirm conversion of the Mre11^{cond} allele to Mre11^{-} in lymphoid organs including bone marrow, lymph node, and spleen (Fig. 2.1C). Western blot analyses of B cells from spleen demonstrated severe deficiency of all three MRN components in Mre11$^{-/-}$ cells, whereas in the presence of nuclease- deficient Mre11 (Mre11$^{-/H129N}$) the proteins remained at wild- type levels (Fig. 2.1D). Thus, by this method we could examine the impact of complete MRN deficiency and distinguish this from the impact of an intact MRN complex lacking endonuclease and exonuclease activities.

Mice lacking MRN or Mre11 nuclease activities in the B lineage produced normal numbers of mature IgM^{+} lymphocytes in bone marrow and had spleens of normal size and cellularity (Fig. 2.5 and data not shown). Therefore, early B cell development is not blocked by Mre11 deficiencies generated by CD19-cre, permitting studies that examine switching from IgM surface expression to other antibody isotypes.

Mre11 deficiencies confer defects in isotype switching

Dr. Maria Dinkelmann and I assessed isotype switching by inducing CSR in B cells isolated from spleens of 6 to 12 week old mice. Exposure to IL-4 and anti-CD40 antibody for 4 days in culture stimulates switching to IgG1 (and IgE) (Fig. 2.2A). Control (Mre11$^{-/+}$), Mre11 nuclease-deficient (Mre11$^{-/H129N}$) and MRN deficient (Mre11$^{-/-}$) cells were induced to switch, and I measured AID protein levels by western blot. Whereas AID was not detected in resting cells, it was present upon stimulation in each of the three Mre11 genotypes, confirming that stimulation was successful in each (Fig. 2.1D).

Dr. Maria Dinkelmann and I analyzed switching from IgM to IgG1 by flow cytometric determination of the class of cell surface immunoglobulin receptor in three to five mice of each genotype. Switching was induced in approximately 30% of control B cells ($Mre11^{-/+}$) (Fig. 2.2B-C). In the absence of Mre11 nuclease activities ($Mre11^{-/H129N}$), switching occurred in 14.5 % of cells; 50% less than control (Fig. 2.2B-C). This impact is relatively minor, but is significant ($P < 0.01$, Student's *t*-test). Next, Dr. Dinkelmann and I examined the impact of MRN loss ($Mre11^{-/-}$), in which the nuclease activities of Mre11 and all other functions of the complex are deficient. In this case, the effect was more severe, with an 80% reduction in switching to IgG1 ($P < 0.0001$) (Fig. 2.2B-C). The greater severity caused by MRN deficiency relative to Mre11 nuclease deficiency was statistically significant ($P < 0.01$ Student's two- tailed *t*-test). We also quantified the relative amounts of IgG1 antibody in the media from the experiments described above, because the only source of this isotype is from cells that have successfully switched. Consistent with the cell surface analyses, IgG1 levels were reduced in both Mre11 mutants ($P < 0.01$) (Fig. 2.2D).

IL-4 and anti-CD40 also induce switching to IgE, the levels of which were measured by flow cytometry by Dr. Dinkelmann. Although positivity for IgE cannot be quantified precisely owing to binding of IgE antibody to Fc receptors, a trend similar to that of IgG1 was observed (Fig. 2.6). Therefore, the roles of MRN in CSR differ from those in DSB repair by HR, in which nuclease deficiency had the same impact as MRN loss [71].

The isotype switching defect caused by MRN loss could merely reflect reduced activation of the ATM kinase, because MRN controls ATM activation, and mice harboring knockout alleles of ATM display a CSR defect [101, 102]. As expected, NBS1 deficiency causes a defect similar to that of $ATM^{-/-}$, because NBS1 acts as the primary interface between MRN and ATM [103,

104]. Therefore, Dr. Dinkelmann directly compared isotype switching in B cells from MRN and ATM deficiencies. MRN loss clearly caused a more severe defect compared to ATM deficiency ($P < 0.001$), which was approximately 50% as efficient as control (Fig. 2.2B-C). The greater impact of MRN loss compared to $ATM^{-/-}$, along with the minor defect caused by Mre11 nuclease deficiency (which does not affect ATM activation), collectively argue that MRN plays multiple roles during CSR.

Because CD19-Cre begins expression in early B cell development, we addressed the possibility that reduced isotype switching results from an undetected defect in V(D)J recombination that does not block the development of an IgM^+ population but instead compromises later attempts to switch. To this end, I generated mice with Mre11 genotypes described above, but containing CD21-cre, which expresses the recombinase after cells develop to the IgM^+ stage [105]. I observed an overall trend similar to that observed with CD19-cre mediated deletion ($P< 0.01$, Student's *t*-test for $Mre11^{-/+}$ vs. $Mre11^{-/H129N}$, $Mre11^{-/+}$ vs. $Mre11^{-/-}$ and $Mre11^{-/H129N}$ vs. $Mre11^{-/-}$) (Fig. 2.7). Western blot analyses of splenic B cell extracts tended to show residual Mre11 in CD21-cre mice, likely accounting for the less severe Mre11 phenotypes relative to those associated with CD19-cre (Fig. 2.7 and data not shown). Therefore, we pursued further experimentation using CD19-cre.

Proliferation defects do not account for CSR phenotypes

Isotype class switching involves several rounds of cellular division in addition to the end joining recombination reaction [96]. Therefore we determined whether the quantitative isotype switching defects merely reflect reduced proliferation. Dr. Dinkelmann utilized the cell tracking dye CFSE to distinguish sub-populations of cultured B cells having undergone different numbers

of cell divisions (Fig. 2.3A). First, these analyses show that the Mre11 deficiencies do slow proliferation, with MRN loss and Mre11 nuclease deficiency having a similar impact. After 4 days in culture, a higher percentage of mutant cells relative to wild type cells had undergone only two or three divisions (Fig. 2.3A). Conversely, a higher percentage of control cells had undergone four divisions. Importantly, within the populations at each cell division, the mutants showed lower percentages of cells switched to IgG1 (Fig. 2.3A). Therefore, the reduced isotype switching in the Mre11 mutants cannot be accounted for by proliferation defects.

MRN deficiency causes persistent IgH locus chromosome breaks

Defects in the joining phase of CSR cause DSBs to persist, and a subset can manifest as chromosome breaks at the immunoglobulin heavy chain (IgH) locus on mouse chromosome 12, where CSR occurs [106]. For example, these breaks are readily detected in the context of C-NHEJ defects such as Lig 4 or Xrcc4 deficiency [38]. Therefore, to directly address whether the complex has a role in end joining, I determined whether MRN deficiency causes such a phenotype.

Standard karyotyping cannot distinguish chromosome breaks at IgH from those arising elsewhere on chromosome 12 that are caused by general genomic instability. Therefore I employed a two- color fluorescence *in situ* hybridization (FISH) assay that uses two bacterial artificial chromosomes (BACs) as probes, located 5' and 3' of the IgH locus (Fig 2.3B). Chromosome breaks at IgH are identified as separation of the probes, and previous work has shown that these events are dependent on AID [38]. For each genotype, I examined 100 to 200 total metaphases derived from three mice, and the Fisher Exact Probability test was performed to determine if the percentage of breaks accumulating in the IgH locus was significantly different in

the Mre11 mutants compared to control. Loss of MRN ($Mre11^{-/-}$) resulted in a significant increase in chromosome breaks (P = 0.0003) while loss of Mre11 nuclease activity ($Mre11^{-/H129N}$) did not (P = 0.3482). This observation strongly supports the notion that MRN is required for joining of ends and provides further distinction between Mre11 nuclease and full MRN deficiencies.

Analysis of CSR sequence joins

The established end joining factors Lig 4 and Xrcc4 operate exclusively in C-NHEJ [38, 85, 86]. MRN could potentially be restricted to A-NHEJ, operate with established factors in C-NHEJ, or overlap with both pathways. To distinguish these hypotheses, former lab member Trina Stoneham cloned and sequenced CSR joins from stimulated B lymphocytes. Examination of join sequences from B cells with MRN deficiency and Mre11 nuclease deficiency reveals that both blunt (C-NHEJ) and microhomology mediated (A-NHEJ) joins are represented (Fig. 2.3C, Tables 2.1- 2.3). Trina preformed χ^2 tests using the Mre11 control ($Mre11^{+/-}$) percentages as the expected results. The P-value for $Mre11^{-/H129N}$ joins is 0.764, and for $Mre11^{-/-}$ joins is 0.215, indicating that the Mre11 deficiencies have no significant impact on the ratio of outcomes. Therefore, unlike Lig4 and XRCC4, the MRN complex appears to function in both NHEJ pathways.

MRN and the H2AX/MDC1/53BP1 DNA damage response

H2AX is a specialized core histone, which undergoes phosphorylation in megabase regions surrounding DSBs [107]. Phosphorylated H2AX (γ-H2AX) is bound by MDC1 protein, which in turn interacts with 53BP1, facilitating localization of these proteins to DSB sites. Mouse knockouts of any member of the H2AX/MDC1/53BP1 axis cause a B lymphocyte

development phenotype similar to what we observe for MRN deficiency, that is, progression of a substantial population of cells through early stages and defective CSR in mature cells [106, 108-111]. The similarity of these phenotypes raises the possibility that MRN could control functions of these proteins. Alternatively, MRN could provide functions at DSBs independent of γ-H2AX/MDC1/53BP1. Former post- doctoral fellows Dr. Jeff Buis and Dr. Yipin Wu were able to distinguish these hypotheses by determining the impact of MRN loss, or Mre11 nuclease deficiency, on γ -H2AX formation, and localization of MDC1 and 53BP1 to DSBs as marked by Immunofluorescent foci. The induction of DSBs must be well synchronized to investigate kinetic differences in DNA damage responses, yet CSR occurs over a time span of days. To circumvent this problem, Dr. Buis and Dr. Wu induced DSBs with ionizing radiation (IR) in mouse embryonic fibroblasts (MEFs) harboring the same Mre11 alleles[71]. In this case, the $Mre11^{cond}$ allele was converted to $Mre11^{-}$ prior to IR by delivering the Cre recombinase via adenovirus as previously described [71].

At 1 and 8 hours after IR, Dr. Yu performed western blots using an antibody specific to phosphorylated H2AX (γ -H2AX). No reduction of γ -H2AX levels was evident in the Mre11 mutants, in contrast to phosphorylated-SMC-1 levels, which are known to be dependent on MRN (Fig. 2.4A)[71]. Immunofluorescent studies revealed that Mre11 mutations had no effect on Mdc1 or 53bp1 foci formation (Fig. 2.4B-C). Although a subtle influence on these proteins cannot be ruled out, these experiments support the notion that CSR defects conferred by Mre11 deficiencies cannot be ascribed to a defective γ -H2AX/MDC1/53BP1 response.

Discussion

We have demonstrated that MRN plays multiple roles during CSR in B lymphocytes, and that it operates in both major end joining pathways. In considering the precise roles of MRN in any DSB repair process, distinguishing the impact of reduced ATM activation from direct repair functions can be challenging. We have employed two means to provide this distinction. First, we have directly compared the impact on CSR of ATM deficiency to that of total MRN loss, which disables ATM activation and all other functions of the complex. ATM deficiency clearly causes a milder CSR defect than does the loss of MRN. If the role of MRN were restricted to control of ATM, the degree of CSR deficiency would be equivalent. Secondly, we have examined the impact of Mre11 nuclease deficiency ($Mre11^{H129N}$) on CSR. We have shown previously that this single amino acid change does not impede activation of the ATM kinase. Therefore, phenotypes conferred by this mutation reflect roles of MRN independent of ATM activation. Mre11 nuclease deficiency did indeed cause an appreciable CSR defect, but milder than that of total MRN loss. Therefore, the MRN complex plays at least two independent roles during CSR that ensue after localization to DSBs: (i) activation of the ATM kinase, and (ii) nucleolytic processing of DNA ends.

It is possible that the sum of minor phenotypes conferred by deficient Mre11 nuclease activity and ATM activation accounts entirely for the severe defect caused by total MRN loss. However, the MRN complex possesses additional functions that likely contribute to its roles in end joining. Mre11 forms a dimer, which has recently been shown to bind and hold two double stranded DNA ends in juxtaposition, and in close proximity to the Mre11 nuclease active site [53]. Rad50 features two long coiled-coil arms that can engage in intermolecular interactions through a terminal hook domain [112-114]. Studies using atomic force microscopy have

visualized Mre11-Rad50 complexes bridging DNA ends at distances up to 1,200 Ångstroms [62]. These bridging functions might be particularly suited for CSR, because recombination requires ligation of ends that originate over 100 kb apart. This imposes a requirement for synapses of distant ends, as opposed to standard DSB repair, which entails ligation of broken ends to restore the original sequence. It could be argued that 1,200 Ångstroms (a little over 350 bp) is not comparable to 100 kb. There are several ways to answer this criticism, however. First, it is likely that microscope technology has limited the distance of DNA bridging/MRN scaffolding that is currently detectable. Additionally, it has been shown that S region DNA becomes involved in a macromolecular complex during CSR, which stabilize the binding of factors such as AID and UNG to the DNA[115]. It is possible that these macromolecular complexes contain factors that would bring two S regions into closer proximity, allowing for the bridging by the Mre11/Rad50 heterotetramers.

In mammals and single-celled organisms, MRN is required for DSB repair by homologous recombination [71, 116, 117]. Thus, MRN is required for all three major DSB repair pathways. However, the precise requirements for specific functions of the complex likely differ in each case. For example, we have demonstrated that the Mre11 allele with defective nuclease activities ($Mre11^{H129N}$) confers an HR defect that is equally as severe as absence of the entire MRN complex [71]. This likely reflects the need for the nuclease activities of Mre11, along with other factors such as CtIP (known as Sae2 in yeast) and Exo1, for generation of single stranded DNA to facilitate invasion of homologous duplex DNA [118, 119]. Although the 3'-5' polarity of Mre11's exonucleolytic activities suggest that it should not play a role in resection, it has indeed been shown to be necessary for its initiation. Studies suggest that resection initiation requires MRN and CtIP to catalyze the removal of short oligonucleotides from the 5' end of a

DSB[120]. This intermediate can then be extensively processed by Sgs1-Top3-Rmi1 (STR), in concert with Exo1, which provides the 5'-3' exonucleolytic activities.

In contrast, within NHEJ during CSR (this work), Mre11 nuclease deficiency confers a defect that is milder than that conferred by a total loss of MRN. We postulate that nucleolytic processing might only be necessary in a subset of end joining events to generate DNA ends that are compatible for ligation, a role for Mre11 supported by previous *in vitro* studies [49, 121].

Notably, the requirements for specific MRN functions in each pathway may be influenced by context. For example, in contrast to our findings for CSR, alternative end joining of specialized DSBs initiated by a mutant form of RAG1/2 endonuclease requires NBS1, but not the nuclease activities of Mre11 [122]. Furthermore, it now seems that a subset of V(D)J recombination events completed by C-NHEJ in the T lymphocyte lineage involve MRN [122, 123]. These studies used hypomorphic mutant alleles of MRN that permit viability in mammals, and therefore likely have minimal impact on non-ATM related functions of the complex. In the future it will be interesting to determine if essential functions of MRN are required in the T lymphocyte lineage.

Collectively, our work and recent studies [64, 65, 122-124] support the following model for early events during end joining. The γ-H2AX/MDC1/53BP1 axis provides long-range stabilization of ends, which involves modification and movement of chromatin over distances that can be cytologically visible [106, 125, 126]. Interactions among Rad50 coiled coil arms then stabilize DNA ends over closer distances [62], followed by ends being held in proximity within an Mre11 dimer interface [53], where a subset undergo nucleolytic processing to render them compatible for ligation [121]. Finally, the ends are shuttled to either NHEJ pathway for

final repair. Because C-NHEJ and A-NHEJ operate in DSB repair in contexts other than CSR, our observations likely apply broadly to end joining in mammals.

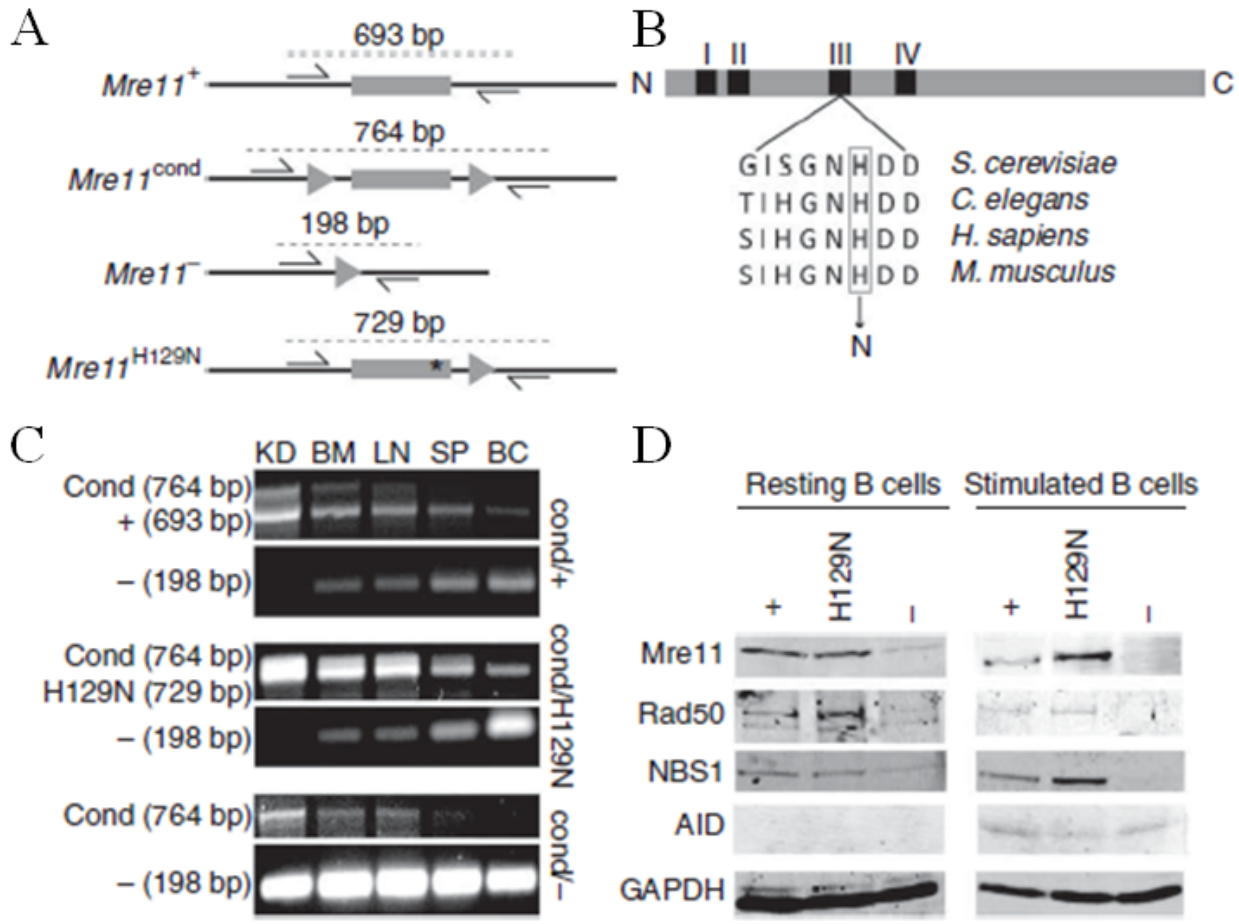

Figure 2.1: Mre11 deficiencies in the B lymphocyte lineage. (A) Four germline mouse alleles of Mre11: Mre11 wild type ($Mre11^{+}$), Mre11 conditional ($Mre11^{cond}$), Mre11 null ($Mre11^{-}$), and Mre11 deficient in nuclease activities ($Mre11^{H129N}$). Mre11 exon 5 (gray rectangle), intronic sequence (black line), LoxP sites (triangles), histidine to asparagine mutation at amino acid 129 (asterisk). Base pair (bp) numbers indicate allele specific PCR products resulting from the two primers depicted (arrows). (B) Location of the invariant active site histidine within nuclease motif III. Mouse histidine 129 was changed to asparagine as described. (C) PCR analyses distinguishing the four Mre11 germline alleles. Conversion of $Mre11^{cond}$ to $Mre11^{-}$ is detected only in sites containing substantial numbers of B lymphocytes (BM - bone marrow, LN - lymph node, SP - whole spleen, BC - enriched B cell population from spleen), but not in kidney (KD). Primers used depicted in (a). (D) Western blot analyses of MRN components and AID in splenic B lymphocytes from mice harboring one allele of CD19-cre. GAPDH was used as a protein loading control. Left - resting B cells, right - B cells stimulated to undergo class switch recombination for 4 days in culture. Each mouse contains the Mre11 allele indicated, and a second allele, which is $Mre11^{-}$ in the B lineage ($Mre11^{cond}$ elsewhere).

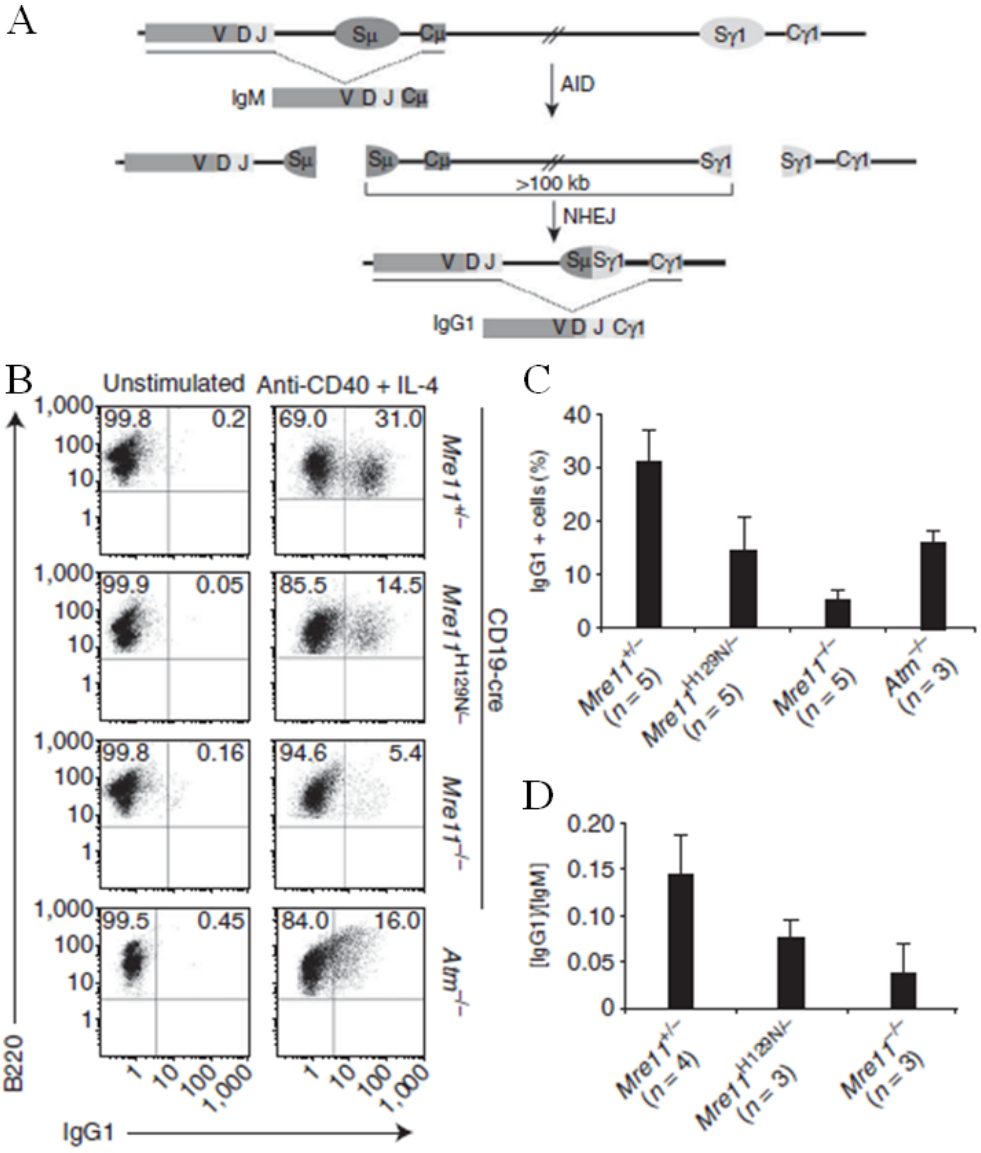

Figure 2.2: Distinct deficiencies in isotype switching conferred by MRN and ATM mutations. (A) Schematic of class switching from default IgM to the IgG1 isotype. AID initiates the formation of DSBs in switch regions (Sμ and Sγ1) upstream of their corresponding constant regions (Cμ and Cγ1). The intervening sequence (>100 kb) is excised, and the remaining DNA ends are ligated by NHEJ pathways generating a new heavy chain gene encoding Cγ1. Schematic is not to scale. (B) Flow cytometric analyses of class switching from IgM to IgG1 in B cells cultured with IL-4 and anti-CD40 for four days. Numbers in upper right quadrants represent the average percentage of IgG1+ cells from three to five mice of each genotype. $ATM^{-/-}$ mice were mixed 129/SvEv and NIH Black Swiss background. (C) Bar graph depicting direct comparisons of IgG1+ cell populations in (B) (average +/- S.D). (D) Antibodies secreted by stimulated B cells after 4 days in culture. Y axis indicates the ratio of IgG1 to IgM. No difference in IgM levels were detected (not shown).

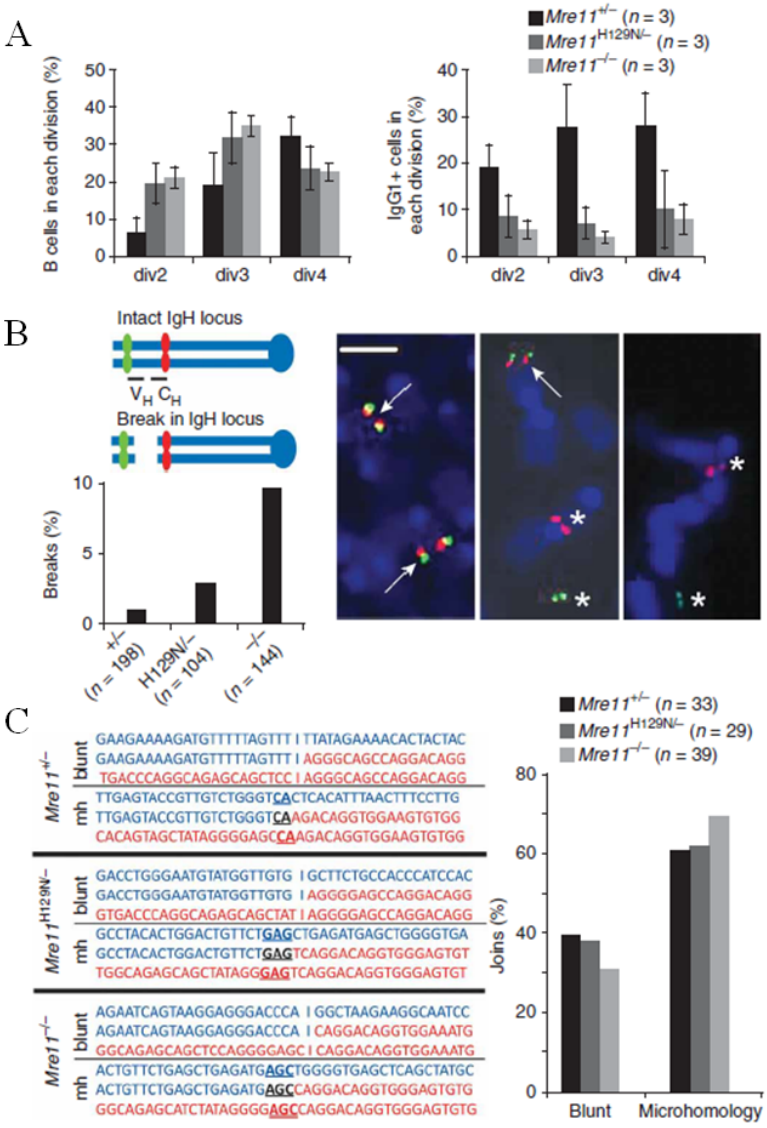

Figure 2.3: Requirement for MRN in the repair process. (A) Reduced class switching in MRN deficiencies does not result from proliferation defects. Left - The cell tracking dye CFSE was used to distinguish populations of stimulated B cells having undergone the indicated number of divisions (x axis). The percentage of cells in each population is shown on the Y axis. Reduced proliferation in the Mre11 deficiencies is evident. Right - the percentage of cells in each population (x axis) having switched to IgG1. Reduced switching is evident in each population. (B) Chromosome breakage in the IgH locus. Two color FISH with BACs flanking IgH on mouse chromosome 12 reveals IgH breaks by separation of red (BAC 199) and green (BAC 207) signals. The representative examples show a normal metaphase (left) and two with an IgH break (center and right). Arrows indicate co-localized signals (intact). Asterisks indicate separated signals (broken). The bar graph depicts the percentage of metaphases with an IgH break. Three mice of each genotype were analyzed. The total number of metaphases analyzed are indicated below each genotype. (C) Mre11 deficiencies impact the classic and alternative end joining pathways. Left - Representative sequences of cloned joins involving the mu and gamma 1 switch regions. Right - The distribution of joins containing blunt ends (Lig 4/XRCC4 dependent, classic NHEJ) and microhomologies (Lig 4/XRCC4 independent, alternative NHEJ) are shown. Three mice of each genotype were analyzed. The total number of sequenced joins are indicated.

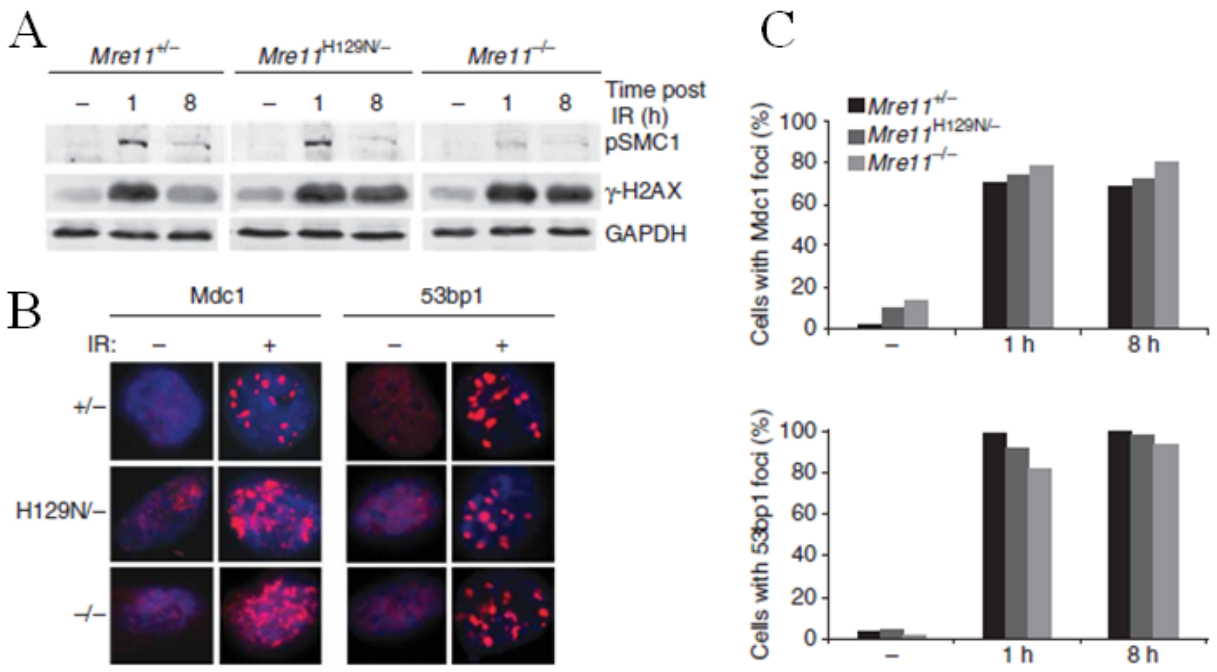

Figure 2.4: Independence of γ-H2AX-MDC1-53BP1 and MRN. (A) Distinct requirements for phosphorylation of SMC1 versus H2AX during the response to DSBs. Western blot analyses of the indicated proteins (right) prior to 10 Gy IR (–), and 1 or 8 hours post-IR. Phosphorylated SMC1 is used as a control to demonstrate functional MRN deficiency. GAPDH is a protein loading control. (B) Representative Immunofluorescent foci prior to (–), or 8 hours after (+) 10 Gy IR. (C) The formation of MDC1 and 53BP1 foci at 1 and 8 h post-IR does not require Mre11 nuclease activities or MRN. Bar graphs represent quantification of MDC1 and 53BP1 foci-positive cells at the indicated times (X axis) after 10 Gy IR. (–) no IR. Positive cells defined as > 5 foci.

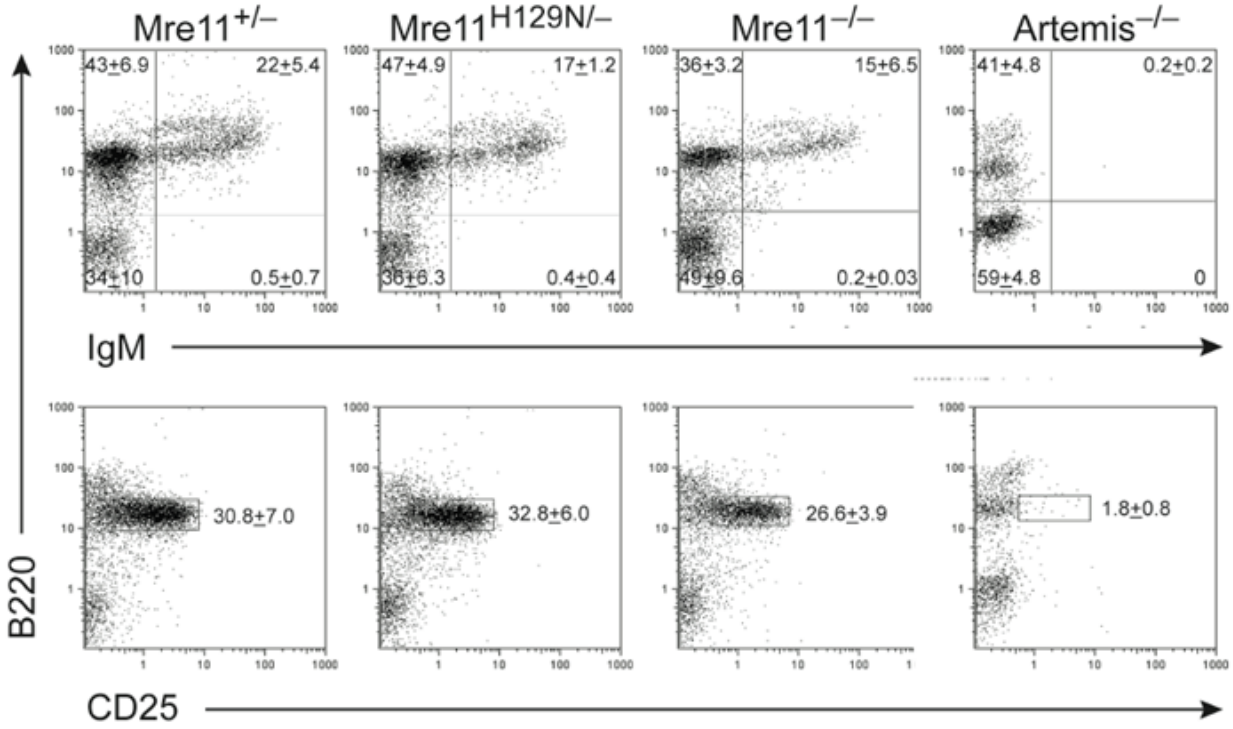

Figure 2.5: MRN deficiencies generated by CD19-Cre do not block early B cell development. Flow cytometric analyses of bone marrow using the indicated antibodies. Artemis deficiency was used as a control for early developmental block resulting from defective V(D)J recombination. Three mice of each genotype were analyzed. Numbers in the quadrants represent the averages +/- S.E.M. B220/IgM positive populations reflect B cells having supported successful V(D)J recombination at the heavy and light chain loci. B220/CD25 positive populations have supported heavy chain, but not light chain, recombination.

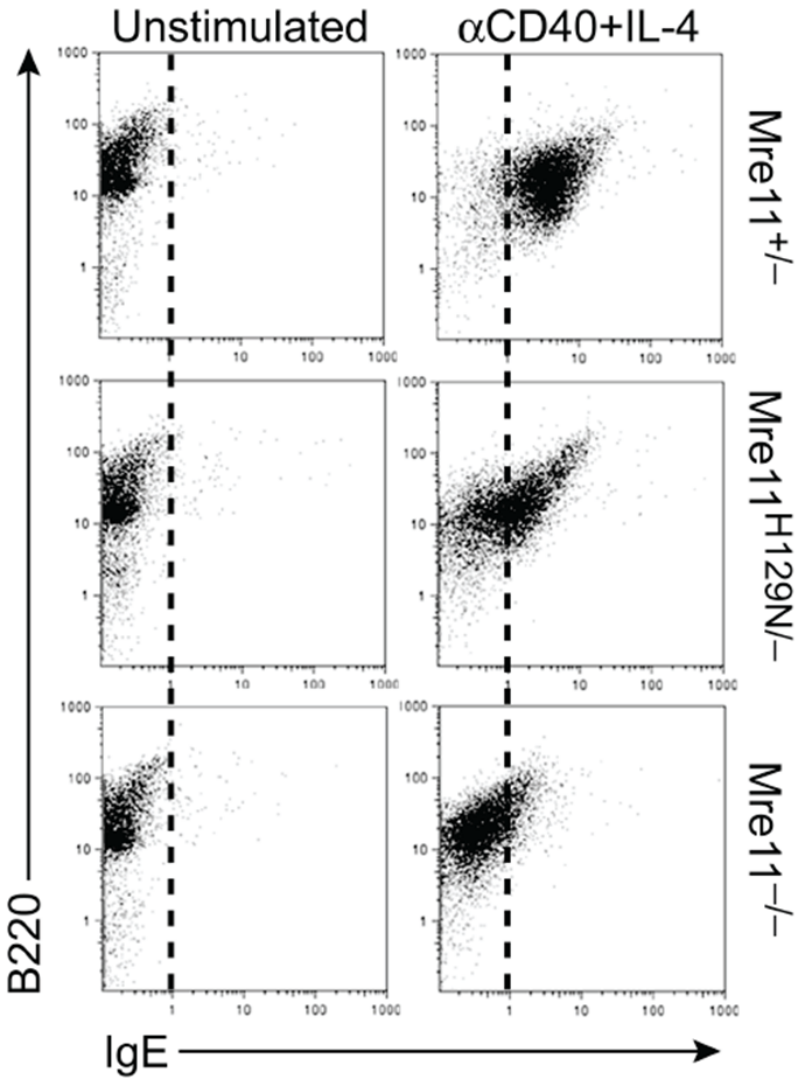

Figure 2.6: Requirement of MRN for switching to IgE. Representative flow cytometric analysis of class switching from IgM to IgE in B cells cultured with IL-4 and anti-CD40 for four days. IgE positivity cannot be quantitated precisely due to IgE antibody binding to Fc receptors.

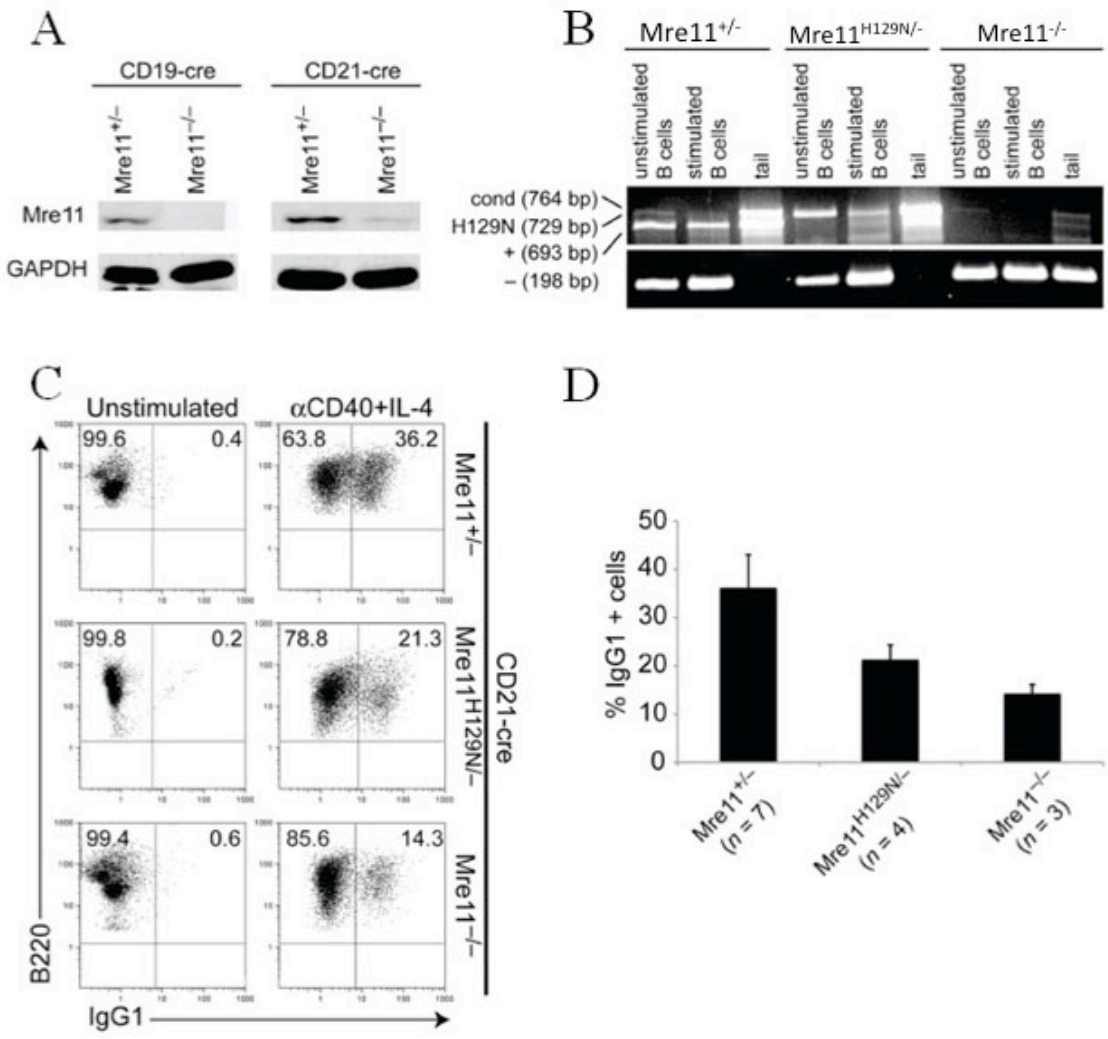

Figure 2.7: Conversion of Mre11cond to Mre11– by CD21-Cre. (A) Western blot analyses comparing Mre11 protein levels in CD19-cre and CD21-cre containing mice. Enriched splenic B cells stimulated with IL-4 and anti-CD40 were used. More residual Mre11 protein was reproducibly observed in CD21-cre relative to CD19- cre Mre11–/– B cell cultures. (B) PCR analyses confirming conversion of Mre11cond to Mre11– by CD21-cre in B lymphocytes. Primers used are depicted in figure 1a. (C) Flow cytometric analyses of class switching from IgM to IgG1 in mice harboring CD21- cre, which begins expression in mature IgM+ B cells. Numbers in upper right quadrants represent the average percentage of IgG1+ cells from three to five mice of each genotype. (D) Bar graph depicting direct comparisons of IgG1+ cell populations in (C) (average +/- S.D).

Table 2.1: Sequences of CSR joins from Mre11+/- stimulated B cells. Column on left shows blunt ended joins between Sμ and Sγ1 or Sε in Mre11$^{+/-}$ B cells after undergoing switching. Insertions and deletions are shown in red. Column on right shows microhomology- mediated joins (black sequence).

Table 2.2: Sequences of CSR joins from Mre11H129N/- stimulated B cells. Column on left shows blunt ended joins between Sμ and Sγ1 or Sε in Mre11$^{H129N/-}$ B cells after undergoing switching. Insertions and deletions are shown in red. Column on right shows microhomology- mediated joins (black sequence).

Table 2.3: Sequences of CSR joins from Mre11-/- stimulated B cells. Column on left shows blunt ended joins between Sμ and Sγ1 or Sε in Mre11$^{-/-}$ B cells after undergoing switching. Insertions and deletions are shown in red. Column on right shows microhomology- mediated joins (black sequence).

Chapter 3

Mice possessing Mre11 deficient B lymphocytes do not succumb to B cell lymphoma

Abstract

Non-homologous end joining (NHEJ) is one of the two main pathways of DNA double strand break repair, and is the pathway responsible for DNA rearrangements during B lymphocyte development. In the absence of classical NHEJ factors such as Artemis, DNA Ligase IV, or Xrcc4 on a p53 deficient background, mice develop B cell lymphomas. These lymphomas develop from B cells that have attempted V(D)J recombination or immunoglobulin class switching, and harbor translocations to the immunoglobulin heavy chain locus (IgH). The Mre11-Rad50-Nbs1 complex has multiple roles in response to DNA DSBs, including functioning within both the classical and alternative NHEJ pathway, the latter of which is thought to be responsible for oncogenic translocations. Mice harboring MRN deficiencies in B cells possess a strong defect in CSR. However, in contrast to other NHEJ factors, mice that harbor Mre11 deletions in B cells on a p53 deficient background do not succumb to B cell lymphomas, despite containing abundant genomic instability including IgH: Myc translocations.

Introduction

DNA double-strand breaks (DSBs) are highly toxic chromosomal lesions that can be caused by a myriad of endogenous and exogenous stresses. Left unrepaired, DSBs result in cell cycle stalling, growth arrest and cell death, while misrepair of DSBs can lead to a breadth of chromosomal abnormalities. These abnormalities, specifically chromosomally rearrangements, can cause cancer, birth defects, and other genetic diseases [82]. Luckily, mammals have evolved highly complex mechanisms to recognize these breaks, stop the cell from continuing to cycle, and repair the DNA. There are two main pathways for mammalian DSB repair, homologous recombination (HR) and non-homologous end joining (NHEJ) [83]. The HR machinery utilizes template sequences with long stretches of homology for repair. This template, usually a sister chromatid or homologous chromosome, is used it to fill in missing nucleotides, and thus HR predominates in S/G2 phases of the cell cycle [127]. NHEJ facilitates repair by ligating the broken ends together without a need for a homologous sequence, permitting it to function during all phases of the cell cycle [4]. In recent years, it has been discovered that NHEJ is actually comprised of at least two pathways, the classical pathway (C-NHEJ), and the alternative (A-NHEJ), or microhomology mediated pathway or pathways. C-NHEJ is classified mainly from its dependence on key proteins such as DNA Ligase IV (Lig 4) and its binding partner Xrcc4 [32, 86, 128]. Absence of these proteins allows for the A-NHEJ pathway(s) to take over. Although its exact mechanism and acting factors remain elusive, what is known about A-NHEJ is that it is able to utilize a microhomologous sequence (1-25 bp) between the two broken strands to align the DNA before ligation [38]. A-NHEJ is thought to be the primary mediator of translocations in mammalian cancers, specifically those involved in hematologic tumors [23, 129, 130].

Despite the fact that DSBs have the potential to be very dangerous to a cell, there are certain processes that require programmed DSBs to occur, such as meiotic crossover and B and T lymphocyte development. During B lymphocyte development, there are two programmed rearrangement reactions that require the generation of double strand breaks. The first is V(D)J recombination, which is a developmental step necessary to produce the diverse antibody repertoire of vertebrates and is initiated by the RAG1/2 endonucleases [131]. Upon the completion of V(D)J in the bone marrow, B lymphocytes migrate to peripheral lymph organs and secrete antibodies with the IgM heavy chain class. When presented with antigen, B cells then undergo the second programmed rearrangement requiring DSBs, class switch recombination (CSR). With a few exceptions, the purpose of CSR is to change the immunoglobulin heavy chain class from IgM to an isotype more effective for the given antigen [132]. During CSR, double strand breaks are initiated by the activation induced cytosine deaminase (AID), which targets specific sequences in highly repetitive switch (S) regions. S regions are comprised of 2-8 kb stretches of DNA that precede the constant (C) region exons which encode each isotype [133]. Recombination joins the DSBs generated in Sμ and a downstream S region, bringing the exon encoding the IgH variable region into proximity with the new IgH C region exon and effector function [134]. C-NHEJ is absolutely necessary for V(D)J recombination, as evidenced by the fact that both humans and mice with mutations in C-NHEJ proteins suffer severe combined immune deficiency [16, 28-33, 135]. While C-NHEJ also predominates in CSR, A-NHEJ can participate in as much as 50% of the joins [38].

The Mre11/Rad50/Nbs1 (MRN) complex plays several crucial roles in DSB repair. Its importance is underscored by the fact that murine knockouts of any of the three members result in early embryonic lethality [71-73], while humans harboring hypomorphic mutations of

complex members cause syndromes with hallmarks such as developmental delay, neurodegeneration and cancer predisposition [82]. Following a double strand break, the complex immediately localizes to the DNA, where the Mre11/Rad50 heterotetramer will bind to and stabilize one or both broken ends [60, 90-92]. The nucleolytic activities of Mre11 then initiate HR through resection [71, 136]. Nbs1 interacts with the ATM kinase, resulting in autophosphorylation of ATM and subsequent signaling to downstream proteins that control pathways such as cell cycle checkpoints and DNA repair. Both the scaffolding functions of MRN and the nucleolytic activities of Mre11 function in both classical and alternative NHEJ [63-65].

Pro-B cell tumors arise in mice lacking C-NHEJ factors Ku80, Xrcc4, Lig 4, or Artemis on a $p53^{-/-}$ background, while tumors that arise in conditionally deleted $Xrcc4^{-/-}p53^{-/-}$ mature B cells carry CSR induced translocations [29, 137-140]. Since the MRN complex is involved upstream of both the C-NHEJ and more translocation prone A-NHEJ pathways [63-65], we seek to determine a role for Mre11 in the development of B cell lymphomas. We hypothesize that Mre11 deletions in B lymphocytes will lead to B cell lymphomas, and there is strong evidence to support this hypothesis. First, we know that MRN functions within C-NHEJ, so it is possible that loss of then complex will shuttle CSR breaks to the more error prone A-NHEJ pathway. Studies have also shown that the absence of MRN leads to widespread genomic instability and defective checkpoint activation due to defective ATM activation, which are conditions that are necessary for cancer cell transformation [71]. Finally, human mutations in ATM, Nbs1, and Mre11 lead to cancer predisposition.

Materials and Methods

Generation of mice

Generation of $Mre11^{+/-}$, $Mre11^{-/-}$, and $Mre11^{H129N/-}$ mice with CD19- Cre expression was previously described in Chapter 2. $Mre11^{+/-}$, $Mre11^{-/-}$, and $Mre11^{H129N/-}$ mice containing CD19-Cre were crossed onto a $p53^{-/-}$ background (C57BL/6J) (Jackson Labs). Class switch experiments and translocation analysis was done on 6-12 week old mice. Mice were aged until moribund for survival curves and tissue analysis.

Mouse genotyping

Mre11 and Cre genotyping conditions were carried out as described in Chapter 2. p53 genotyping was performed using thermocycling conditions of 32 cycles of 94°C for 45 sec, 60°C for 45 sec, 72°C 2 min 30 sec with the following PCR primers: *Jaxp53-69*: 5'- ATA GGT CGG CGG TTC AT -3', *Jaxp53-70*: 5'- CCC GAG TAT CTG GAA GAC AG -3', and *Jaxp53-1300*: 5'- CTC GAC GTT GTC ACT GAA GC -3.

Mouse necropsy

Mice were aged until they were determined to be moribund by the standards of the University of Michigan Unit for Laboratory Animal Medicine (ULAM). Upon morbidity, mice were euthanized using CO2, and necropsied. Lymph organs including lymph nodes, bone marrow, spleen, and thymus were collected and fixed in 10% formalin. Visible tumor masses and spleen were and assayed for abnormal expression of B220 via flow cytometry. Spleen weight was taken in the event of splenomegaly.

Histology

Tissues removed during necropsy were fixed in 10% formalin and taken to the University of Michigan Histology and Immunohistochemistry Service (HIS). There, tissues were embedded, mounted, and stained for hematoxylin and eosin. Slides were viewed and photographed on an Olympus BX51 microscope, courtesy of the lab of Yuan Zhu.

B lymphocyte enrichment and culture

B cells were isolated from mice and cultured as described in Chapter 2. For cells to be assayed via translocation PCR, the cultures were washed and infected with an AID-expressing retrovirus after 24 hours as previously described [141]. This overexpression of AID allowed us to isolate 10- to 100-fold more translocations. DNA was prepared from these cultures 48 h after retroviral infection using the Qiagen DNeasy kit.

Flow cytometry

Cell surface markers were analyzed on a BD Accuri C6 Flow Cytometer using C6 software. Cells were washed with PBS + 10% (v/v) FBS, and incubated on ice in the dark for 30 - 60 min using various combinations of the following antibodies: αB220 (1:200, eBioscience), αIgG1 (1:100, BD Pharmingen), αIgE (1:100, Southern Biotech), αIgM (1:200, Southern Biotech), αCD25 (1:100, eBioscience). Data was analyzed using FlowJo software.

2- color FISH

B lymphocytes were incubated in colcemid (KaryoMAX) for 3 hours, washed twice with PBS, and incubated in 75 mM KCl for 15 min at 37°C. Cells were then fixed with 3:1 methanol/acetic acid and dropped onto glass slides, which were dried on a 42°C hot plate. 2-

color FISH labeling was done as described using BAC 199 (aka 199M11, Invitrogen) and BAC 207 (aka RP22-207123, BAC PAC Resources), and a BAC to c-myc (generous gift from Wes Dunnick). Slides were stained with DAPI (Invitrogen) according to manufacturer's instructions. FISH images were acquired on an Olympus BX61 microscope using a 60x objective, DAPI, FITC, and Texas Red filters, a CCD camera, and FISHview software (Applied Spectral Imaging).

Translocation PCR

IgH:Myc translocation PCR was a nested PCR reaction performed using the Expand Long Template PCR System (Roche) with the following thermocycling conditions. First round was 96C for 5 min followed by 25 cycles of 94C, 15 s; 62C, 15 s; and 68C, 7 min with 20 s of additional extension time per cycle. Second round was 25 cycles with 4 min of elongation time extended for 20 s per cycle. The following primers were used: for derivative chromosome 12 translocations first round, 5′-TGA GGA CCA GAG AGG GAT AAA AGA GAA-3′ and 5′-GGG GAG GGG GTG TCA AAT AAT AAG A-3′; for derivative chromosome 12 translocations second round, 5′-CAC CCT GCT ATT TCC TTG TTG CTA C-3′ and 5′-GAC ACC TCC CTT CTA CAC TCT AAA CCG-3′; for derivative chromosome 15 translocations first round, 5′-ACT ATG CTA TGG ACT ACT GGG GTC AAG-3′ and 5′-GTG AAA ACC GAC TGT GGC CCT GGA A-3′; and for derivative chromosome 15 translocations second round 5′-CCT CAG TCA CCG TCT CCT CAG GTA-3′ and 5′-GTG GAG GTG TAT GGG GTG TAG AC-3′. c-myc loading control primers were 5′-GGG GAG GGG GTG TCA AAT AAT AAG A-3′ and 5′-GTG AAA ACC GAC TGT GGC CCT GGA A-3′. PCR products were purified, cloned (TOPO-TA, Invitrogen), and sequenced.

For the GFP:Chr 2 translocation PCR, cells were infected with Adeno I-Sce1 with an MOI 500:1 at 50% confluency. 72 hours later the cells were harvested and genomic DNA was prepared using DNeasy Blood and Tissue Kit (Qiagen). First round was 96C for 5 min followed by 30 cycles of 94C, 15 s; 55C, 45 s; and 72C, 1.5 min. Second round was 96C for 5 min followed by 30 cycles of 94C, 15 s; 55C, 45 s; and 72C, 1.5 min. Primers used were *MMP2_4* 5'- GGT CAC TAA CTC ATG CCC CAC C -3'and *DR-GFP_400* 5'- GGT TCG GCT TCT GGC GTG -3' for the first round and *MMP2_5* 5'- GAG GAG ACG GAA GTG AAG CTC TG -3'and *DR GFP* 5'- GGT AGC GGC TGA AGC ACT GC -3'for the second round.

Results

Mice with Mre11 mutations in the B cell lineage on a p53- deficient background do not succumb to B cell lymphomas

Our lab has engineered alleles of Mre11 that function as wild type until conditionally inactivated by the Cre recombinase. Previous work with these alleles has shown that conversion of the conditional allele ($Mre11^{cond/-}$) to null ($Mre11^{-/-}$) results in loss of Mre11 and subsequent instability of the entire MRN complex [71]. Additionally, we engineered a point mutation in Mre11 (H129N) that abrogates both endo and exonucleolytic activities of Mre11without disrupting the integrity of the MRN complex or the ability of the complex to activate ATM in the presence of DSBs [71]. To bypass embryonic lethality and examine roles for MRN in lymphoma development, we generated mice that lack MRN or Mre11 nuclease activity in the B lymphocyte lineage by breeding in a CD19-cre allele [63]. CD19-cre activates in B lymphocytes during the progenitor stage in bone marrow [100]. Mice lacking MRN or Mre11 nuclease activities in B

cells because of CD19-cre expression ($C^{+}Mre11^{-/-}$ and $C^{+}Mre11^{H129N/-}$, respectively) produce normal numbers of IgM+ lymphocytes in bone marrow and produce spleens of normal size and cellularity. However, CSR is significantly affected in these cells, with the absence of nuclease activity decreasing switching by 50%, and loss of the complex causing an 80% decrease in CSR [63]. These B cells exhibit an accumulation of breaks in IgH following CSR induction, and both lymphocytes and fibroblasts harboring Mre11 deficiencies exhibit an overall increase in genome instability [63, 71].

The abundance of accumulated DSBs and genomic instability exhibited by B lymphocytes with Mre11 deficiencies, as well as the cancer predisposition in human patients harboring partial-loss of function alleles of Mre11 caused us to ask if these mice would develop B cell tumors. Former post-doctoral fellow Dr. Maria Dinkelmann and I began by aging a cohort of mice with B cells with genotypes $C^{+}Mre11^{-/-}$ and $C^{+}Mre11^{H129N/-}$, using mice containing one wild type allele, $C^{+}Mre11^{+/-}$, as the control cohort. Surprisingly, mice with B cells possessing Mre11 deficiencies have a normal life span, with a median survival of 27.5 months (compared to 29 months for the controls), and are not cancer prone (Fig. 3.1A). It is possible that cells harboring breaks in IgH and other types of genomic instability are eliminated from the cell population due to p53 related cell cycle arrest. To investigate this possibility, Dr. Dinkelmann and I bred our $C^{+}Mre11^{+/-}$, $C^{+}Mre11^{-/-}$, and $C^{+}Mre11^{H129N/-}$ mice onto a p53 deficient background to generate mice with $P^{-}C^{+}Mre11^{+/-}$, $P^{-}C^{+}Mre11^{-/-}$, and $P^{-}C^{+}Mre11^{H129N/-}$ B cells.

$P^{-}C^{+}Mre11^{-/-}$, and $P^{-}C^{+}Mre11^{H129N/-}$ mice became moribund about 16-18 weeks of age (Fig. 3.1B). However, the control $P^{-}C^{+}Mre11^{+/-}$ mice also became moribund around 16-18 weeks of age (Fig. 3.1B). Upon necropsy, the majority of mice presented with an enlarged thymus that was negative for the B cell marker, B220, and was therefore likely a product of p53 deficiency

(flow data not shown). A smaller percentage of mice succumbed to non- lymphoid tumors (Figure 3.1C). No mouse succumbed to B cell lymphoma, regardless of genotype. These results indicate that deficiencies in Mre11 on a $p53^{-/-}$ background do not cause mice to succumb to B cell tumors, at least before 16-18 weeks of age.

Mice conditionally deficient of the C-NHEJ factor Xrcc4 on a p53 null background developed mature B lineage lymphomas that presented in mesenteric lymph nodes [140]. To rule out the possibility that microscopic B cell tumors were present in our mice in addition to thymic tumors, I removed all lymph organs from these mice upon necropsy. In order to detect microscopic B cell tumors, spleens and mesenteric lymph nodes were fixed with 10% formamide and sent to the histology core for sectioning and staining. A preliminary 4 spleens and mesenteric lymph from each genotype were stained using hematoxylin and eosin.

Preliminary results from four spleens and mesenteric lymph nodes from each of the three genotypes suggest that there is no difference in histology between the genotypes (Fig. 3.2). Several of the spleens show disorganization of structure with poorly defined germinal centers, but rather than this phenotype being specific to any genotype, it seems to correlate with the absence or presence of a thymic mass upon mortality. Specifically, disorganized spleens were only seen in mice that presented with a thymic mass upon necropsy. However, a number of mice presenting with a thymic mass also maintained a structured and organized spleen. These results suggest that either the thymic lymphomas spread to the spleen in a subset of mice, or enlarged, disorganized spleens may be a symptom of thymic lymphoma. Additionally, histology from the mesenteric lymph nodes showed a range of phenotypes, including some disorganized and enlarged nodes (Fig. 3.2B). These phenotypes did not correlate with a specific Mre11 genotype, however. Although more histology needs to be examined in order to make a statement about the

significance of the tissue structure, initial data suggests that there are not B cell tumors developing in these mice, at least not in the peripheral lymph.

p53 loss does not rescue Mre11 related CSR defects

I next assessed levels of CSR and end joining in our $P^{-}C^{+}$Mre11 mice. Absence of p53 in $C^{+}Mre11^{+/-}$ and $C^{+}Mre11^{H129N/-}$ lymphocytes has no effect on the percentage of B cells that are able to complete CSR as compared to cells with wild type p53 (Fig. 3.3A). However, $P^{-}C^{+}Mre11^{-/-}$ mice showed a statistically significant increase in the percentage of B cells that express IgG1 on their surface as compared to $C^{+}Mre11^{-/-}$ B cells (Fig. 3.3 A). Cell counts show indicate less cell death in $P^{-}C^{+}Mre11^{-/-}$ B cells as compared to their p53 wild type counterparts (data not shown), thus it is likely that the increase in the percentage of IgG1 presenting cells is the result of the elimination of p53 related apoptosis that might otherwise accompany an unrepaired DSB in IgH.

Previously, decreased levels of CSR in $C^{+}Mre11^{-/-}$ mice coincided with increased levels of accumulated breaks in IgH. To determine if this holds true upon loss of p53, I employed several 2- color fluorescence *in situ* hybridization (FISH) assay that uses BAC probes flanking the IgH locus to look for chromosome breaks in IgH. Breaks were identified as separation of probes (Fig. 3.3B). For each genotype, 100-200 metaphases were examined, and the Fisher exact probability test was used to determine if the number of breaks was significant. Loss of p53 did not significantly impact the number of IgH breaks accumulated in $C^{+}Mre11^{+/-}$ and $C^{+}Mre11^{-/-}$ B cells as compared with p53 wild type $C^{+}Mre11^{+/-}$ and $C^{+}Mre11^{-/-}$ B cells (Fig. 3.3B). However, $P^{-}C^{+}Mre11^{H129N/-}$ B cells show a significant increase in IgH breaks as compared to those $C^{+}Mre11^{H129N/-}$ B cells with wild type p53 (Fig. 3.3B). Cells harboring the $Mre11^{H129N}$ allele still

have intact ATM signaling, so it would make sense that knocking out p53 in these cells would have a greater impact than in cells without the MRN complex, in which checkpoint signaling is already defective due to insufficient ATM activation. This data suggests that Mre11 nuclease activities may play a more important role for end joining during CSR than we initially understood, but intact cell cycle checkpoint signaling was masking that role.

Translocations are detectable in p53 and Mre11 deficient B cells

We show in Chapter 2 that the MRN complex is involved in both C- and A-NHEJ, in addition to its other known functions in DSB repair. Since A-NHEJ is thought the primary mediator of translocations in mammalian cancers and MRN functions in its pathway, it is possible that the absence of the complex or the Mre11 nuclease activities leads to an inability to generate translocations. To test this hypothesis, I used several 2- color fluorescence *in situ* hybridization (FISH) assays to look for translocations. Two bacterial artificial chromosomes (BACs) were used as probes, located at the 3' and 5' of the IgH locus (Fig. 3.4A). Chromosome breaks are identified as a separation of the probes, and translocations are identified as reattachment of the 3' probe to another chromosome (Fig. 3.4A). Although this is a crude assessment of translocation, the percentage of metaphase spreads with 3' probes that appeared to be attached to another chromosome was significantly higher in the $P^{-}C^{+}Mre11^{-/-}$ B cells than the controls (Fig. 3.4B). The number of metaphases with probes that appeared to be attached to another chromosome was higher in $P^{-}C^{+}Mre11^{H129N/-}$ B cells than in controls, but this was not statistically significant (Fig. 3.4B).

Pro-B cell tumors that arise in mice lacking C-NHEJ factors Ku80, Xrcc4, Lig 4, or Artemis on a $p53^{-/-}$ background harbor translocations from JH to the proto-oncogene c-myc

(Myc) [29, 137-139], while tumors that arise in conditionally deleted $Xrcc4^{-/-}p53^{-/-}$ mature B cells carry CSR induced translocations between S regions and Myc [140]. Therefore, I used a similar 2- color FISH assay to evaluate possible IgH:Myc translocations in Mre11 and p53 deficient B cells. Molecularly, IgH:Myc translocations join the 3' ends of both loci, so I utilized BAC probes that were 3' of both Myc and IgH. Co-localization of the probes would indicate translocation between the two loci (Fig. 3.4C). No translocations were observed using this assay (Fig. 3.4D). This result could indicate that translocations do not occur in the absence of the MRN complex, or that the metaphase spread assay is not sensitive enough to detect such a rare chromosomal event.

To determine whether IgH:Myc translocations occur in Mre11, p53 deficient B cells in a more sensitive manner, I employed a previously established PCR based assay [142]. This PCR utilizes primers that can amplify translocations that occur anywhere between J_H4 and the Cμ of IgH and exon 1 of c-myc(Fig. 3.5A). Preliminary data from this assay shows that IgH translocations occur in $P^-C^+Mre11^-$ and $P^-C^+Mre11^{H129N}$ B cells, as well as $P^-C^+Mre11^+$ B cells (Fig. 3.5B). Translocations were confirmed by Southern Blot (Fig. 3.5B) and sequencing.

Because IgH translocations occur in roughly 1 in 10^6 B cells, former post-doctoral fellow Dr. Jeff Buis employed another PCR technique to assay translocations in mouse embryonic fibroblasts (MEFs) in which MRN or the Mre11 nuclease activity absent. In this assay, a plasmid containing a GFP cassette surrounding a cut site for the rare cutting nuclease I-Sce1 is stably introduced into $Mre11^{-/-}$ MEF lines expressing $Mre11^+$, $Mre11^{H129N}$, or $Mre11^-$ cDNA. Cryptic I- Sce1 cut sites have been described in the mouse genome, in which sequences diverge 1-5 nucleotides from the 18bp target site [143]. These sites were identified as AID- independent targets of translocation for Myc in a genome wide translocation assessment [143]. The PCR

strategy employed uses primers between the introduced GFP cassette and the cryptic I-Sce1 site found in the Mmp24 gene on chromosome 2 (Fig. 3.5C). After introduction of I-Sce1, translocations between GFP and the I-Sce1 cryptic cut site in chromosome 2 were detected in $Mre11^{+}$, $Mre11^{H129N}$, and $Mre11^{-}$ MEF lines (Fig 3.5D). Although this PCR data is inconclusive in that it is not quantitative, it does show that there is some level of translocation happening in p53, Mre11 deficient cells.

Discussion

My goal was to determine possible roles for Mre11 in the development of B cell lymphomas following CSR induction. It has been shown that deletion of C- NHEJ factors Ku [137], Xrcc4 [138], Lig 4 [29], and Artemis [139] on a p53 deficient background in mice overwhelmingly leads to pro-B cell lymphomas that harbor translocations to the J_H region, indicating a failure to correctly complete V(D)J recombination. Furthermore, when Xrcc4 is knocked out in mature B cells on a p53 null background, mice develop tumors caused by translocations involving the S region, indicating a failed attempt at CSR [140]. Since Mre11 has been shown to be involved in C-NHEJ, it seems likely that deletion of the MRN complex, on top of p53 deficiency, would lead to B cell tumors. The fact that patients with deficiencies in Mre11 and other members of the MRN complex are predisposed to neoplasms, while deletion of Mre11 in fibroblasts and B cells shows significant genomic instability, including chromosomal translocations seems to reinforce the hypothesis that Mre11 would be involved in preventing oncogenic translocations. However, the data presented here indicates that neither the MRN complex nor the Mre11 nuclease activities are important for the prevention of tumors, at least in

B cells. $P^{-}C^{+}Mre11^{-/-}$ and $P^{-}C^{+}Mre11^{H129N/-}$ mice died presenting with p53 related thymic tumors, and B cell tumors were preliminarily not visible on a cellular level.

We cannot completely rule out the presence of microscopic B cell tumors. To do this, we would need to perform more histology, and possibly immunohistochemistry on peripheral lymph, to rule out the possibility that clonal populations of B cells are not present. Additionally, it would be advantageous to histologically examine bone marrow from $P^{-}C^{+}Mre11^{-/-}$ and $P^{-}C^{+}Mre11^{H129N/-}$ mice, although it is unlikely that CD19-cre would delete Mre11 that early in B cell development. We also cannot exclude the possibility that B cell tumors could arise later in the life of these mice, but they succumb to thymic lymphomas before they can be detected. The introduction of a conditional p53 allele would help us to resolve this issue.

In the case that there are no microscopic B cell tumors present or that these mice will not develop B cell tumors later in life, perhaps this could have been anticipated. Mre11 and the MRN complex have been shown to have roles in the alternative end joining pathway or pathways, which studies indicate is repressed when C-NHEJ is intact [23]. Loss of C-NHEJ factors such as Xrcc4 and Ku seem to shuttle DNA breaks to the more error prone A-NHEJ pathway, leading to tumor formation [137, 138]. It is possible that removing a factor (Mre11) that has been shown to have roles in both end joining pathways may repress tumor formation through the A-NHEJ pathway.

One hypothesis that could explain the lack of tumors in our p53/Mre11 deficient B cells is that the MRN complex is required for the joining of ends into translocations. The data presented in this thesis is inconclusive on this front, and more work is required to answer this question definitively. Because 2- color FISH is limited both in its ability to examine only cells in

M phase as well as in the fact that time and equipment is required to look at hundreds of metaphases, we turn to PCR based assays. After employing a well established PCR assay that was designed to detect translocations between IgH and Myc [144], I was able to see a detectable level of translocations in all three Mre11 genotypes (Fig. 3.5). However, in order to be able to comment on how efficiently cells that harbor Mre11 deficiencies can undergo translocation, this assay needs to be repeated hundreds of times per Mre11 genotype. Only then will this assay be qualitative and quantitative enough to conclude on the role of MRN in translocation formation. This applies to the PCR assay done by Dr. Buis as well. I show that translocations between a GFP reporter and a cryptic I-Sce1 cut site in chromosome 2 are detectable in MEFs containing Mre11 deficiencies. Again, this assay must be repeated enough times to reach a quantitative and qualitative conclusion about these translocations. This is certainly something that can be done in the future.

Another hypothesis that might explain why our mice do not succumb to B cell lymphomas is that Mre11 has other roles in cell growth that, when removed, are not compatible with malignancy. It was recently published that Mre11 functions to regulate homologous recombination during the normal mammalian cell cycle [145]. The protein CtIP functions with MRN and the BRCA1 tumor suppressor to resect broken DNA ends during HR, and must therefore interact with them in S and G2 phases of the cell cycle. In order to maintain this cell cycle specific interaction, CtIP is targeted to the proteasome for degradation during G1 phase of the cell cycle but is phosphorylated by cyclin dependent kinases (CDKs) during S- phase [146, 147]. Buis et al. discovered that Cdk2 is the major kinase responsible for phosphorylation of CtIP in S-phase, and that this phosphorylation event is dependent upon the C-terminus of Mre11 [145]. Ongoing and yet unpublished studies in the Ferguson lab indicate that this interaction

between Cdk2 and the Mre11 C-terminus might be required for the activation of Cdk2 substrates other than CtIP.

If Mre11 truly functions to control Cdk2 activity, there are several conceivable implications that arise that could impact tumorigenesis. First, it is possible that Mre11 could have other undiscovered roles in the normal cell cycle that could prevent growth of tumor cells upon removal. Second, it is possible that Cdk2 targets proteins that are necessary for tumorigenesis and that removal of Mre11 suppresses their action. One example of a target of Cdk2 that could affect tumor growth in our system is Myc. Several studies have shown that Myc is responsible for the repression of Ras induced senescence in a Cdk2 phosphorylation dependent manner [148, 149]. Thus, it is imaginable that removal of Mre11 from $P^{-}C^{+}Mre11^{-/-}$ B cells allows for the activation of senescent pathways in cells that would otherwise begin to abnormally proliferate, which is particularly compelling given the IgH: Myc translocations detectable in our B cells as well as the regularity with which this translocation occurs in general.

One caveat in this theory is that the $Mre11^{H129N}$ allele is still capable of associating with and activating Cdk2. Therefore, there would have to be a second function of Mre11 that could explain why $P^{-}C^{+}Mre11^{H129N/-}$ mice do not succumb to B cell lymphomas. Buis et al. published that both $Mre11^{-/-}$ and $Mre11^{H129N/-}$ MEFs are hypersensitive to aphidicolin and harbor chromatid anomalies such as radials that are indicative of a role in replication stress during S-phase [71]. The activation of ATR and its downstream effector Chk1 are important for cell survival during replication stress in S-phase [150]. Studies suggest that the deregulated S-phase caused by oncogenes such as Myc increases replication stress, thus intensifying the importance of ATR and Chk1 in these cells. Defective ATR signaling caused by the Mre11 defects in our system could conceivably increase replication stress in cells and explain why neither $P^{-}C^{+}Mre11^{-/-}$ nor P^{-}

$C^{+}Mre11^{H129N/-}$ mice die of B cell tumors. Furthermore, chromosome spreads of MEFs and B cells that harbor Mre11 deficiencies show a significant increase in general chromosome instability [71]. The combination of oncogenic stress and genome instability in $P^{-}C^{+}Mre11^{-/-}$ and $P^{-}C^{+}Mre11^{H129N/-}$ B cells could produce a level of genome instability that exceeds compatibility with cell survival.

Collectively, this data suggests that loss of Mre11 or the MRN complex protects cells against oncogenic transformation. Mice with Mre11 deficiencies in their B cells do not succumb to B cell lymphomas, even in the absence of p53. Additionally, these cells harbor detectable levels of translocations, signifying that the block in transformation occurs after DNA mutagenesis by DNA repair failure. Investigation of Cdk2 activation and oncogenic stress in these cells may help to define these roles more clearly in future studies.

A

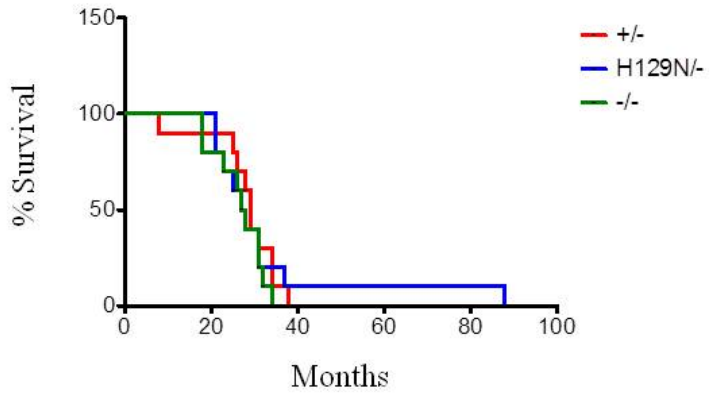

B

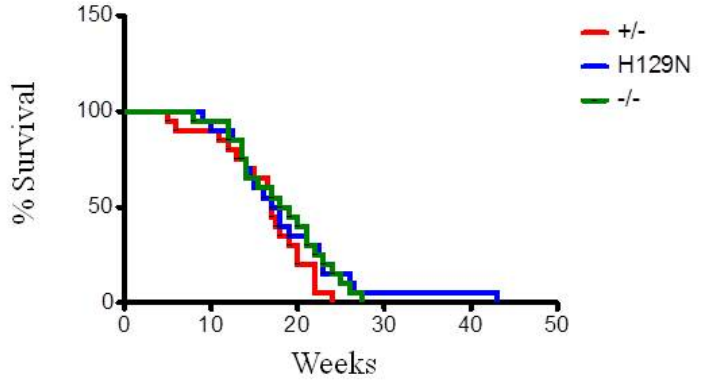

C

Genotype ($p53^{-/-}$, $CD19cre^{+}$)	Cause of Death				
	B cell lymphoma	Thymic lymphoma	Non-lymph tumor	Non-tumor	Total
+/-	0	14	2	4	20
H129N/-	0	13	3	4	20
-/-	0	15	1	4	20

Figure 3.1: $P^{-}C^{+}Mre11^{-}$ and $P^{-}C^{+}Mre11^{H129N}$ mice do not succumb to B cell lymphomas. (A) Mice harboring Mre11 deficiencies in B cells show a survival curve similar to control mice, with median survival of 27.5 months compared to 29 months (P=0.7272 for $C^{+}Mre11^{H129N}$ and 0.4794 for $C^{+}Mre11^{-}$). (B) $P^{-}C^{+}Mre11^{-}$ and $P^{-}C^{+}Mre11^{H129N}$ die earlier, but show similar survival to $P^{-}C^{+}Mre11^{+}$ mice (median survival 17.5 weeks, 18.5 weeks and 17 weeks respectively where P= 0.3575 for $P^{-}C^{+}Mre11^{H129N}$ mice and 0.2482 for $P^{-}C^{+}Mre11^{-}$ mice). (C) The cause of death for the majority of mice of all genotypes was thymic lymphoma related to loss of p53. No mice developed B cell lymphoma.

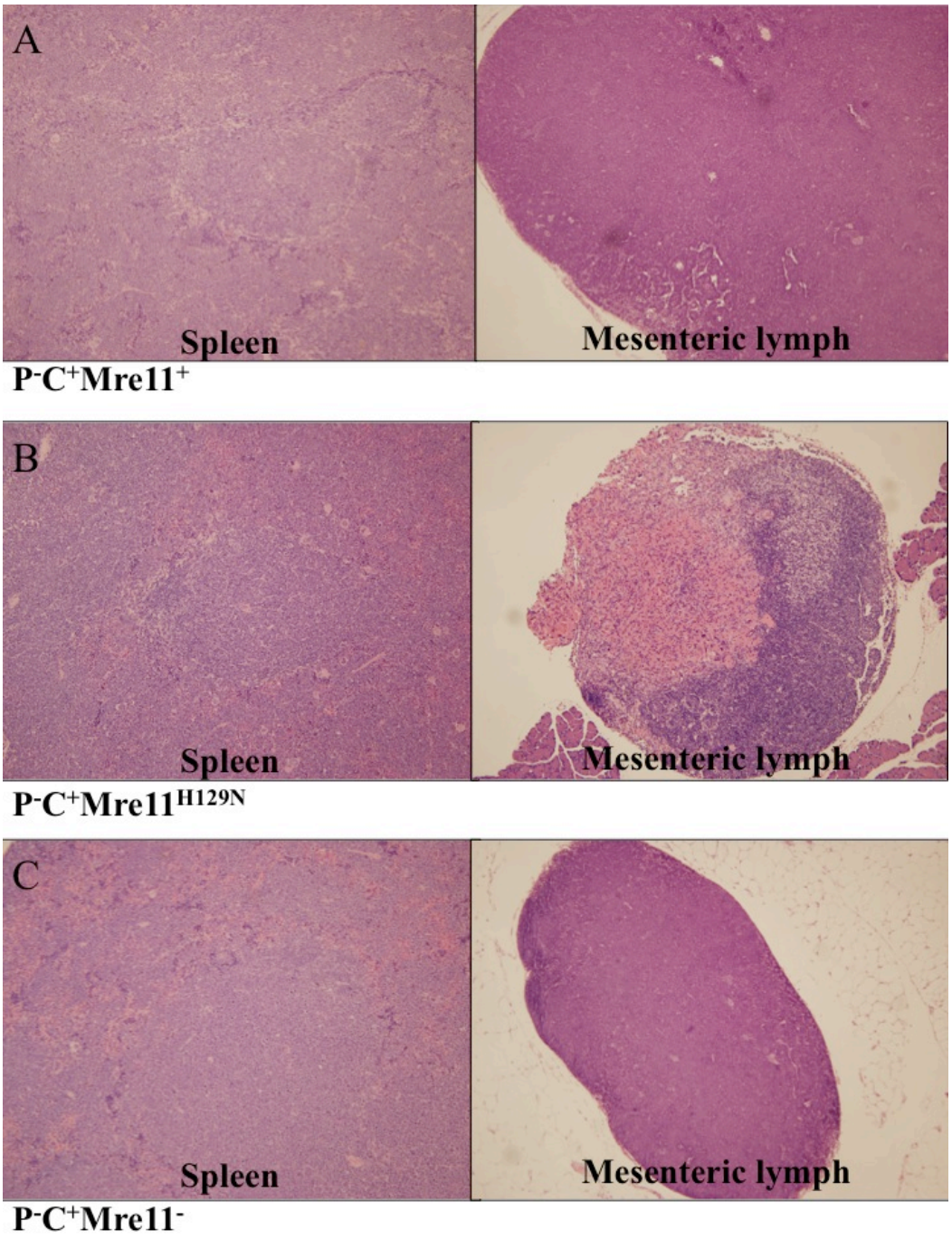

Figure 3.2: Spleens and mesenteric lymph appear histologically similar between genotypes. Representative H&E stained spleen (left) and mesentery (right) of $P^{-}C^{+}Mre11^{+}$ (A), $P^{-}C^{+}Mre11^{H129N}$ (B), and $P^{-}C^{+}Mre11^{-}$ (C) mice. Although some spleens appear more disorganized than others, no obvious differences appear between genotypes. Mesenteric lymph in one $P^{-}C^{+}Mre11^{H129N/-}$ mouse (B) appears inflamed, but no significant differences were able to be determined between genotypes overall. 10x magnification.

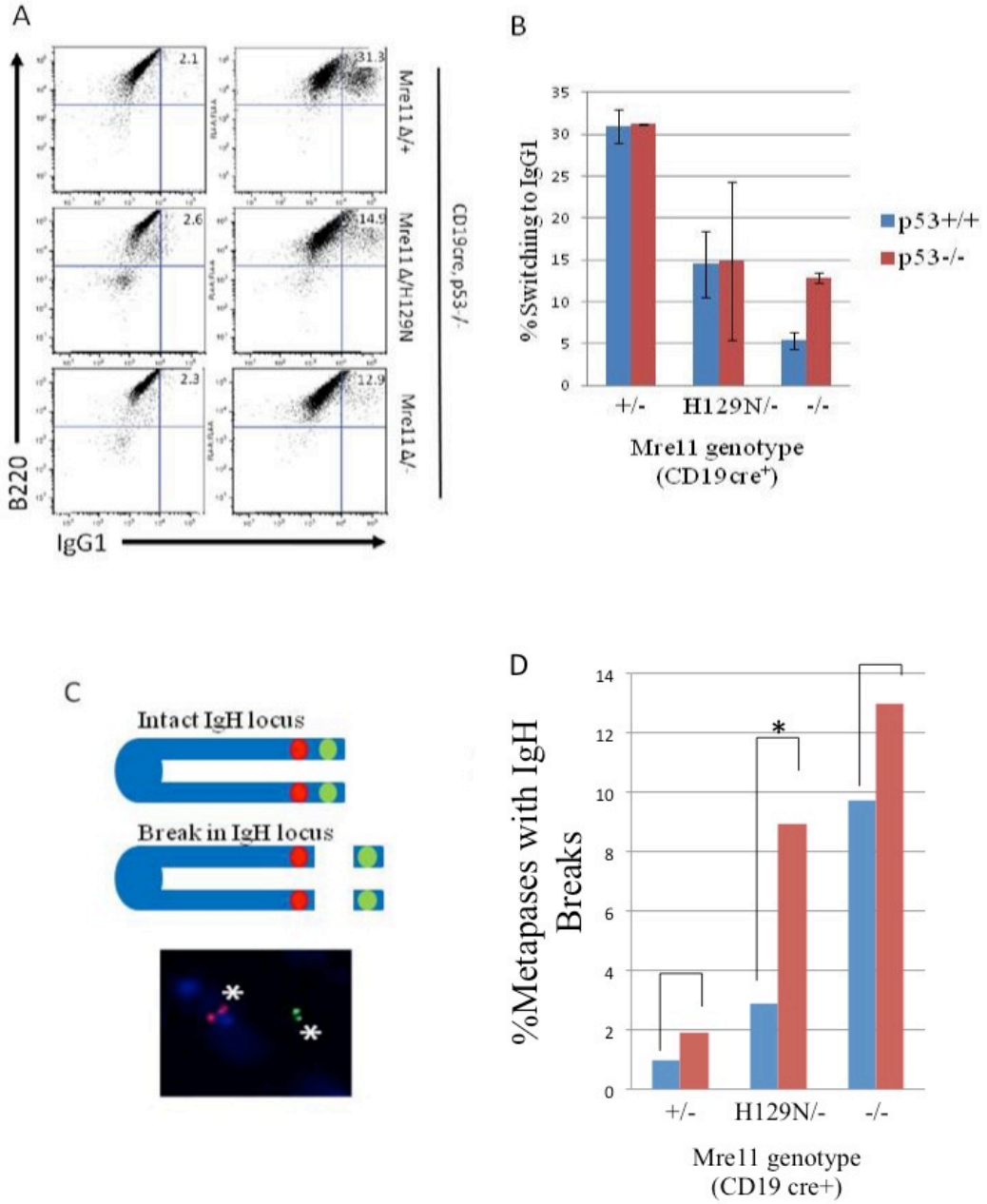

Figure 3.3: Isotype switching and end joining remain significantly reduced in Mre11 deficient B cells on a p53-/- background. (A, B)Nuclease deficient B cells show a 50% decrease in switching, regardless of p53 status. MRN deficient B cells, however, show an 80% decrease in CSR with p53, but only a 40% decrease without p53. Cell counts indicate that this is due to an increase in cell survival. (C, D) Loss of MRN caused an accumulation of unrepaired breaks in the IgH locus, with or without p53. Loss of p53 significantly increases the number of detectable unrepaired breaks in nuclease deficient B cells, likely because the loss of p53 is allowing more cells to survive with breaks and progress to M-phase.

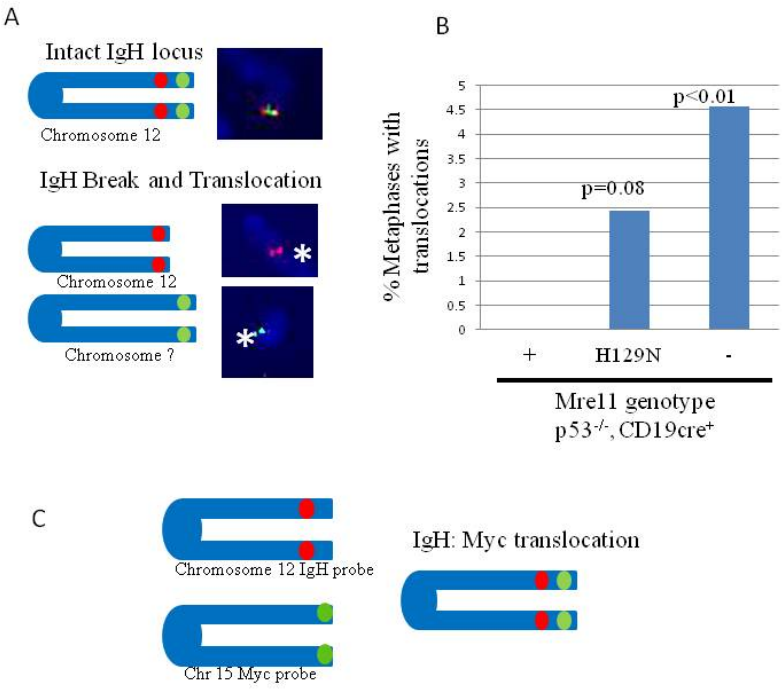

D

Genotype	# Metaphases	# Separated	#Co-localized	N=
$P^{-}C^{+}Mre11^{+}$	150	150	0	3
$P^{-}C^{+}Mre11^{H129N}$	146	146	0	3
$P^{-}C^{+}Mre11^{-}$	153	153	0	3

Figure 3.4: Detecting translocations in B cells using 2- color FISH. We use 2- color FISH to look for general translocations as well as specific translocations (IgH: Myc). (A) Schematic of the broad translocation assessment assay. A break in the IgH locus manifests as separation of probes, whereas a "translocation" is scored when the telomeric probe appears attached to another chromosome. (B) B cells with Mre11 deficiencies show significantly more "translocations" than controls. (C) Detecting IgH:Myc translocations via 2-color FISH. BAC probes to IgH and c-myc allow for the detection of translocations between the genes via co-localization of the probes. (D) Translocations are not detectable using this method, likely because this assay is not sensitive enough to detect such a rare chromosomal event.

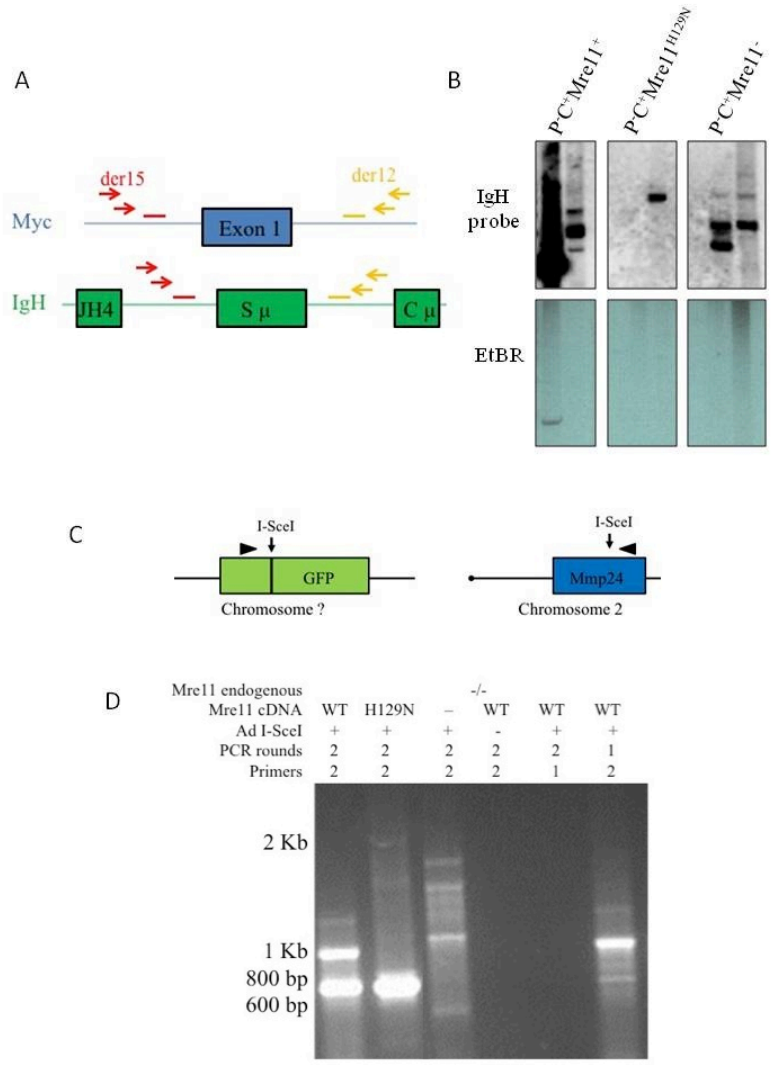

Figure 3.5: PCR reveals translocations in P-C+M B cells with Mre11 deficiencies. (A) Schematic of IgH:Myc translocation PCR performed in B cells. Nested primers (arrows) flanking exon 1 of Myc and Sμ of IgH detect translocations made in this area, deriving either from IgH (der12) or Myc (der15). Southern Blot probes are represented as bars (B) B cells overexpressing AID were stimulated to undergo CSR in culture. Each lane represents der12 PCR done on roughly 5 x 10^5 cells per reaction. PCR products were run on a 1% gel stained with ethidium bromide (EtBr) and then probed using the der12 IgH probe (represented by the yellow bar in A). PCR products were sequenced to confirm translocations. (C) Schematic of translocation PCR in mouse embryonic fibroblasts (MEFs). Mre11$^{cond/-}$ MEFS were stably transfected with a plasmid (DR-GFP) containing an I-SceI cut site. This line was then stably transfected with a plasmid expressing wild type, H129N, or no Mre11 cDNA. (D) Adeno-Cre was used to convert the endogenous Mre11 conditional allele to null, followed by Adeno- I-Sce1 to induce targeted DSBs shown in (C). Nested PCR between the I-SceI cut site and a "cryptic" I-SceI site found in chromosome 2[143] detected translocations between the two chromosomes in MEFs of each genotype (confirmed by sequencing) (work done by Dr. Jeffrey Buis). Controls include empty Adenovirus (lane 4), use of one primer only (lane 5) and one amplification reaction (lane 6).

Chapter 4

Oncogenic *Myc* translocations are independent of chromosomal location and orientation of the immunoglobulin heavy chain locus

Abstract

Many tumors are characterized by recurrent translocations between a tissue- specific gene and a proto- oncogene. The juxtaposition of the Ig heavy chain gene and Myc in Burkitt's lymphoma and in murine plasmacytoma is a classic example. Regulatory elements within the heavy chain constant region locus are required for Myc translocation and/or deregulation. However, many genes are regulated by cis- acting elements at distances up to 1,000 kilobases outside the locus. Such putative distal elements have not been examined for the heavy chain locus, particularly in the context of Myc translocations. We demonstrate that a transgene containing the Ig heavy chain constant region locus, inserted into five different chromosomal locations, can undergo translocations involving Myc. Furthermore, these translocations are able to generate plasmacytomas in each transgenic line. We conclude that the heavy chain constant region locus itself includes all of the elements necessary for both the translocation and the deregulation of the proto- oncogene.

Modified from Spehalski E*, Kovalchuk AL*, Collins JT, Liang G, Dubois W, Morse HC, Ferguson DO, Casellas R, Dunnick WA. Oncogenic *Myc* translocations are independent of chromosomal location and orientation of the immunoglobulin heavy chain locus. Proceedings of the National Academy of Sciences, 2012 Aug 21; 109(34):13728-32.

Introduction

Many tumor types, including most leukemias and lymphomas, are characterized by reciprocal translocations of the same two chromosomal loci in independent tumors. A number of B lineage lymphomas harbor recurrent translocations that involve the immunoglobulin locus (Ig), whereas the T cell receptor locus is involved in most T lineage lymphoma translocations [151, 152]. As a result of these recurrent translocations, promoters or enhancers in one translocation partner often change the regulation of the proto- oncogene in the other partner. A classic example of this is the translocation of the Myc proto-oncogene on human chromosome (Chr) 8 (mouse Chr 15) to the immunoglobulin heavy chain locus (IgH) on human Chr 14 (mouse Chr 12) [2, 153-155]. This translocation results in Myc being placed under the strong translational control of IgH. The Myc:IgH translocation occurs in more than 85% of human Burkitt's lymphoma and mouse plasmacytoma, and it is one of the earliest events in tumorigenesis, indicating it to be the driving force of these tumors. Molecularly, the translocation junction occurs most frequently in the first (noncoding) exon or first intron of the Myc gene, joining the "tail" (second and third exons) of Myc to the tail (3' or constant region) end of IgH. Because it is retained in the majority of these translocations, enhancer elements in the tail (3' regulatory region) of the IgH locus presumably deregulate Myc expression, a primary event in the tumorigenesis [134]. In part, the prevalence of this recurrent translocation is due to strong selection for deregulated Myc expression [2, 153-155].

Chromosomal location also has a role in recurrent translocations. Although the Myc and N-myc genes are very similar, Myc, but not N-myc, is found as a translocation partner in murine pro- B cell lymphomas that arise in mice deficient in the DNA repair factors p53 and DNA Ligase IV (Lig4). Gostissa et al. have tested whether this cell- type specific use of Myc in

translocations was due to selection for specific activities of the protein encoded by the Myc gene, by replacing Myc coding exons with the N-myc coding exons [156]. They found translocations in pro- B cell lymphomas now joined heavy chain genes to the N-myc gene in the Myc location. The investigators in the study concluded that, at least for this pair of genes in this genetic background, selection for the activities of the specific protein is less important than cis- acting elements in the Myc locus that target translocations with some degree of cell type preference [156]. Apparently, preferential targeting of specific loci can vary depending on the cell type and on DNA repair pathways used; the N-myc locus is a target for chromosomal rearrangements in other genetic backgrounds [157, 158].

Myc:IgH translocations in plasmacytoma are thought to result from aberrant heavy chain class switch recombination [151, 152]. Normal switch recombination occurs through double-stranded breaks that are introduced into 2- to 8- kb switch regions (S) that precede the IgH constant region genes [132]. S regions are characterized by multiple copies of simple sequences, some of which are preferred sites of action for the activation-induced cytosine deaminase (AID), the enzyme that initiates class switching [133, 159]. Recombination joins double-stranded breaks in two S regions, bringing the exon encoding the IgH variable region into physical and functional association with a new heavy chain constant region with a different effector function [132]. Like class switch recombination, translocations to Myc usually involve S regions [2, 151, 154, 155] and depend on AID [78, 160, 161].

The known regulatory elements contained within the IgH locus have been examined for a role in Myc translocation and deregulation. The IgH intronic enhancer (Eμ) is not physically associated with the Myc coding sequences after translocation and is, therefore, unlikely to be important for Myc deregulation [2, 153-155]. Gostissa et al. demonstrated that elements in the

IgH 3' regulatory region are required for Myc translocation and/or deregulation [81]. The potential for additional cis- acting elements outside of the IgH constant region locus has not been investigated. In this study, we addressed a fundamental question: Are DNA sequences flanking the IgH constant region locus in its normal chromosomal location required for tumorigenic translocations? Or, are the sequences within the constant region locus sufficient? We utilized an IgH transgene in five genomic locations and determined that all five different chromosomal locations are permissive for translocations with Myc that result in plasmacytoma.

Materials and Methods

Induction of Plasmacytomas

Transgenic mice were produced by injection of fertilized eggs with the 230-kb NotI insert isolated from the parent BAC [162]. Mice from IgH transgenic lines 995, 820, 336, and 234 were crossed to coexpress a Bcl-xL transgene. For lines 820, 336, and 234, additional rounds of breeding were completed, selecting for mice with the IgH transgene, knock-in of the B1-8 V_H region [163], and the Bcl-xL transgene [164], with a background of mixed C57BL/6, 129, and BALB/c. Mice from lines 820, 336, and 234 were maintained in a conventional facility. Mice from line 995 were maintained in a facility free of specific pathogens. Mice were injected with 0.5 mL of pristane intraperitoneally at 2 and 6 months of age. Tumor development was evaluated by visual inspection of the mice, sampling of ascites fluid, and determination of ascitic cell morphology. The tumors evaluated in this study arose 2–8 months after the first injection of pristane. Transgenic mice from IgH transgenic line 556 were crossed to BALB/cAn mice to

generate N3 mice carrying the IgH transgene. The tumor evaluated in this study (mouse no. 1854) arose 13 months after the first injection of pristane.

All tumors used in this study grew as ascites. Tissue sections, stained with hematoxylin and eosin, were evaluated for line 820 plasmacytoma and found to be typical. Tumors were also characterized for cell morphology on cytospin slides, CD138 expression by flow cytometry, and secretion of a single Ig isotype by sandwich ELISA.

Cell lines were established from primary tumor ascytic cells or first-generation transplants into pristane-primed SCID mice by culturing for 30–60 d in 6- or 24-well plates in complete RPMI medium 1640 supplemented with 10% (vol/vol) FCS and 10 ng/mL IL-6.

Two-color FISH and SKY analysis.

For preparation of cells in metaphase, ascites cells (with red blood cells lysed) were cultured at 10^6 per mL in RPMI medium 1640 supplemented with 10% FCS, 2 mM glutamine, penicillin, streptomycin, 20 μM 2-mercaptoethanol, and 10 ng/mL IL-6 for 20 h. Colcemid (0.2 μg/mL) was added, and 4 h later, nuclei were fixed in 3 parts methanol and 1 part acetic acid.

For two-color FISH, BACs were labeled by using Digoxigenin (Dig) or Biotin nick translation kits (Roche). Detection was done with anti-Dig FITC-labeled Fab fragments (Roche) or/and Streptavidin-Alexa Fluor 568 (Invitrogen). Slides were counterstained and coverslipped using Vectashield mounting medium with DAPI (Vector Laboratories). Images were acquired by using an Olympus IX81 fluorescent microscope and processed by using Slidebook software v.5.0.25 (Intelligent Imaging Innovations).

SKY was performed by using mouse SKYPaint probe kit from Applied Spectral Imaging according to the manufacturer's instructions (optional steps of pepsin digestion and blocking

were omitted). SKY image acquisition was performed by using the SpectraCube SD200 (Applied Spectral Imaging) connected to an epifluorescence microscope (DMXRA; Leica).

Molecular Cloning of Translocation Sites

Splenocytes from transgenic mice, depleted of red cells and T cells, were cultured at 1.5×10^6 per mL in medium described for the preparation of cells in metaphase, with LPS (25 μg/mL) or with 15×10^4 Sf21 cells per mL expressing CD40L[165], with IL-4 (35 ng/mL) or IFN-γ (100U/mL). After 22 h, the cultures were washed and infected with an AID-expressing retrovirus [141]. This overexpression of AID allowed us to isolate 10- to 100-fold more translocations. DNA was prepared from these cultures 48 h after retroviral infection. IgH:Myc translocations were amplified by nested PCR, using the primers listed in Table 4.4[166, 167], cloned into pGEM T Easy, and sequenced. The sequence of the IgH portion of the cloned translocation was compared with the strain 129 (transgenic) and C57BL/6 (endogenous) sequences. Both the 5′ to 5′ and 3′ to 3′ IgH:Myc translocations in DNA from tumor no. 1854 ascites (line 556) were amplified by using the primers described for preneoplastic translocations in tissue culture. The 3′ to 3′ IgH:Myc translocation in DNA from tumor no. 4816 ascites (line 995) was isolated after digestion with TaqI and ligation to form circles. Primers from the first intron of the Myc gene were used to amplify the unknown sequences (which turned out to be Sμ) around the ligated circle. The sequence of the tumor no. 4816 translocation site was confirmed by using direct PCR with different primers. The 3′ to 5′ IgH:Pvt1 translocation in DNA from tumor no. 74219 ascites (line 820) was isolated after digestion with TaqI and ligation to form circles. Primers from the 3′ end of Sα were used to amplify the unknown sequences (in the Pvt1 fourth intron) around the ligated circle. The sequence of the tumor no. 74219 translocation site was confirmed by using direct PCR with primers in the Pvt1 locus and in Sα (Table 4.4). The

translocation site in tumor no. 74163 was determined by sequencing of a product of direct PCR with primers in the Pvt1 locus and in Sα (Table 4.4). The translocation sites from both derivative Chr in tumor no. 79130 were determined by sequencing of a product of direct PCR with primers in the Myc locus and in Cγ2b (Table 4.4).

Results

An *IgH* transgene is able to undergo translocations with *Myc* at multiple chromosomal locations

To determine whether the chromosomal environment impacts the development of Myc:IgH translocations, these events were analyzed in transgenic mouse models expressing IgH from five different chromosomes as a collaborative effort between the labs of Wes Dunnick, Rafael Casellas, and myself in David Ferguson's lab. The transgene consists of a 230 kb bacterial artificial chromosome (BAC) carrying a pre-rearranged V(D)J exon and the entire heavy chain constant domain, including the 28 kb 3' regulatory region [134] and an additional 15 kb (Fig. 4.1A) [168]. This heavy chain transgene undergoes normal class switch recombination that is qualitatively and quantitatively comparable to that of the endogenous locus, regardless of the chromosomal insertion site [168]. To determine whether this construct can also participate in Myc translocations, transgenic B cells were induced *ex vivo* to undergo class switching by Dr. Wes Dunnick. To examine a reasonable number of translocation events, Dr. Wes Dunnick and his research assistant John Collins increased their frequency in transgenic B cells by overexpressing AID from a retrovirus. Three days after activation, Myc:IgH translocations were cloned by using a PCR-based approach [166, 167] and characterized by DNA sequencing. Three

independent transgenic lines were studied. Line 995 contains three complete copies of the transgene on chromosome 4. The variable region-encoding exon of at least one transgene copy in line 995 is proximal to the centromere and inverted compared to the endogenous locus (Fig. 4.1B). Line 820 contains a single copy of the IgH transgene inserted into chromosome 7 and inverted with respect to the endogenous locus. Line 556 contains two complete and two partial copies of the transgene inserted near the telomere of chromosome 17 in the same orientation as the endogenous IgH. The IgH transgenes were found by John Collins and Dr. Dunnick to be frequent partners for Myc translocations in tissue culture; 79% of translocations were to the transgene (Fig. 4.1B). The translocations to the transgene were indistinguishable from translocations to the endogenous locus, in that they were distributed over a 2 kb region including the 5'-most Myc exon and intron, and the translocations were widely distributed in S regions (Table II). The interpretation of these experiments includes the assumption that the ratio of translocations involving the transgene to translocations involving the endogenous genes will not be changed significantly by AID overexpression. Even considering this assumption, these results established that the IgH transgene, in three different chromosomal locations, can undergo recombination with the Myc proto- oncogene. Recombination of Myc with the transgene is at least as efficient as recombination with the endogenous IgH gene.

Myc:IgH translocations to the transgene are found in plasmacytoma

To determine whether these translocations involving the IgH transgene could promote tumor development, mice from each of the three transgenic lines, and two additional transgenic lines designated line 336 (two copies integrated near the centromere of Chr 14) and 234 (two copies integrated near the telomere of Chr1), were injected with pristane, in order to induce plasmacytomas, in the laboratories of Dr. Dunnick at University of Michigan and Dr. Rafael

Casellas at the NIH. Many of the mice developed abundant ascites containing cells with the characteristic cytology of malignant plasma cells. Primary tumor cells, tumor cells adapted to tissue culture, or tumor cells transferred to SCID or *nude* mice were characterized for chromosomal translocations by two-color fluorescent *in-situ* hybridization (FISH) and spectral karyotyping (SKY) by Alexander Kovalchuk at the NIH and myself [169]. For FISH, metaphase or interphase chromosome spreads were hybridized with a BAC probe spanning the Myc gene on Chr 15. The same chromosome spreads were also hybridized with a second BAC (labeled with a different fluorochrome) that spans the insertion site of the transgene for the given line (Fig. 4.2A). This second probe lacks any IgH sequence; it has only sequences from chromosomes 1, 4, 7, 14, or 17. Translocation between the IgH transgene and Myc would be detected as a co-localization of the two BAC probes. Representative two-color FISH data are shown in Fig. 4.2B-D. For example, the tumor from line 995 (Fig. 4.2B,i) contains multiple chromosomes with co-localization of the Myc and IgH transgene probes. SKY analysis confirmed the presence of both derivative (4, 15) and derivative (15,4) chromosomes within this tumor (Fig. 4.2B,ii). Notably, chromosome 12 carrying the endogenous IgH was not rearranged. Seven tumors with translocations between Myc and the IgH transgene in line 820 had no rearrangements involving Chr 12 (Table 4.1). In a single tumor with a T(7;15) translocation, Chr 12 was involved in another translocation (Table 4.1). More than 50% of the plasmacytomas demonstrated co-localization of the Myc probe and the IgH transgene probe and, therefore, contained translocations between Myc and the IgH transgene (Table 4.1 and Figures 4.5-4.7). As expected, the plasmacytomas that lacked a translocation between Myc and the IgH transgene had translocations involving the endogenous IgH locus and Myc (Table 4.1). Of the five chromosomal locations we tested, all were permissive for translocations to Myc. Apparently, the

chromosomal location for line 234 (telomeric on Chr 1) is relatively inefficient for translocations to Myc that lead to plasmacytoma.

A concern of the transgenic approach is that unusual transcription rates or chromosomal structure of the IgH transgenes may create a nonphysiologic target for Myc translocations. It is possible that multiple copies of large IgH transgenes, with their strong regulatory elements, result in nonphysiologic chromatin structures. Such a criticism is difficult to rule out in the absence of any experimental data for or against this possibility. To equalize the IgH transgenic and endogenous loci to the extent possible, an assembled V_H region segment was "knocked-in" with its physiologic promoter, into one of the endogenous loci in the single- copy line 820 by Dr. Casellas and Dr. Dunnick. In line 820, where the transcriptional activity of the transgene and the endogenous genes should be similar, the frequency of translocation to the transgene and endogenous IgH genes was virtually identical (Table 4.1). Analogous results were obtained with the two-copy line 336 (Table 4.I).

Either orientation of the IgH transgene is able to undergo translocations

In approximately 85% of mouse plasmacytomas and human Burkitt lymphomas, the IgH locus is translocated 5' of Myc coding exons [2, 153-155]. Conversely, the remaining 15% of plasmacytomas juxtapose the light chain (Igκ or Igλ) sequences 3' of Myc, to a region known as plasmacytoma variant translocation locus or Pvt1 [153, 170, 171]. This bias is best explained by the orientation of heavy and light chain loci relative to their respective centromeres. Light chain gene rearrangements 5' of Myc are thought to be precluded because they would generate dicentric chromosomes that are incompatible with cell viability. Because the orientation of the transgene in line 820 is the same as Igκ or Igλ (Fig. 4.1B), we speculated that translocations

involving the IgH transgene in this line would deregulate Myc primarily through Pvt1 rearrangements. Indeed, two- color FISH analysis done by Alexander Kovalchuk showed colocalization of Pvt1 and the IgH transgene in tumors from this line (Fig. 4.2C, iii). Furthermore, two- color FISH revealed that Myc and part of the Pvt1 probe are rearranged to separate chromosomes, as would be expected if the Pvt1 locus was used in the translocation (Fig. 4.2C, iv). SKY confirmed the presence of a T(7;15) translocation (Fig. 4.2C, ii and Fig. 4.7).

Translocations of Myc to the transgene and to endogenous IgH are similar at the molecular level

To characterize the translocations at the molecular level, the translocation site from at least one tumor from each of four transgenic lines was cloned and sequenced by Dr. Wes Dunnick and John Collins (Fig. 4.3). The translocation event from a line 995 tumor was typical of Myc:IgH translocations, joining exons 2 and 3 of Myc to the 3' end of IgH, in the opposite transcriptional orientation (Fig. 4.3B and Table 4.3). The recombination event occurred in the first intron of Myc and in the Sμ region of the IgH transgene. Recombination sites in two tumors from line 336 were also typical Myc:IgH translocations. Recombination in the first intron of Myc and in IgH Sγ2 joined exons 2 and 3 of Myc to the 3' end of the IgH locus (Table 4.3). Both products of the reciprocal translocation from a tumor from line 556 were cloned and sequenced. Both recombination products from the tumor were similar to Myc:IgH translocations involving the endogenous IgH in terms of translocation sites in Myc, Sμ, and Sα, and in terms of orientation (Fig. 4.3B). Molecular cloning of the translocation site in a tumor from line 820 was consistent with the results of FISH and SKY analysis—sequences in the fourth intron of the Pvt1 gene were joined to the Sα of the transgene in a 3' to 5' orientation (Fig. 4.3B and Table 4.3). Molecular cloning revealed that the translocation sites in a second line 820 tumor and in a line

336 tumor were also in the fourth intron/fifth exon of Pvt1 (Table 4.3). The fourth intron/fifth exon/fifth intron of the Pvt1 gene may be unusually susceptible to DNA double-stranded breaks in B cells, as it is a site of RNA polymerase initiation or pausing and of AID binding [172]. Most Pvt1:kappa light chain translocations are located in this part of the Pvt1 gene (Fig. 4.3C) [173]. Frequent translocation to the IgH transgene in line 820 suggests that the orientation of the IgH locus is more or less irrelevant for oncogenic rearrangements. Apparently, the cell population examines all possible translocations [143, 174], and those translocations that allow cell viability and neoplastic transformation are selected.

Discussion

We sought to determine whether the recurrent IgH:Myc translocations in human Burkitt lymphoma and in murine plasmacytoma depend on the particular chromosomal location of IgH and its orientation relative to the centromere. To determine the role of chromosomal location, we used a 230- kb IgH transgene inserted into five different chromosomal locations and in both orientations relative to the centromere. Each of the five IgH transgenes is capable of class switch recombination at near physiologic levels [162, 168], a likely prerequisite for translocation [2, 151, 154, 155]. We found that the Myc proto- oncogene can translocate to a 230- kb IgH locus inserted into any of five different chromosomal locations (Figure 4.2, Table 4.1). Not only was the transgene able to undergo translocations with Myc, but the frequency of translocation to the transgenic IgH was at least equal to the frequency of translocation to the endogenous IgH. At the molecular level, Myc translocations to the IgH transgene are similar, if not identical, to translocations to the endogenous IgH (Figure 4.3, Table 4.2, Table 4.3).

Lymphoid cells expressing the RAG endonuclease or AID can suffer any of one of thousands of different translocations that are spread throughout the genome [143, 174-176]. Presumably it is selection for the IgH:Myc translocation, and its resulting deregulated Myc expression, that leads to the recurrence of this translocation in human lymphoma and murine plasmacytoma. However, IgH:Myc translocations are overrepresented in the primary pool of translocations [143, 174, 175, 177]. Several factors have been hypothesized to increase the frequency of IgH:Myc translocation, including gene proximity due to chromosome territories[178, 179], gene proximity perhaps due to shared transcription factors [180, 181], high frequency of DNA breaks after AID activity [175], gene proximity after DNA breaks perhaps due to sharing of repair machinery [178], and failure to repair after DNA breaks [89, 161]. Chromosome environment is likely to play a role in some or all of these factors. The IgH transgene therefore represents a valuable model for future studies on the effect of different chromosome environments on translocation and each of the potential factors mentioned above.

The 230- kb transgene is sufficient not only for the recombination event with Myc, but it also includes all of the regulatory elements necessary for oncogenic deregulation of Myc (Table 4.1). Because the IgH 3' regulatory region is required for the genesis of plasmacytomas [81, 182-184], it is likely that the 3' regulatory region in the IgH transgene both enhances Myc recombination to the transgene and deregulates Myc expression, resulting in tumor development. Thus, putative regulatory elements outside of the 230- kb constant region gene play only a minor role for oncogenic translocation and for Myc deregulation.

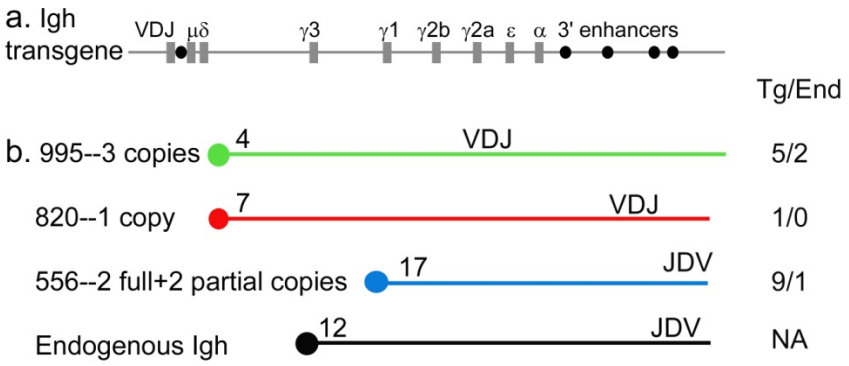

Figure 4.1: Myc:IgH translocations. (**A**) Structure of the 230-kb IgH transgene. Coding exons are depicted as grey rectangles and regulatory elements are depicted as black circles. The transgene is drawn approximately to scale. (**B**) The three main transgenic lines used in this study are shown, with copy number and a schematic of chromosome location, with transgene orientation relative to the centromere depicted by the orientation of the VDJ exon. For comparison, the location of the endogenous IgH locus on Chr 12 is shown. To the right of each chromosome schematic is shown an enumeration of Myc:IgH translocation sites cloned from in vitro cultures. Translocation to the transgene or to the endogenous genes (number of sequences of each type shown, separated by a slash) was determined by evaluation of three to 52 polymorphisms in the various S regions.

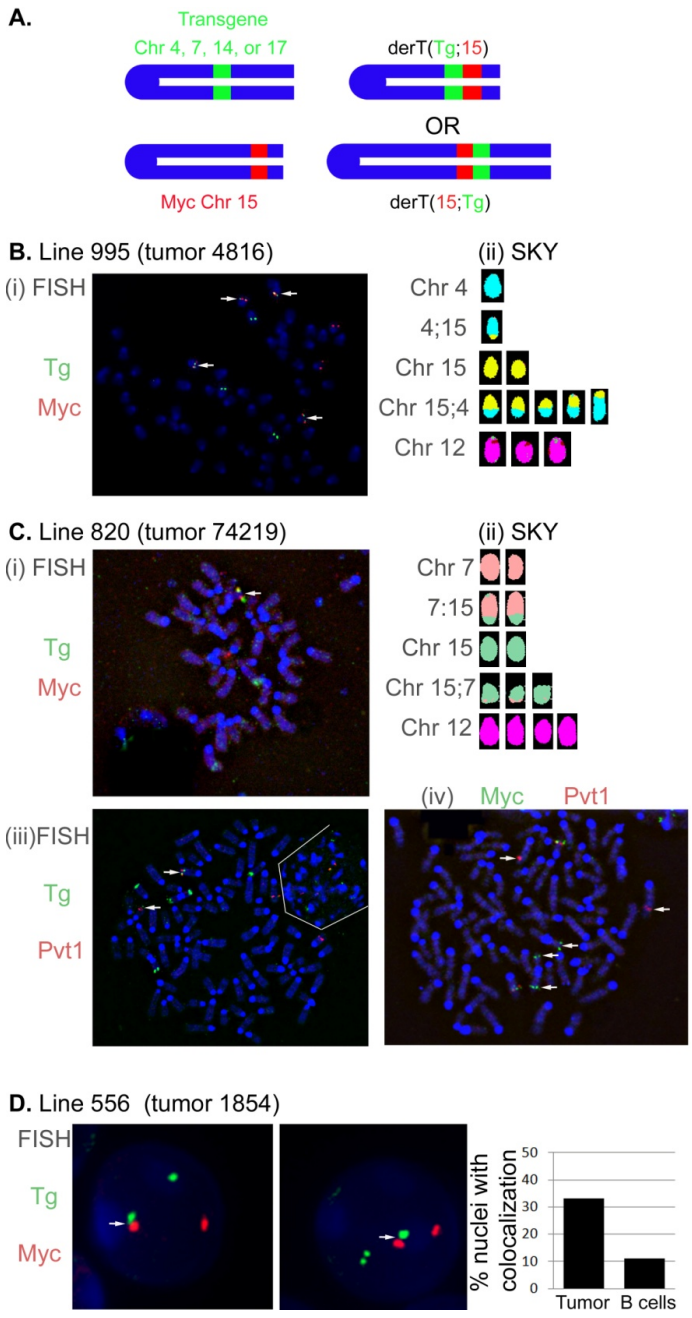

Figure 4.2: Plasmacytomas harbor translocations to the IgH transgene. (**A**) Co-localization of the IgH transgene with Myc or Pvt1. Co-localization of BACs spanning the IgH transgene insertion site on Chr 4 (line 995), 7 (line 820), 14 (line 336), or 17 (line 556) and either Myc or Pvt1 reveal translocations involving the two loci. White arrows note separation of probes (Part C, iv) or colocalization (all other Parts). Asterisks denote chromosomes of interest not involved in translocations. (**B**) Two-color FISH (i) and SKY (ii) on metaphase spreads from tumor #4816, line 995. The color coding for Chr 15 for the SKY analysis of these metaphases was changed to yellow, to better contrast with the aqua color coding for Chr 4. (**C**) Two-color FISH and SKY analysis of tumor #74219, line 820. (i) The IgH transgene is shown to co-localize with Myc. (iii) The IgH transgene is shown to co-localize with Pvt1. The white lines delineate a second, interphase cell that lies next to the metaphase. (iv) The Myc and Pvt1 probes are rearranged onto different chromosomes. (**D**) Interphase two-color FISH analysis of tumor #1854, Line 556 (two representative cells shown). Myc and the IgH transgene were co-localized in 33% of the interphases from #1854 ascites, but in 11% of the interphases from normal B cell controls ($p<0.001$, Fisher's exact test).

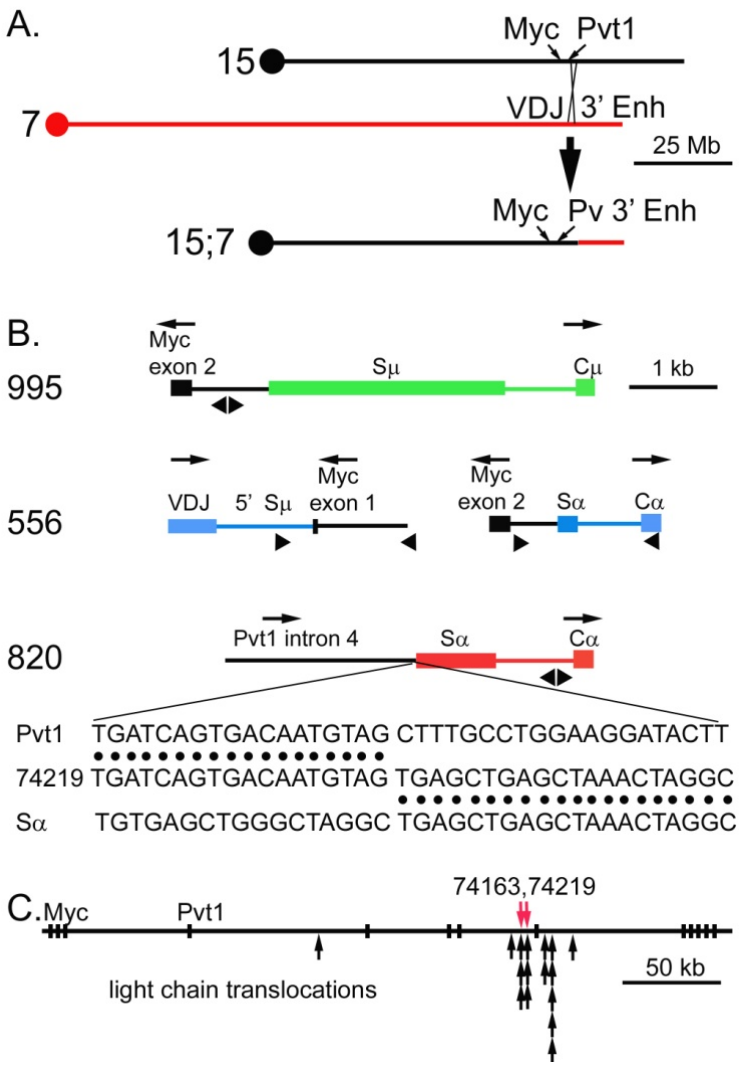

Figure 4.3: Molecular characteristics of translocations between the IgH transgene and Myc. (**A)** Schematic diagrams of murine Chr 15 with the approximate location of the Myc and Pvt1 genes, murine Chr 7 with the heavy chain transgene, and the resulting derivative Chr 15 after translocation. (**B)** Molecular clones of translocations to the transgenic heavy chain genes. These molecular clones are from primary tumor #4816 (line 995), from primary tumor #1854 (line 556, both der(15) and der(17) translocation products), and from primary tumor #74219 (line 820). Transgenic heavy chain sequences at the translocation site are color coded according to the chromosome on which the transgene resides. Myc- or Pvt1-associated sequences (Chr 15) are shown in black. The direction of transcription of each gene is shown above each schematic. Triangles below each schematic approximate the location of PCR primers used to clone these translocation sites. The sequence data corresponding to the structure shown in the line 820 schematic is presented below the schematic. Sequence data for other translocation sites in tumors is shown in Table 4.3. (C) Structure of the Myc and Pvt1 loci on Chr 15. Exons are depicted as black rectangles. The Myc gene is encoded by the three exons on the left of the map; the Pvt1 transcripts are encoded by the next exon designated "Pvt1" and the remaining nine exons (and other exons not shown). The translocation sites in tumors 74163 and 74219, located in the fourth intron of Pvt1, are shown as red arrows. Translocation sites to light chain genes in plasmacytomas[173] are shown below as black arrows.

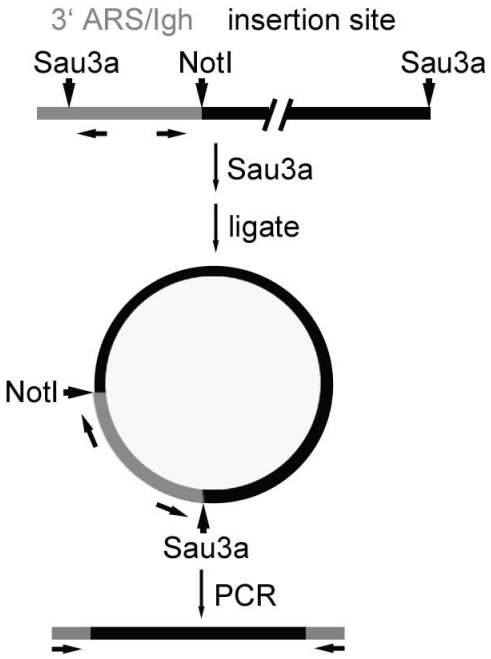

Figure 4.4: Cloning and sequencing of transgenic insertions sites. Transgenic ARS/IgH sequences are shown in grey; mouse genomic sequences at the transgenic insertion site are shown in black. PCR primers are shown as arrows. The location of the *Sau*3a site in the mouse genomic sequence is unknown.

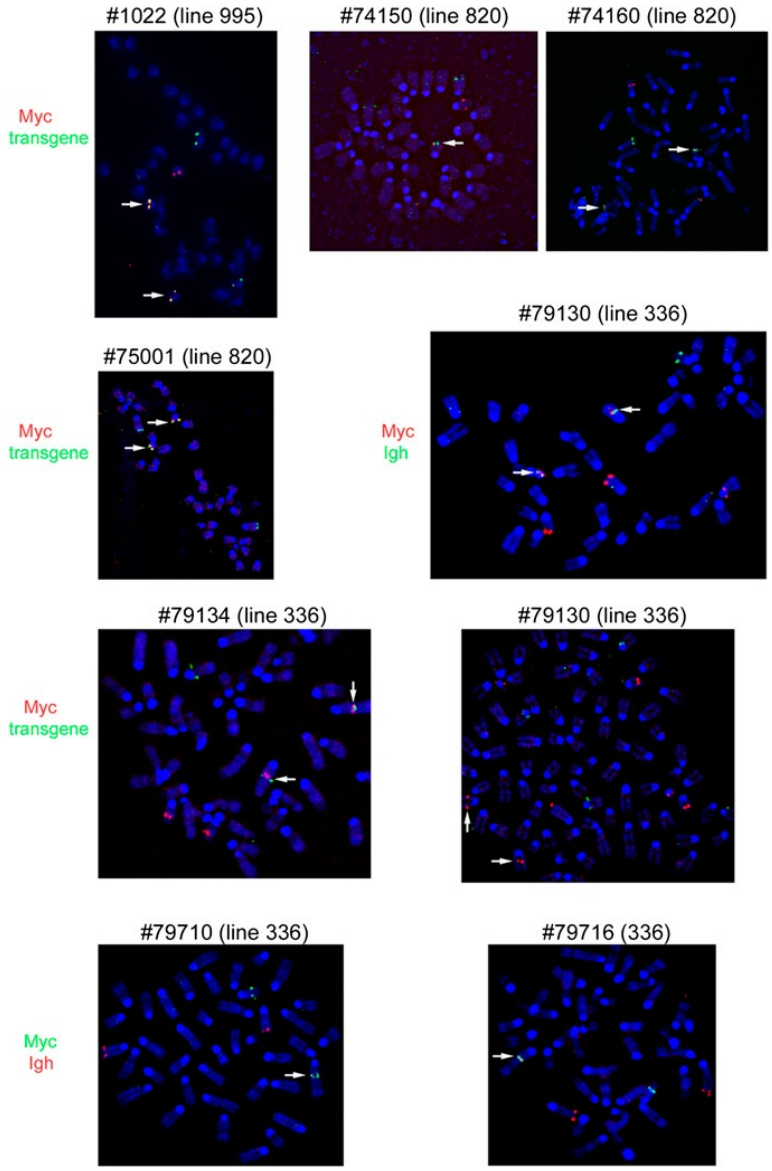

Figure 4.5: Two-color FISH analysis of translocations between IgH transgenes and Myc from transgenic lines 995, 820, and 336. Derivative chromosomes are noted by a white arrow. Chromosomal analysis of line 336 tumors: The transgene in line 336 integrated near the centromere of Chr 14. I used BAC RP24-329N9 from Chr 14 as a surrogate for the transgene insertion site as it colocalizes with IgH sequences in metaphases from line 336 spleen cells. However, we have not mapped the location of the transgene insertion relative to this BAC probe. Three tumors from line 336 (nos. 79134, 79710, and 79716) have a derT(15;14) on which RP24-329N9 colocalizes with Myc. SKY analyses (Fig. 4.8) are consistent with a T(14;15) translocation, with the breakpoint near the centromere of Chr 14. Tumor no. 74130 has a short derivative Chr with colocalized Myc and IgH hybridization near the centromere, consistent with a T(14;15) translocation. However, the RP24-329N9 probe does not colocalize with Myc on this derivative Chr. SKY analysis is inconclusive concerning a 14;15 derivative Chr but reveals a 1;4 balanced translocation and a 15;18 derivative Chr. SKY revealed no evidence for translocations involving Chr 12 (Fig. 4.8). Hence, our tentative conclusion is that there is a translocation involving Myc and the IgH transgene in tumor no. 79130, which may have been followed by translocations involving other Chr.

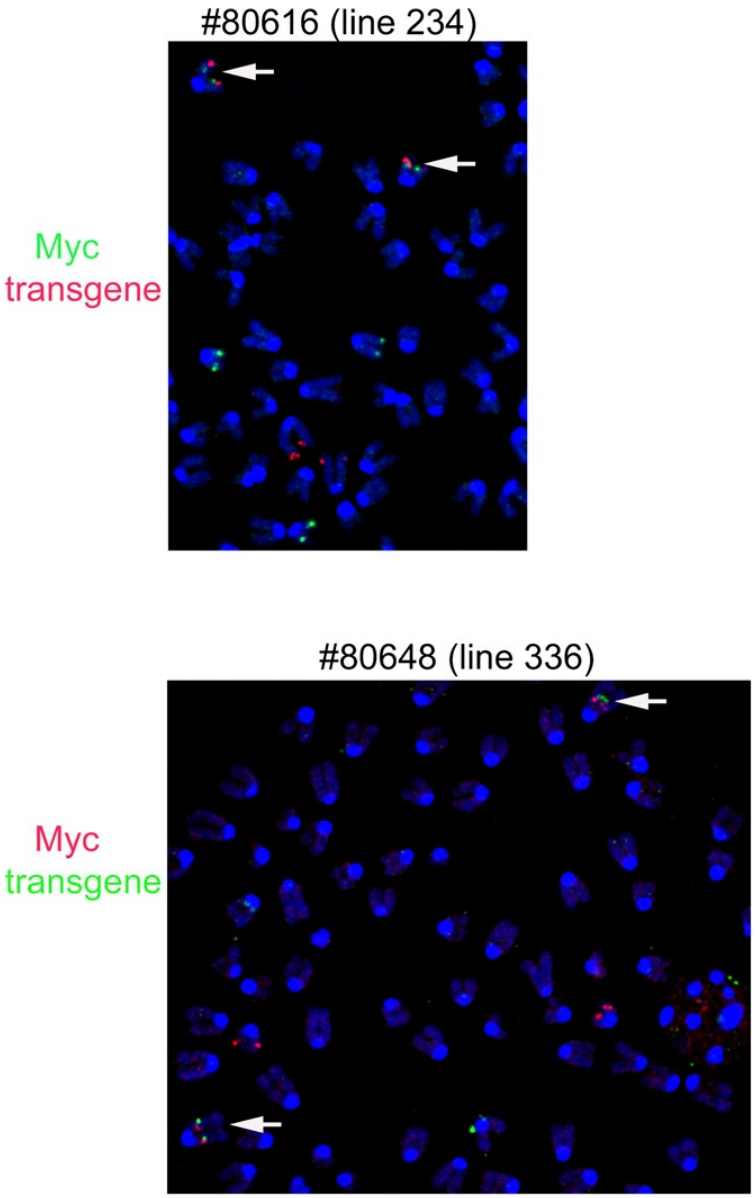

Figure 4.6: Two-color FISH analysis of translocations between IgH transgenes and Myc from transgenic lines 336 and 234. Derivative chromosomes are noted by a white arrow.

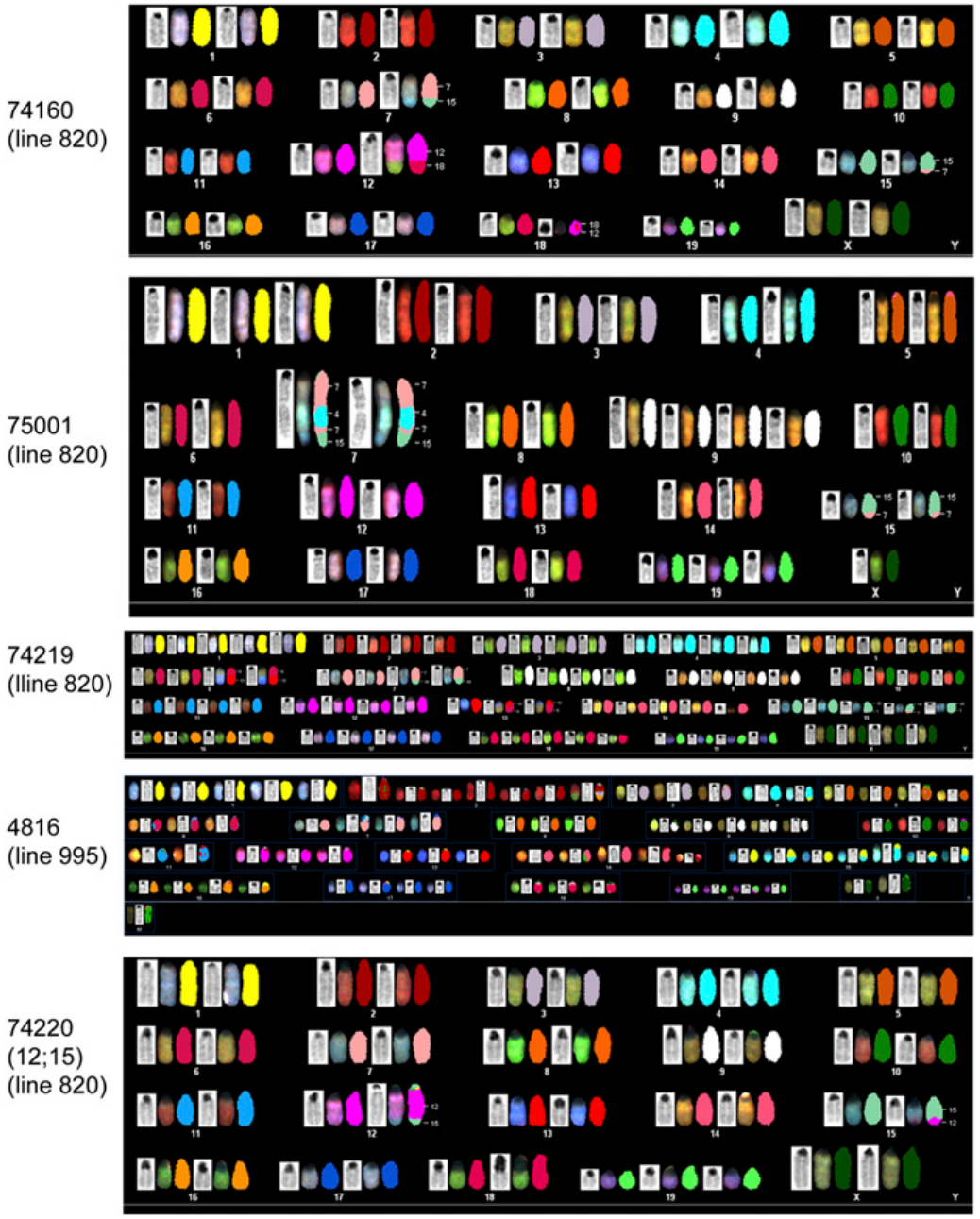

Figure 4.7: SKY analysis of translocations between IgH transgenes and Myc from transgenic lines 820 and 995. SKY analysis of tumor no. 74220 is also shown as an example of a translocation between Myc and the endogenous IgH locus.

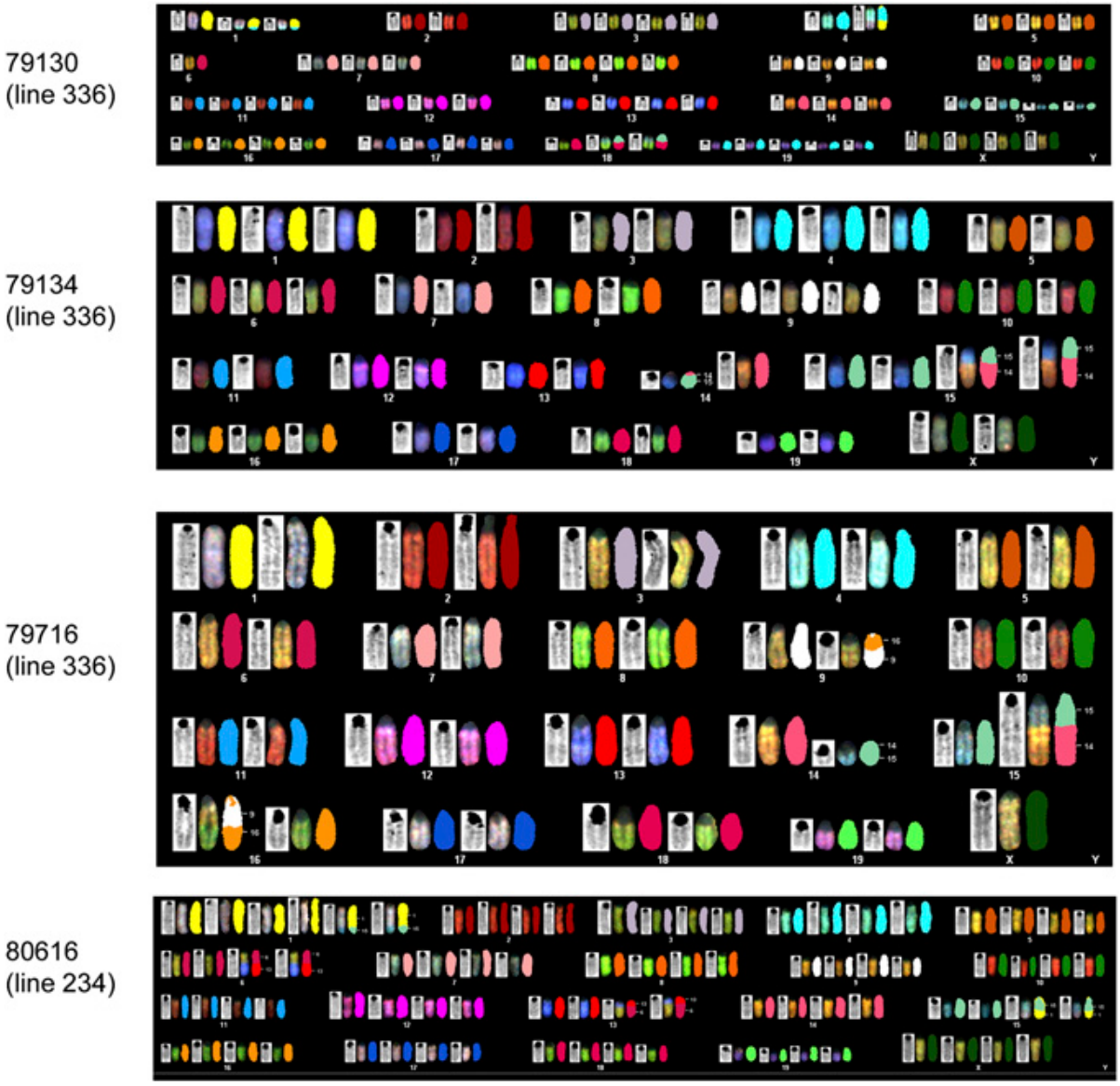

Figure 4.8: SKY analysis of translocations between IgH transgenes and Myc from transgenic lines 336 and 234.

Transgenic line	Primary tumor	Genetic background	Translocations	Other
995 Chr 4 at 98.3 of 154.3 Mb	4816	C57BL/6, Bcl-xL	4;15	*Myc*-Sμ (cloning), secretes IgA
VDJ centromere proximal	1022	C57BL/6, Bcl-xL	4;15	
820 Chr 7 at 122 of 145 Mb	74149	Mixed, Bcl-xL*	7;15	
VDJ centromere proximal	74150	Mixed, Bcl-xL	7;15	
	74160	Mixed, Bcl-xL	7;15 and 12;18	Secretes IgA
	74162	Mixed, Bcl-xL	12;15	
	74163	Mixed, Bcl-xL	7;15	Secretes IgA, *Pvt1*-Sα (cloning)
	74219	Mixed, Bcl-xL	7;15 and 6;13	
	74220	Mixed, Bcl-xL	12;15	
	74223	Mixed, Bcl-xL	7;15	
	74997	Mixed, Bcl-xL	12;15	
	75000	Mixed, Bcl-xL	12;15	
	75001	Mixed, Bcl-xL	7;15	Chr 4 insertion into 7;15
	75002†	Mixed, Bcl-xL	7;15	Secretes IgA and IgG2a
	75002†	Mixed, Bcl-xL	12;15	
	75004	Mixed, Bcl-xL	12;15	
336 Chr 14 near centromere	78286	Mixed, Bcl-xL*	14:15	
orientation unknown	79130	Mixed, Bcl-xL	14?;15‡, 15;18, and 1;4	*Myc*-Sγ2a (cloning)
	79134	Mixed, Bcl-xL	14;15	
	79710	Mixed, Bcl-xL	14;15	
	79711	Mixed, Bcl-xL	14;15	
	79716	Mixed, Bcl-xL	14;15 and 9;16	
	80635	Mixed, Bcl-xL	14;15	
	80639	Mixed, Bcl-xL	12;15	
	80648	Mixed, Bcl-xL	14;15	
	82028	Mixed, Bcl-xL	12;15	
	82043	Mixed, Bcl-xL	14;15	
	82048	Mixed, Bcl-xL	12;15	
	82181	Mixed, Bcl-xL	14;15	
	83353	Mixed, Bcl-xL	12;15	
556 Chr 17 at 89.6 of 95.2 Mb	1854	BALB/cAn	15;17	Interphase, *Myc*-Sα (cloning)
VDJ centromere distal	2731	C57BL/6, Bcl-xL	not 15;17	Interphase
234 Chr 1 near telomere	78709	Mixed, bclxL*	12;15	
	79145	Mixed, bclxL	12;15	
	80616	Mixed, Bcl-xL	1;15 and 6;13	
	80621	Mixed, Bcl-xL	12;15	
	83366	Mixed, Bcl-xL	12;15	

Table 4.1: Myc:IgH translocations
*In addition, lines 820, 336, and 234 had a B1-8 VH recombined into one of the endogenous IgH loci [164].
†The ascites in mouse no. 75002 included two tumor clones.
‡The ambiguity concerning the translocation in tumor no. 79130 is detailed in the data and legend of Figure 4.5.

Clone Designation	Sequence	Tg/End	Polymorphic residues
	16,555 – 578* 1,419,586 – 562* (Sμ)		
der15.3.1†	TCCTGTGCTTTTGACACCTTTCTCA|CTCAGCCCAGCTCAGCTCACTCCAG	Tg†	(6/6)
	16,842 – 818 1,421,882 – 858 (Sμ)		
18.10	AATCCCTTCTCCAAAGACCTCAGGA|GCTGAGCTGAGCTGGGGTGAGCTGA	Tg	(11/12)
	16,504 – 479 1,421,792 – 814 (Sμ)		
11.9	ACACAGGGAAAGACCACCAGATCTG|G|TGAGCTGAGCTGTGCTGGAGTGA	Tg	(13/13)
	15,085 – 061 (Sμ, 21 bp inversion§,then 1,421,832)		
12.1	GTGGTGTGGAGGCGGCTCTTTCCCC|CAGCTCATCCCAGCTTACCCCAGCT	Tg	(9/9)
	16,694 – 670 1,421,922-946 (Sμ)		
10.1	CCTCCCGGTTTGACCCCTCAAAGGA|GGTGAGCTGAGCTGAGCTGGGGTGAG	Tg	(4/4)
	16,798 – 822 1,416,707 – 682 (Sμ)		
2.3	TCGCTTCGTGGTGGCCAAAGAAAGC|CCTAGGAACCACTTAAGAGTAAAAGC	End	(5/5)
8.1	ca. 15,133¶ ca. 1,416,040	End	(9/9)
23-89-ml	ca. 16,471¶ ca. 1,557,000 (Sγ2a)	Tg	(18/18)
	16,885 – 861 1,422,474 – 498 (Sμ)		
10.2	AGTCAGAAACTACGGAGCCTTCTCG|GGCCTGGTTGAGATGGTTCGAGATG	Tg	(3/3)
	16,915 – 891 1,421,516 – 540 (Sμ)		
15.5	GAAATTTAAATGCCCTCTCAGAGAC|CTGAGCTGAGCTGGGTGAGCTGAGC	Tg	(31/31)
	16,905 – 881 1,419,010 – 034 (Sμ)		
36.2	TGCCCTCTCAGAGACTGGTAAGTCA|TGGACTGTTCTGAGCTGAGATGAGC	Tg	(>31/31)
	16,796 – 772 1,419,079 – 055 (Sμ,152 bp inversion§)		
37.3	ACCACGAAGCGACCTCCCGGTTTGA|GCTCACCCCAGCTCAGCTCACCCCA	Tg	(3/3)
	16,913 – 889 1,422,115 – 139 (Sμ)		
4.1	AATTTAAATGCCCTCTCAGAGACTG|AACTGAGCTGTGTGAGCTGAGCTGG	End	(4/4)
	15,085 – 061 1,419,559 – 535 (Sμ, 36 bp inversion§)		
12.4	GTGGTGTGGAGGCGGCTCTTTCCCC|CAGCTCAGCTCACCCCAGCTCATCC	Tg	(51/52)
	17,095 – 071 1,421,631 – 655 (Sμ)		
6.3	AGCCCAACATCAAGTCCTAGTGCCG|TGAGCTGGGCTGAGCTGGGCTGAGC	Tg	(16/19)
	16,896 – 872 1,421,898 – 922 (Sμ)		
2.9	AGAGACTGGTAAGTCAGAGTCTACG|CTGGGGTGAGCTGAGCTGAGCTGGG	Tg	(7/7)
	16,208 – 184 1,421,908 – 932 (Sμ)		
21.10	GGCGGCAGGCTCGGAGGCAAAGCCC|CTGAGCTGAGCTGGGGTGAGCTGAG	Tg	(8/8)

Table 4.2: Sequences of preneoplastic Myc:IgH translocations from tissue culture.

* AC153008.4 is the Genbank accession number for the 25 bp of the Myc part of the translocation (left) and AJ851868.3 is the GenBank accession number for the IgH part (strain 129) of the translocation (right). Residue numbers from these accessions are shown above each sequence. The S region of origin is also shown above the sequence of the IgH part. For comparison to the endogenous IgH (C57BL/6) sequence, accession NT_166318.1 was used. A vertical line in each sequence notes the translocation site. Nucleotides between vertical lines represent insertions. Nucleotides that are underlined are shared between the IgH and Myc or Pvt1 sequences.

†der 15.3.1, 18.10, etc. are the laboratory designations of the cloned translocation sequence. The first seven sequences are from transgenic line 995 B cells, "23-89-ml" is from transgenic line 820 B cells, and the last nine sequences are from transgenic line 556 B cells. The full sequences are available in GenBank, accessions JX080033-JX080049.

‡The transgenic (Tg) or endogenous (End) origin of the IgH sequence was determined by the examination of all potential polymorphic residues in the sequence. In the right-most column the number of residues that matched the "Tg" or "End" designation/number of polymorphic residues examined is shown in parentheses.

§In these translocation site sequences, there was a 21, 36, or 152 bp inversion of Sμ sequences at the exact translocation site, followed by Sμ in the orientation dictated by the PCR primers.

¶We did not determine the exact translocation site location by accurate sequences, as the translocation site was far removed from the sequencing primer. However, the residues shown are within 100 bp of the actual translocation site, and the Sμ sequences near the sequencing primer allowed unambiguous designation of transgenic or endogenous sequences.

Tumor	Sequence*	Tg/End	Polymorphic residues
	16,905 – 881 1,419,010 – 034 (Sμ)		
4816	TGCCCTCTCAGAGACTGGTAAGTCA|TGGACTGTTCTGAGCTGAGATGAGC	Tg	(24/24†)
	23,286,370 – 394‡ 1,586,911 – 935 (Sα)		
74219	TGACGGTTGATCAGTGACAATGTAG|TGAGCTGAGCTAAACTAGGCTGAAA	Tg§	
	23,288,305 – 329‡ 1,418,724 – 700 (Sμ¶)		
74163	TTCTGAAAACAGGAATATGTGCAAG|CAAGCTTTATGAGTCTGGCCTTCTC	Tg§	
	15,709 – 684 1,537,648 – 672 (Sγ2b)		
79130	TACTCCGGCTCCGGGGTGTAAACAG|AGCACTGGGCCTTTCCAGAACTAAT	Tg§	
	15,283 – 314 1,555,377 – 357 (Sγ2a)		
79130	TACGTGGCAGTGAGTTGCTGAGTAA|CCCAGATTCCCCATAGCTGCTCTGC	Tg§	
	23,295,296 – 6,018‡ 1,509,641 – 618 (Sγ1)		
79134	CTTTCTTCCAGGCTAATTCATATTT|G|TTATCACAGGGCTCAGCTGCCTT	Tg§	
	16,786 – 762 1,587,313 – 337 (Sα)		
1854	GACCTCCCGGTTTGACCCCTCAAAG|CTGAGCTGGGCCTAAGATGGACTTG	Tg§	
	16,340 – 364 1,416,532 – 508 (Sμ)		
1854	CCCAGGCTCCGGGGAGGGAATTTTT|CTCCTTCCAACAAATGAAGTTTTAA	Tg§	

Table 4.3: Sequences of Myc:IgH translocations sites from tumors.
*The organization of this Table is identical to Table 4.2. Relevant GenBank accession numbers are listed in the footnotes to Table 4.2. Tumor 4816 was derived from transgenic line 995. Tumors 74219 and 74163 were derived from transgenic line 820. Tumors 79130 and 79134 were derived from transgenic line 336. Tumor 1854 was derived from transgenic line 556. These sequences are available in GenBank, accessions JX080050-JX080057.
†The alignment of the Sμ part of the translocation from the tumor in mouse 4816 required two deletions relative to the germline sequences. The first was at residue 1,419,156 and was 90 bp for the 129 sequence and 105 bp for the C57BL/6 sequence. The second deletion was at residue 1,419,441 and was 2145 bp for the 129 sequence and 145 bp for the C57BL/6 sequence. These putative deletions resulted in the best alignments for both 129 and C57BL/6.
‡Chr 15 sequence (Pvt1) is from accession NT_039621.7. Consistent with the sequence of the translocation site, Pvt1-Cα transcripts[185] were amplified from the RNA of tumor #74219 and #79134. Pvt1-Cα transcripts were also cloned from the RNA of tumor #74163.
§These tumors were derived from mice with an endogenous IgH allele, and therefore the origin of the IgH part of the translocation cannot be determined from sequence polymorphisms. The "Tg" designation is derived from two-color FISH.
¶213 bp of Sμ (the 3' end of the Sμ sequence is joined to 5' end of the *Pvt1* sequence) is followed by 84 bp of Sγ1 sequence (the 3' end of the Sγ1 sequence is joined to the 5' of end of the Sμ sequence). The Sγ1 sequence is followed by Sα sequences (joined to Sγ1 5' to 5'). The orientation of the Sμ and Sγ1 sequences relative to one another and to the Sα sequences suggest that the Sμ and Sγ1 sequences are derived from a switch deletion circle.

Purpose	5'/3'	Sequence	Location	Other
Cloning	5'	AAGCCAAACTACCCTGGTGCC	BAC vector	
Transgene	3'	CATTAATTGCGTTGCGCTCACTGC	BAC vector	
Insertion site				
Cloning	5'	GTGAAAACCGACTGTGGCCCTGGAA	14932-56	first round
Myc:Igh	3'	ACTATGCTATGGACTACTGGGGTCAAG	1416007-33 (Sμ)	first round
head-to-head	5'	GTGGAGGTGTATGGGGTGTAGAC	14961-83	second round
	3'	CCTCAGTCACCGTCTCCTCAGGTA	1416037-60 (Sμ)	second round
	5'	GGGGAGGGGGTGTCAAATAATAAGA	17395-71	tumor #79130 der (14;15)
	3'	GGAGGGAAGATGAAGACGGATGGT	1560298-275 (Sγ2b)	tumor #79130 der (14;15)
Cloning	5'	GGGGAGGGGGTGTCAAATAATAAGA	17395-71	first round
Myc:Igh	3'	TGAGGACCAGAGAGGGATAAAAGAGAA	1423540-14 (Sμ)	first round
tail-to-tail	3'	CGGTTTGTTTGAGAATGTCAGCGG	1558331-308 (Sγ2a)	first round
	3'	CGTGAATCAGGCAGCCGATTATCAC	1588781-57 (Sα)	first round
	5'	GACACCTCCCTTCTACACTCTAAACCG	17370-44	second round
	3'	CACCCTGCTATTTCCTTGTTGCTAC	1423459-35 (Sμ)	second round
	3'	CTCAATCAGACAACTCTCCTGG	1558280-259 (Sγ2a)	second round
	3'	GAGCTGACCAACAGTTCTGGCTGTATAGAC	1588548-19 (Sα)	second round
	5'	AGATCACGACTCACCGCAGTC	17246-226	inverse cloning #4816
	3'	GGTTCCGTAACAGCTGCTACC	17251-271	inverse cloning #4816
	5'	GTGAAAACCGACTGTGGCCCTGGAA	14932-56	tumor #79130 der (15;14)
	3'	CTGTGGGTTGGGAGAAGTGTAGTGT	1537457-481(Sγ2a)	tumor #79130 der (15;14)
Cloning	5'	CATTACATTCTGTCCATCCAATCATC	23285634-56	tumor #74219
Pvt1:Igh	3'	TCTAGGTAAGCTCAGCCTTGTTCAG	1587230-06 (Sα)	tumor #74219
	5'	ATGACTACACCCCCTGAGCAGTC	1588432-411 (Sα)	inverse cloning #74219
	3'	ACAGCCAGAACTGTTGGTCAGC	1588525-46 (Sα)	inverse cloning #74219
	5'	TGGAGATGTGACTTCCTGGATC	23286702-23	tumor #74163
	3'	CGTGAATCAGGCAGCCGATTATCAC	1588781-57 (Sα)	tumor #74163

Table 4.4: PCR primers for cloning transgene insertion sites and Myc:IgH translocation sites. Residues numbers for Myc primers are from accession AC153008.4; residues for Pvt1 primers are from accession NT_039621.7; residues for IgH primers are from accession AJ851868.3

Name	Chromosome	Location
RP24-388I5	1	175,551,438-175,696,869
RP24-398H12	4	98,439,094-98,594,754
RP24-221C18	7	129,437,953-129,597,875
189A22 (Igh)	12	114,400,224-114,510,168
RP24-329N9	14	9,118,407-9,306,395
D15MIT17 (Myc)	15	61,732,863-61,867,227
RP23-96F18 (Pvt1)	15	62,022,418-62,186,675
RP24-172M11	17	90,046,770-90,191,451

Table 4.5: BAC probes used in this study

Chapter 5

Discussion

The goal of the studies executed in this thesis was to identify factors that both contribute to the formation of translocations between an oncogene and the IgH locus and lead to subsequent deregulation of that oncogene. We show that although the MRN complex plays significant roles in CSR, it is unnecessary for the formation of translocations to the IgH locus, and its absence in B cells does not lead to early B cell lymphoma related mortality. Additionally, this work establishes that IgH contains all of the elements necessary for both the translocation to, and the deregulation of, proto-oncogenes.

Roles for MRN in CSR

It is known that translocations to IgH are often caused by mistakes made during B lymphocyte development, in an antigen dependent process known as class switch recombination [151]. CSR forces a cell to induce potentially dangerous lesions, double strand breaks, into its DNA, which require the non-homologous end joining pathway for repair. The studies shown in this thesis utilize a mouse model in which the MRN complex or the Mre11 nuclease activity is knocked out specifically in B cells. Using this model, our study is one of the first to establish multiple roles for the complex in CSR. Importantly, we are able to identify novel roles for the MRN complex outside of the activation of the ATM kinase by the introduction of the Mre11

nuclease deficient allele. This allele exhibits defects in CSR while maintaining signaling through ATM, establishing the nuclease activity as a separate and necessary function of Mre11.

Previous studies have identified roles for the Mre11/Rad50/Nbs1 complex in homologous recombination [71]. Our data shows unrepaired breaks in the IgH locus in the absence of MRN and Mre11 nuclease activity following induction of CSR, which establishes roles for MRN in end joining[63]. Sequencing of the few CSR joins that form in the absence of MRN or Mre11 nuclease activity reveals that MRN functions in both the C-NHEJ as well as the more poorly defined A-NHEJ pathway or set of pathways. Two other studies that were published with this one reinforce our conclusion that MRN is involved in NHEJ, and that it is involved in both classic and alternative pathways. Rass et al., use a reporter substrate and siRNA knockdowns to show that levels of C-NHEJ are reduced following silencing of Mre11, Rad50, and CtIP. Additionally, inhibition of Mre11 on a C-NHEJ deficient background ($Xrcc4^{-/-}$) reduces end joining further, leading the authors to conclude that MRN is involved in A-NHEJ. The authors go on to show that overexpression of Mre11 in their model increases the number of ends that are joined by the alternative pathway[65]. Xie et al. also use a reporter system that requires I-Sce1 to induce DSBs in the substrate. They, too, use siRNA to silence Mre11 and Nbs1 on top of Xrcc4 deficiency, revealing decreases in end joining[64]. These reporter assay studies, together with our *ex vivo* data, makes a highly convincing argument that MRN is important for classical and alternative NHEJ in mammalian cells (reviewed in [186]).

While the studies mentioned above provide the first evidence for the importance of MRN in end joining in mammals, there has been convincing data for over a decade that MRX (Mre11/Rad50/Xrs2, Xrs2 being a functional analog of Nbs1) has roles in end joining in *S. cerevisiae*. Involvement of the Mre11/Rad50/Xrs2 complex in NHEJ in the budding yeast

originated from findings that showed significantly reduced frequency of integration of transforming DNA that shares no homology with the host genome in the Rad50 mutant[187]. Later i*n vivo* experiments using an HO endonuclease-induced chromosomal DSB and a plasmid repair assay definitively established a role of the Mre11/Rad50/Xrs2 complex in *S. cerevisiae* NHEJ. Plasmid repair assays showed that strains, from which Mre11, Rad50, or Xrs2 was deleted, showed up to a 40-fold decrease in NHEJ compared to the wild type strain[188]. Finally, strains of *S. cerevisiae* harboring double mutants of MRX members with known NHEJ factors such as yeast Ku and Lig 4 did not show a larger decrease in end joining than single mutants[188].

The data presented in this thesis, combined with the knowledge previously established in the field in yeast, allows us to propose a model in which the MRN complex senses and localizes to a double strand break and, by using its bridging and tethering functions, links broken ends at distances up to 1,200 Angstrom. The DNA ends are then brought into close proximity by the Mre11/Rad50 heterotetramer, allowing Mre11 to nucleolytically process a subset of the ends. Because the breaks that are made during CSR are so imprecise, there are likely to be a range of end substrates that need to be nucleolytically processed by Mre11, as well as other nucleases. Mre11's exonucleolytic activities are likely important for the processing of at least some of these substrates. Finally, the complex then hands off the break to either the C-NHEJ or A-NHEJ machinery for resolution [63].

Roles for MRN in B cell lymphoma development

Because we observe an accumulation of breaks in the IgH locus of cells harboring Mre11 deficiencies following CSR induction, we proceeded to examine the likelihood that these unresolved breaks result in oncogenic translocations due to faulty DSB repair. B cell specific deletion of C-NHEJ factors, such as Xrcc4 and Ku, in mice on a p53 deficient genetic background, result in mortality due to B cell lymphoma development[24, 138]. It seems that loss of these C-NHEJ factors shuttles breaks to the more error prone A-NHEJ pathway, leading to oncogenic translocations [23]. Because we establish that MRN functions in NHEJ, we might expect the same outcome from mice with Mre11 deficiencies on a p53 null background. However, what we see is quite unique. Our data shows that the majority of mice harboring B cell specific Mre11 deficiencies die of p53 related thymic lymphomas, while none succumb to B cell lymphoma.

It is possible that these mice succumbed to thymic lymphomas before B cell lymphomas were advanced enough to emerge. Therefore, there could be microscopic B tumors present in the lymph that were undetectable during necropsy. The limited histology that has been done, however, indicates this is not the case. Although histology indicates some abnormalities in lymph nodes and spleen, none appear to exhibit obvious B cell related tumors, and they are certainly not genotype dependent. A more conclusive experiment would be to employ immunohistochemical stains specific to B and T cells to this tissue to look for the abnormal accumulation of these cells in peripheral lymph organs. It may also be useful to histologically examine bone marrow from these Mre11 deficient mice. Although CD19-cre deletes Mre11 late in the bone marrow, we cannot completely rule out the possibility of a phenotype in this tissue.

It is also possible that these mice would have developed B cell lymphomas later in life. However, unpublished data produced by Cheryl Jacobs in the Sekiguchi lab shows that Artemis deficient mice no longer develop progenitor B cell lymphomas in the absence of MRN or Mre11 nuclease activity. This seems to suggest that loss of the MRN complex is not compatible with malignancy. It would be interesting to cross mice containing the Mre11 conditional, null, and nuclease deficient alleles to a T cell specific promoter. Given the current data, the prediction would be that Mre11 deficiencies in the thymus would lead to a suppression of p53 related thymic lymphomas, leading to prolonged tumor free mouse survival. This result would certainly be novel in that it would determine that MRN or Mre11 is an oncogene of sorts, the presence of which is necessary for tumors to develop. There are a number of tumor models that would be curious to cross our Mre11 deficiencies onto to look for absence of tumors. The Eμ- Myc transgenic mice, for example, develop B cell lymphomas due to an inherited IgH-Myc fusion transgene [80]. It would be exciting to see if lymphoma development in this model would be impaired upon the introduction of Mre11 deficiencies.

Although I suggest a number of theories on why our $P^{-}C^{+}Mre11^{H129N}/Mre11^{-}$ mice do not succumb to B cell lymphomas in Chapter 3, I stop short of proposing a mechanism as to why. This is a question that many future experiments can be proposed to answer. I demonstrate that $P^{-}C^{+}Mre11^{H129N/-}/ Mre11^{-/-}$ B cells are able to undergo translocations to the IgH locus, but as of yet I have not been able to qualify and quantify these translocations with respect to genotype. It would be useful to discern if the detectable translocations are more or less frequent in the absence of MRN. Previous data in MEFs indicates that loss of MRN results in more translocations [71], while the data presented in this thesis suggests that translocation levels are similar to controls. It is also probable that the quality of joins is different between genotypes;

that the loss of Mre11 nuclease activity or the MRN complex contributes to a variation in the number of translocation joins being ligated through the A-NHEJ pathway. To address quantitative differences in translocations between B cells with or without Mre11 deficiencies, translocation PCR could be repeated on $P^{-}C^{+}Mre11^{+/-}$/$Mre11^{H129N/-}$/ $Mre11^{-/-}$ B cells until a large enough number of reactions have been completed to allow for quantification and statistics. These results should also be compared to a quantity of translocations in a population of B cells that are devoid of an intact C-NHEJ pathway as a control, such as B cells deficient in Lig 4.

Spectral karyotyping is another way to measure translocation quantity. This assay can easily be done in MEFs in which DSBs are induced by the introduction of IR. Although MEFs and B cells certainly behave differently, SKY would allow for easy quantification of translocations in the absence of MRN and Mre11 nuclease activity, as well as easy comparison of levels of translocation to MEFs with other end joining deficiencies, such as the previously mentioned Lig 4 deficiency.

I also propose that oncogenic stress coupled with replication stress and general genomic instability might be leading to cell death in $P^{-}C^{+}Mre11^{H129N}$/$Mre11^{-}$ B cells. Evaluation of this theory would require assaying cells for the presence of deregulated oncogenes. This could be done by something as simple as rtPCR or western blot to certain known translocation partners such as Myc, Bcl-1 or Bcl-2. It is also possible to overexpress oncogenes in cells isolated from $P^{-}C^{+}Mre11^{H129N}$/ $Mre11^{-}$ mice in order to determine the effect of oncogenic stress on growth and survival rates. A pilot experiment is discussed in Appendix III in which MEFs are immortalized with Myc and assayed for growth and senescence. Although the results of these studies are inconclusive, these cell lines could be valuable for assays that examine aberrant regulation of

senescence or apoptosis. These experiments may give insight into the effect of oncogenic stress and genome instability in $P^{-}C^{+}Mre11^{H129N}/Mre11^{-}$ cells in mice.

An interesting (but expensive) assay would be to evaluate genome wide expression of cells with and without Mre11 deficiencies using array technology. Comparing expression of genes in cells lacking Mre11 that have been immortalized by Myc to cells immortalized by other methods might shed light onto diverging mechanisms of cellular senescence/apoptosis. Arrays could also be performed on $P^{-}C^{+}$ $Mre11^{+}/Mre11^{H129N}/Mre11^{-}$ B cells to look for impacts of Mre11 versus Mre11 nuclease deficiency loss on gene expression patterns.

Array assays could also be interesting when addressing the role of Mre11 in the regulation of Cdk2 in cells. A phosphoproteomic array would allow for the evaluation of the phosphorylation status of a wide range of Cdk2 targets. It would also allow for the identification and evaluation of unique Cdk2 targets, as many remain unknown due to of the propensity of Cdks to compensate for one another. Western blots would be appropriate to investigate the phosphorylation status of known Cdk2 targets as well.

Additionally, Buis et al. determined that the C-terminus of Mre11 is essential for its interaction with Cdk2, and that disruption of this portion of the protein leads to a significant decrease in phosphorylation of Cdk2 targets such as CtIP. It would be interesting to deplete the C-terminus of Mre11 in our B cell specific mouse model and look for tumor development. If the loss of the C- terminus phenocopies the lack of B lymphocyte tumors seen in $P^{-}C^{+}Mre11^{H129N}/Mre11^{-}$ mice, it could indicate that Mre11 regulation of Cdk2 is the mechanism behind the lack of B cell tumor development.

This mechanism would be puzzling due to the fact that $P^{-}C^{+}Mre11^{H129N}$ mice do not succumb to B cell lymphomas, echoing their MRN null counterparts. Since the C-terminus of Mre11 is presumably intact in the presence of the H129N point mutation (indeed cells containing the Mre11 nuclease deficient allele show Cdk2 dependent CtIP phosphorylation [145]), this would suggest that the MRN complex functions through more than one mechanism in tumor development. This possibility could lead to a number of future experiments in the lab. An easy experiment to begin with would be to use Myc to immortalize Mre11 nuclease deficient MEFs and assess growth and senescence to compare with the Mre11 null cells.

Cis- acting elements play a minor role in Myc translocation to and deregulation by IgH

Work described in this thesis also shows that all the elements necessary to form translocations between IgH and an oncogene, as well as deregulate the oncogene are found within the IgH locus. This is the first study to determine that cis-acting elements outside of IgH, either close to or far from the locus in the genome, are essentially unimportant for the development of IgH translocations and tumors. In this study, a transgenic mouse model was used to evaluate translocation and transformation abilities of the IgH locus at several different chromosomal locations and in different orientations relative to the centromere. Our data reveals that regardless of the genomic location or orientation of IgH, it is still able to undergo translocations with Myc, deregulate Myc, and lead to the development of plasmacytoma.

Numerous studies have shown that lymphoid cells expressing the RAG endonuclease or AID can undergo any of one of thousands of different translocations {Klein, 2011 #27;Chiarle, 2011 #28;Hakim, 2012 #30;Hasham, 2010 #31[3]}. However, it seems that the IgH:Myc translocation and its resulting deregulated Myc expression are selected for, and that this leads to

the recurrence of this translocation in human lymphoma and murine plasmacytoma. Much work in the field indicates that IgH:Myc translocations are overrepresented in the primary collection of translocations [143, 174, 175, 177]. Several factors have been hypothesized to increase the frequency of the IgH:Myc translocation such as gene proximity caused by chromosome territories in the nucleus or shared transcription factors and repair machinery [178-181], high frequency of DNA breaks following AID operation [175], and faulty DNA repair [89, 161]. Our transgenic system presents a unique model with which to evaluate the importance of these hypotheses in translocation formation. It would be valuable to measure the proximity of the different IgH transgenes to the Myc locus using 3-dimensional FISH. If we see frequent co-localization of Myc to the transgene, but not to the translocation insertion site alone, it would argue that proximity of two translocation partners is important, and that IgH can somehow control it. Conversely, if we observe co-localization between the Myc and the transgene insertion sites with and without the transgene, it would argue that proximity of certain DNA segments to others is less important for translocation formation due to the fact that Myc does not normally translocate to these chromosomal sites. Our transgenic system could also allows for the assessment of the importance of AID activity and break frequency in this model by measuring AID activity at each chromosomal insertion site.

In summary, this thesis explores mechanisms that control every aspect of transformation of a cell, including misrepair of DNA lesions that lead to translocations, processes that control the formation of translocations, and elements that lead to deregulation of an oncogene following translocation. It is my goal that the knowledge gained by this work can contribute to the development of therapeutics for Non-Hodgkin lymphomas as well as other cancers that are caused by recurring translocations. DNA repair proteins have become an important target for

therapy in many kinds of cancer, and I hope this data can help with the advancement of these therapies, ultimately improving the quality of life for cancer patients worldwide.

Appendix I: A Glycine- Arginine rich motif of Mre11 is not important for class switch recombination

Introduction

Human Mre11 bears a glycine and arginine rich (GAR) motif that is conserved among multicellular eukaryotic species. Methylation of these arginines has been shown to regulate the MRN complex, specifically the first six methylated arginines have been shown to be essential for the regulation of Mre11 DNA binding and nuclease activity [189]. A knock- in mouse allele was generated that substitutes the 9 arginines within the GAR motif with lysines ($Mre11^{RK}$) in the lab of Stephan Richard in Montreal. The $Mre11^{RK/RK}$ mice show hypersensitivity to (IR), while the cells from these mice displayed cell cycle checkpoint defects and chromosome instability, ATR/CHK1 signaling defects, and impairment in the recruitment of RPA and RAD51 to sites of DNA damage. The $M^{RK}RN$ complex was able to form and localize to the sites of DNA damage, as well as activate the ATM pathway in response to IR. The $M^{RK}RN$ complex exhibited exonuclease and DNA-binding defects *in vitro* responsible for the impaired DNA end resection and ATR activation observed *in vivo* in response to IR [190].

Materials and Methods

B lymphocyte enrichment and cell culture

Mature B lymphocytes were isolated from mouse spleens using a B Lymphocyte Enrichment Kit (BD IMag) and cultured B cells in RPMI media supplemented with 10% (v/v)

FBS and 1% (v/v) Pen/Strep (10,000 U ml^{-1} Pen + 10,000 ug ml^{-1} Strep) with or without the following cytokines: 1 μg ml^{-1} αCD40 (BD Bioscience) plus 25 ng ml^{-1} IL-4 (R&D Systems). For cell tracking experiments, cells were incubated in RPMI media containing 10 μM CFDA SE dye (Vybrant CFDA SE Cell Tracer Kit, Invitrogen) at 37°C for 10 min and washed with PBS prior to plating. B lymphocytes were plated at $1x10^6$ cells ml^{-1} and cultured for 4 days.

Flow Cytometry

Cell surface markers were analyzed on a Beckman Coulter FC500 Flow Cytometer using Cytomics RXP software. Cells were washed with PBS + 10% (v/v) FBS, and incubated on ice in the dark for 30 - 60 min using the antibodies αB220 (1:200, eBioscience), and αIgG1 (1:100, BD Pharmingen). Data was analyzed using FlowJo software.

Results and Discussion

MRE11 participates in NHEJ pathways, which are required for class switch recombination (CSR). Absence of MRE11 in developing B lymphocytes causes a significant reduction in CSR, whereas MRE11 defective only in nuclease activities causes a mild CSR defect [63]. To determine if the MRE11 GAR motif is required for its function in NHEJ, I compared CSR levels of $Mre11^{RK/RK}$ B cells to CSR levels of $Mre11^{\Delta/\Delta}$ and $Mre11^{\Delta/H129N}$ B cells. A CD21-cre transgene was crossed to mice with Mre11 deficient alleles to convert $Mre11^{cond}$ to $Mre11^{\Delta}$ in mature IgM+ B lymphocytes. Splenic B cells from $Mre11^{\Delta/\Delta}$ and $Mre11^{\Delta/H129N}$ mice were induced to switch from IgM to IgG1 and defects similar to those reported previously were observed. In contrast, $Mre11^{RK/RK}$ cells display a small statistically significant difference (P = 0.0409), which is not likely to be biologically significant.

It appears as though the methylation of arginines in the Mre11 GAR motif is not important for CSR, and, on a more global scale, it is most likely not important for NHEJ. However, studies on these mice do show significant phenotypes that provide genetic evidence for the critical role of the MRE11 GAR motif in DSB repair. Using these transgenic mice, the Richard lab was able to demonstrate a mechanistic link between post-translational modifications at the MRE11 GAR motif and DSB processing and ATR/CHK1 checkpoint signaling [190].

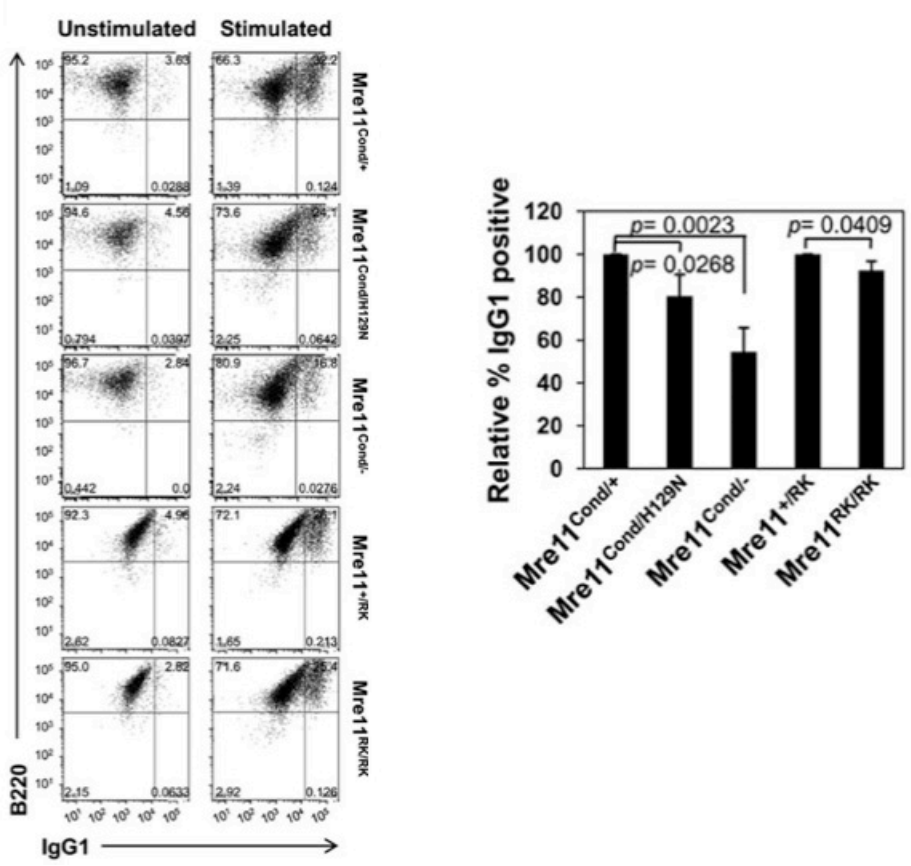

Figure A1: Methylation of arginines in the Mre11 GAR does not affect levels of immunoglobulin switching. Flow cytometric analysis of CSR from IgM to IgG in B lymphocytes cultured with IL-4 and anti-CD40 for four days. Representative flow data is shown on the left. The bar graph depicts comparisons of IgG1+ cell populations relative to $Mre11^{+/cond}$. N=3 mice per genotype.

Appendix II: Looking at the impact of Mre11 deficiencies on somatic hypermutation

Introduction

Somatic hypermutation (SHM) is required for antibody maturation, and is initiated in peripheral lymphoid organs upon introduction of cells to antigen. The purpose of SHM is to increase antibody affinity to the antigen by hypermutating the variable region coupled with selection. Like CSR, AID is responsible for initiating DNA lesions during SHM. Although SHM is largely thought to be a process involving point mutations, 5-10% of resulting mutations are small insertions and deletions, which are suggestive of DSB intermediates [41]. Several groups have used ligation- mediated PCR assays to show DSBs in hypermutation regions [42, 191, 192], while others have shown processing of these lesions still occurs in NHEJ deficient mice [44], leaving the question open for debate.

Materials and Methods

Isolation of B cells from Peyer's Patches

Peyer's Patches were collected from 4-12 month old mice and B cells were isolated using a B Lymphocyte Enrichment Kit (BD IMag). B cells were pooled from 5 mice each of the genotypes $Mre11^{cond/+}$, $Mre11^{cond/H129N}$, and $Mre11^{cond/-}$. Mre11 conditional alleles were excised when these mice were crossed to mice with a CD21- Cre allele. A BD Bioscience FACSVantage cell sorter (University of Michigan core) was used with antibodies αB220-PECy5 (1:200, eBioscience), and αGL7-FITC (1:100, BD Pharmingen).

PCR, cloning, and sequencing

DNA was isolated from each sorted population using a Qiagen DNeazy kit. PCR was performed using primers V 3'- GGA ATT CGC CTG ACA TCT GAG GAC TCT GC-5' and E 3'- GAC TAG TCC TCT CCA GTT TCG GCT CAA TCC- 5' with at 56°C annealing temperature and 2 minute extension time for 35 cycles. PCR products were then purified using a Qiagen QIAquick PCR Purification Kit. PCR products were cloned using a TOPO-TA cloning kit (Invitrogen), diluted 1:20 and sent to the University of Michigan sequencing core with the JH4 primer: 3'- TAT GCT ATG GAC TAC TGG- 5'.

Results and Discussion

Peyer's Patches were collected from 4-12 month old mice and B cells were isolated and sorted for actively hypermutating cells (B220+, GL7+) and non- mutating control B cells (B220+, GL7) (Fig A2). These experiments were piloted by Maria Dinkelmann, a former post doc in the lab, but continued by myself. PCR was done between V_HJ558 and E to ensure only cells that had undergone V(D)J were selected for. These PCR products were cloned and sequenced using a primer to the JH4 intronic region in order to amplify the mutating region (Fig A3). Sequences were then analyzed in order to quantify mutation rates of JH4 in hypermutating and non-mutating B cells with Mrell genotypes of $Mre11^{cond/+}$, $Mre11^{cond/H129N}$, and $Mre11^{cond/-}$. Preliminary data from 5- 12 sequences of each cell state from each genotype show that while we were able to sort hypermutating from non mutating cells in each genotype, there does not seem to be a difference in mutation rates between the genotypes.

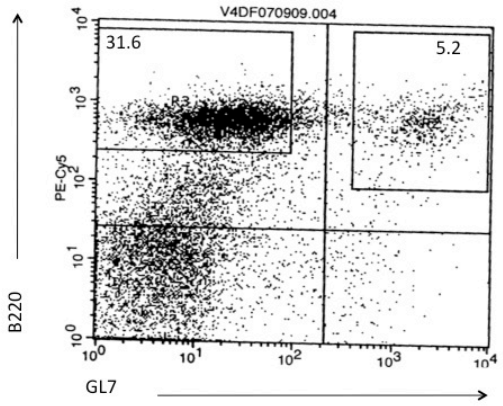

Figure A2: Flow cytometry sorts for hypermutating and non- mutating B cells. Hypermutating cells are B220+, GL7+ and can be compared to B220+, GL7- cells from the same mice.

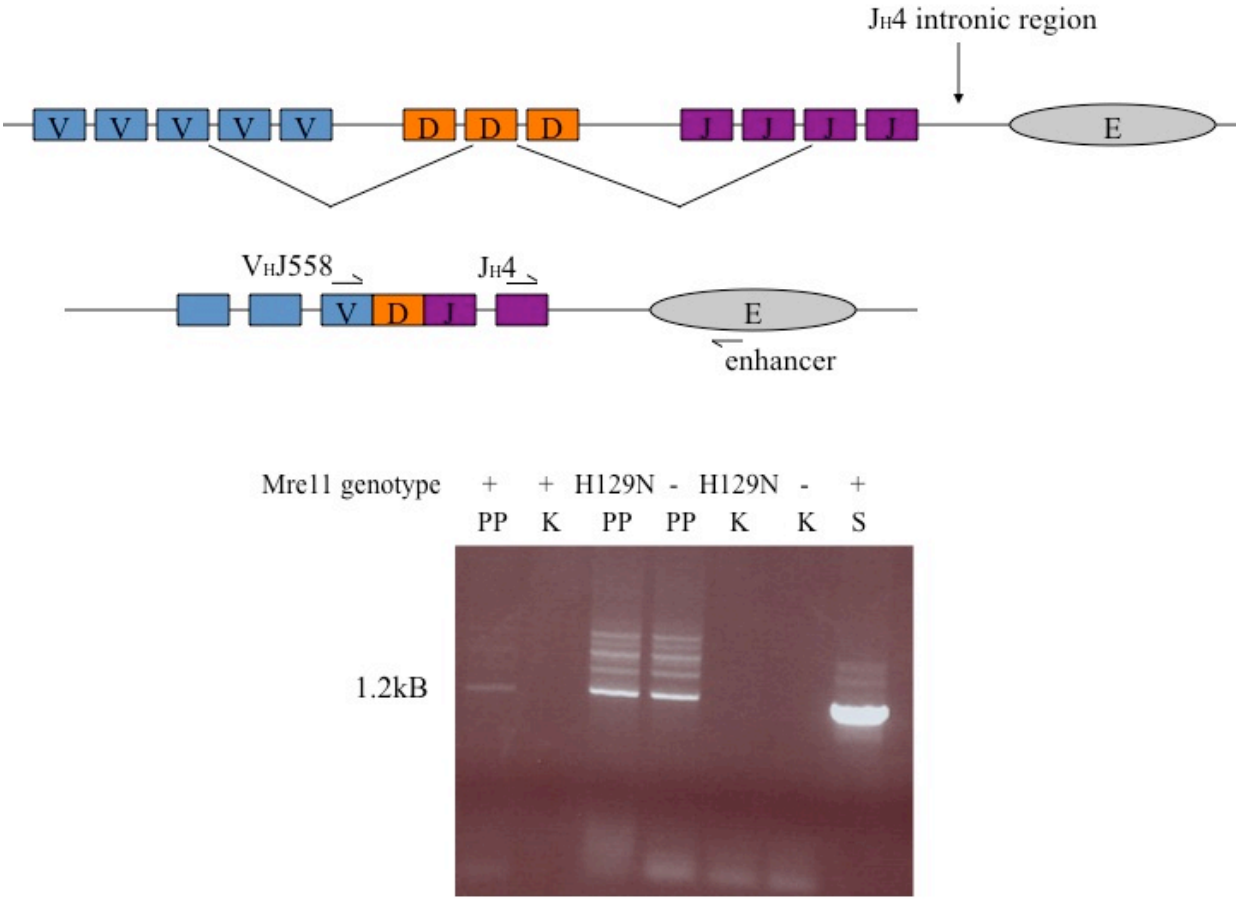

Figure A3: Somatic Hypermutation PCR. V-E PCR primers amplify the JH4 intron specifically in mature B cells with rearranged V(D)J exons from Peyer's Patches (PP) while not amplifying cells from kidney (K). Positive control is B cells isolated from spleen and cultured to undergo CSR for 4 days (S). Multiple bands are indicative of exons joined to different J regions.

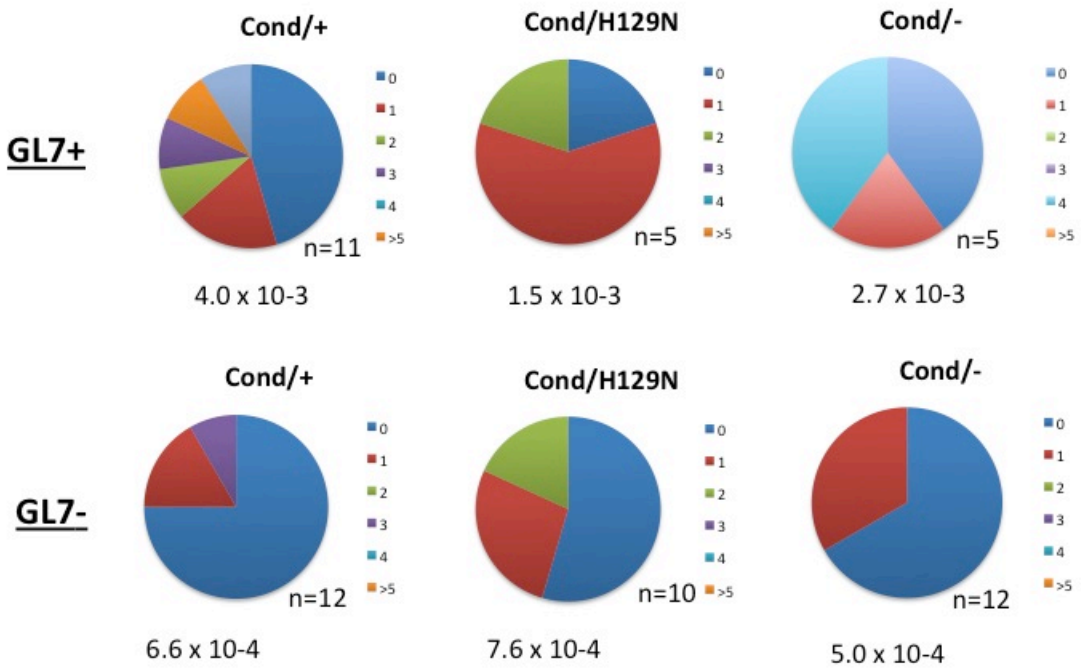

Figure A4: Somatic hypermutation rates in B cells harboring Mre11 deficiencies are similar to controls. Rates of mutation were compared between hypermutating (GL7+) and non-mutating (GL7-) B cells. GL7+ cells show a significant increase in mutation rates compared to controls (rates below graphs are mutations per cell). Pie charts depict percentage of sequences with zero to more than 5 mutations. Data is not significant.

Appendix III: C-myc immortalization of MEFs to assess how oncogenic stress impacts Mre11 deficiencies

Introduction

One hypothesis for $P^{-}C^{+}Mre11^{-/-}$ and $P^{-}C^{+}Mre11^{H129N/-}$ mice not developing B cell tumors is that oncogenes such as Myc play a role in tumor development in conjunction with Mre11. The rationale behind this is two fold. First, studies have shown that c-myc, besides leading to DNA damage itself, plays roles in sensitizing cells to replication stress through oncogenic actions. For example, overexpression of Myc show impaired proliferation and rapid senescence in the absence of the Werner helicase, which is important for the resolution of DNA structures that form following stalled replication forks [193]. Additionally, several studies have shown that overexpression of c-myc becomes synthetically lethal with loss or inhibition of ATR and its downstream effector Chk1 [194-196]. This implies that the stress caused by oncogenes such as Myc makes cells particularly sensitive to replication stress due to deregulated S-phase. Since ATR and Chk1 are crucial for the cellular response to replication stress, it would make sense that inhibition of these kinases compounded with oncogenic stress on cancer cells would lead to cancer cell death. This is the case in mice in which reduced levels of ATR found in a model of ATR- Sickle syndrome prevented the development of Myc- induced lymphomas and pancreatic tumors [196]. Additionally, human neuroblastoma cells with high levels of Myc expression were sensitive to Chk1 inhibitors [195]. Since Mre11 has been shown to have roles in S-phase and cells lacking MRN and Mre11 nuclease activity are sensitive to replication stress [71], it could be that Mre11 deficiencies sensitize cells to oncogenic stresses caused by Myc overexpression.

Myc has also been shown to be downstream of Cdk2. Although it is clear oncogenes promote cancer development through enhanced cell proliferation, it has been shown that they can also trigger senescence pathways [197]. Myc overexpression causes activation of Cdk2 and promotes cell cycle progression [198]. However, there are several studies that show that Cdk2 phosphorylation of Myc leads to repression of cellular senescence [148, 149, 199]. This may be important for the formation of B cell tumors in $P^{-}C^{+}Mre11^{-/-}$ and $P^{-}C^{+}Mre11^{H129N/-}$ mice due to the role of Mre11 in global control of Cdk2. Buis et al. show that Mre11 regulates CtIP through a c-terminal dependent, DNA damage independent interaction with Cdk2 [145]. Unpublished work from Jeff Buis indicates that control of Cdk2 by the Mre11 c-terminus may play a more global role in Cdk2 signaling than just regulation of CtIP. Thus, if Cdk2 does control Myc induced senescence, it may be that the loss of Mre11 in our B cells leads to cellular senescence by inhibiting Myc phosphorylation by Cdk2.

Materials and Methods

Transformation of MEFs

MEFs were isolated in the Ferguson lab and frozen or transformed by Jeff Buis as previously described[71]. Primary MEFs were plated at P3 into a 6 well dish at 1.5 x 10^5 cells per well and cultured overnight at 37°C. 50µL of pLenti-Myc T58A or a pLenti- empty control (gifts from David Lombard) were introduced to the cells with a 1:4000 dilution of polybrene (Santa Cruz) in DMEM without serum on antibiotics. After 24 hours, retrovirus was removed and cells are washed twice with PBS. 24 hours later, cells were split 1:3 with medium

containing 2μg/mL puromycin. After 5 days in selection media, 100% of the cells that were introduced with the control empty vectors were dead.

Growth curve

Myc and T-antigen transformed Mre11$^{cond/-}$ and Mre11$^{cond/+}$ MEFs were plated at 5 x 10^5 in 10cm dishes and cultured overnight. Cells were infected twice with either Adeno-Cre or Adeno-Empty (University of Michigan vector core) at a MOI of 500:1 in DMEM without serum or antibiotics overnight. Four days after the second infection, cells were plated at a low density (1 x 10^5 cells/10cm dish) and counted every 2 days.

β- gal senescence assay

Myc and T-antigen transformed as well as primary Mre11$^{cond/-}$ and Mre11$^{cond/+}$ MEFs were cultured and treated with Adeno- Cre or Adeno-Empty as described above. 5 days after second Adeno infection, cells were plated at a low density (1 x 10^5 cells per well in a 6 well dish) until reaching 50-75% confluency (2-3 days). Cells were stained for senescence using the Senescence β- Galactosidase Staining Kit (Cell Signaling) and the percentage of senescent cells were counted using a Leica DMIL phase contrast microscope and graphed.

Results and Discussion

To address the relationship between Myc and Mre11, we used retrovirus to introduce oncogenic Myc into MEFs harboring the Mre11 conditional allele. After 5 days under puromycin selection, immortalization of MEFs infected with the Myc oncogene can be seen, while the empty vector infected controls die. We then treated the MEFs with either Adeno- Cre or Adeno-Empty to

delete Mre11 and assay for cellular growth and senescence. The growth assay shows impaired growth in all cell lines in which Mre11 was deleted. However, there is no observable difference in growth between Mre11 deleted cells immortalized by Myc versus T- antigen (Fig. A5). The senescence assay reveals a significant increase in senescence following cre- mediated deletion of Mre11 in primary MEFs, but, predictably, does not show increased senescence in immortalized MEFs (Fig. A6). This could be indicative of several things. First, deletion of Mre11 may not have an impact on Myc expression or cell cycle control in MEFs. Second, although we do not see a difference in cell growth or senescence using these assays, it is possible that the programs that the cells are undergoing are different depending on how they were immortalized. Future directions for this line of investigation include assessment of activation of specific members of the senescence/apoptotic pathways to look for differences in mechanism. Possible targets for investigation include Cdk2 and Ras, which are involved in cell cycle control and oncogenic senescence, as well as the apoptotic markers caspase 3, 7, and cleaved PARP.

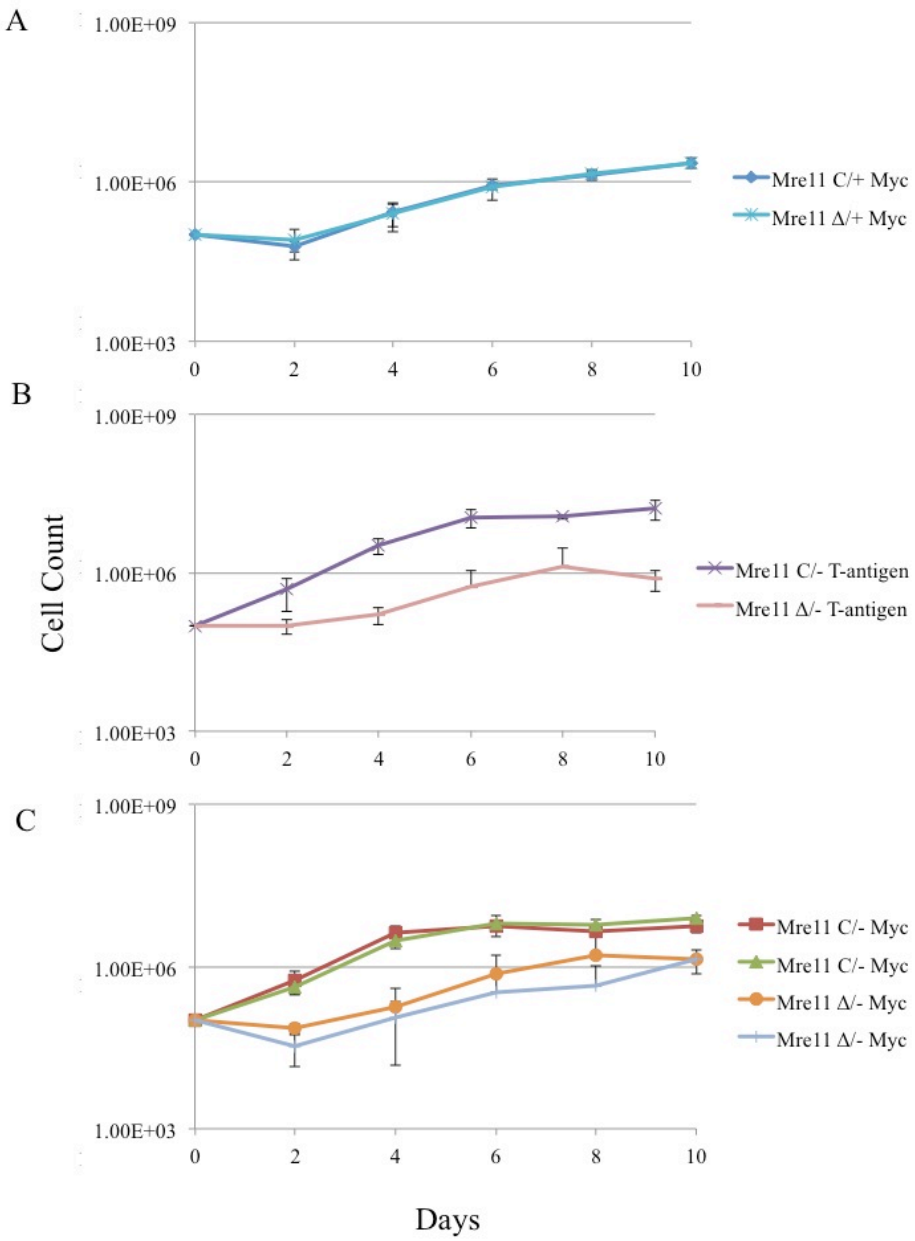

Figure A5: Growth curve of Myc transformed Mre11 deleted MEFs. Cell growth of Mre11 deficient MEF lines transformed with Myc or T-antigen. (A) Growth curves of $Mre11^{cond/+}$ MEFs that were transformed with Myc and treated with either Adeno-cre (Mre11 Δ /+ Myc) or Empty adenovirus (Mre11 C/+ Myc) overlap. (B) Growth curves of $Mre11^{cond/-}$ MEFs that were transformed with T- antigen and treated with either Adeno-cre (Mre11 Δ /- T-antigen) or empty adenovirus (Mre11 C/- T-antigen). MEFs in which Mre11 is deleted (Mre11 Δ /- T-antigen) grow significantly slower than controls. (C) Growth curves of two MEF lines that were transformed with Myc and treated with either Adeno-cre (Mre11 Δ /- Myc) or empty adenovirus (Mre11 C/- Myc). MEFs in which Mre11 is deleted (Mre11 Δ /- Myc) grow significantly slower than controls, but do not show a difference in growth when compared to T-antigen transformed MEFS (B). N=3 for each growth curve.

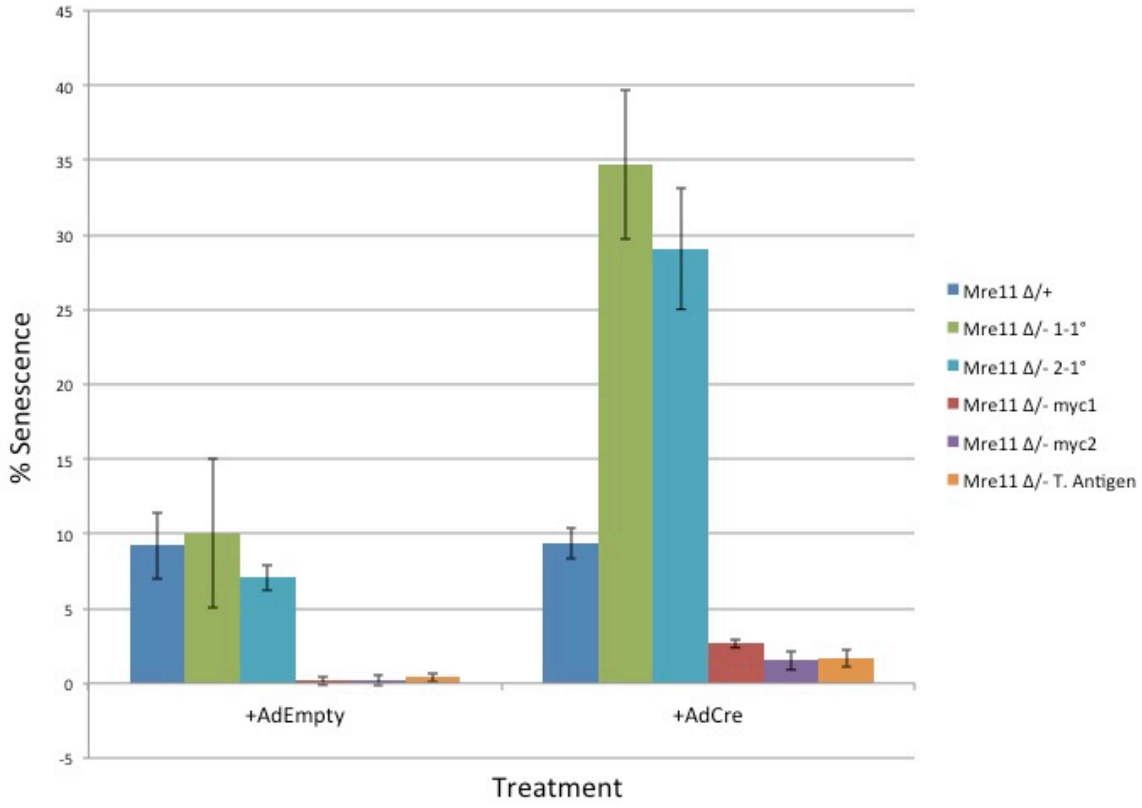

Figure A6: Senescence of Myc transformed Mre11 deleted MEFs. In the presence of Mre11, the three primary cell lines (Mre11Δ/+ and Mre11Δ/- 1-1° and 2-1° +AdEmpty) show no difference in senescence levels. However, upon the deletion of Mre11, senescence increases significantly (Mre11Δ/- 1-1° and 2-1°). In immortalized cell lines, senescence is barely detectable when Mre11 is present (Mre11Δ/- myc1, Mre11Δ/- myc2 and Mre11Δ/- T. Antigen +AdEmpty). Following Mre11 deletion, senescence levels increase slightly in the immortalized cell lines, but show no significant difference due to immortalization mechanism. N=3

Bibliography

1. Dalla-Favera, R., et al., *Human c-myc onc gene is located on the region of chromosome 8 that is translocated in Burkitt lymphoma cells.* Proc Natl Acad Sci U S A, 1982. **79**(24): p. 7824-7.
2. Kuppers, R. and R. Dalla-Favera, *Mechanisms of chromosomal translocations in B cell lymphomas.* Oncogene, 2001. **20**(40): p. 5580-94.
3. Zhang, Y., et al., *The role of mechanistic factors in promoting chromosomal translocations found in lymphoid and other cancers.* Adv Immunol, 2010. **106**: p. 93-133.
4. Lieber, M.R., *The mechanism of double-strand DNA break repair by the nonhomologous DNA end-joining pathway.* Annu Rev Biochem, 2010. **79**: p. 181-211.
5. Symington, L.S. and J. Gautier, *Double-strand break end resection and repair pathway choice.* Annu Rev Genet, 2011. **45**: p. 247-71.
6. Mimitou, E.P. and L.S. Symington, *DNA end resection--unraveling the tail.* DNA Repair (Amst), 2011. **10**(3): p. 344-8.
7. San Filippo, J., P. Sung, and H. Klein, *Mechanism of eukaryotic homologous recombination.* Annu Rev Biochem, 2008. **77**: p. 229-57.
8. Maher, R.L., A.M. Branagan, and S.W. Morrical, *Coordination of DNA replication and recombination activities in the maintenance of genome stability.* J Cell Biochem, 2011. **112**(10): p. 2672-82.
9. Chen, P.L., et al., *Inactivation of CtIP leads to early embryonic lethality mediated by G1 restraint and to tumorigenesis by haploid insufficiency.* Mol Cell Biol, 2005. **25**(9): p. 3535-42.
10. Gowen, L.C., et al., *Brca1 deficiency results in early embryonic lethality characterized by neuroepithelial abnormalities.* Nat Genet, 1996. **12**(2): p. 191-4.
11. Hakem, R., J.L. de la Pompa, and T.W. Mak, *Developmental studies of Brca1 and Brca2 knock-out mice.* J Mammary Gland Biol Neoplasia, 1998. **3**(4): p. 431-45.
12. Lim, D.S. and P. Hasty, *A mutation in mouse rad51 results in an early embryonic lethal that is suppressed by a mutation in p53.* Mol Cell Biol, 1996. **16**(12): p. 7133-43.
13. Kuzminov, A., *DNA replication meets genetic exchange: chromosomal damage and its repair by homologous recombination.* Proc Natl Acad Sci U S A, 2001. **98**(15): p. 8461-8.
14. Featherstone, C. and S.P. Jackson, *Ku, a DNA repair protein with multiple cellular functions?* Mutat Res, 1999. **434**(1): p. 3-15.
15. Dynan, W.S. and S. Yoo, *Interaction of Ku protein and DNA-dependent protein kinase catalytic subunit with nucleic acids.* Nucleic Acids Res, 1998. **26**(7): p. 1551-9.
16. Moshous, D., et al., *Artemis, a Novel DNA Double-Strand Break Repair/V(D)J Recombination Protein, Is Mutated in Human Severe Combined Immune Deficiency.* Cell, 2001. **105**(2): p. 177-186.
17. Dominguez, O., et al., *DNA polymerase mu (Pol mu), homologous to TdT, could act as a DNA mutator in eukaryotic cells.* EMBO J, 2000. **19**(7): p. 1731-42.

18. Bebenek, K., et al., *The frameshift infidelity of human DNA polymerase lambda. Implications for function.* J Biol Chem, 2003. **278**(36): p. 34685-90.
19. Lu, H., et al., *Length-dependent binding of human XLF to DNA and stimulation of XRCC4.DNA ligase IV activity.* J Biol Chem, 2007. **282**(15): p. 11155-62.
20. Gu, J., et al., *XRCC4:DNA ligase IV can ligate incompatible DNA ends and can ligate across gaps.* EMBO J, 2007. **26**(4): p. 1010-23.
21. Boulton, S.J. and S.P. Jackson, *Saccharomyces cerevisiae Ku70 potentiates illegitimate DNA double-strand break repair and serves as a barrier to error-prone DNA repair pathways.* EMBO J, 1996. **15**(18): p. 5093-103.
22. Kabotyanski, E.B., et al., *Double-strand break repair in Ku86- and XRCC4-deficient cells.* Nucleic Acids Res, 1998. **26**(23): p. 5333-42.
23. Simsek, D. and M. Jasin, *Alternative end-joining is suppressed by the canonical NHEJ component Xrcc4-ligase IV during chromosomal translocation formation.* Nat Struct Mol Biol, 2010. **17**(4): p. 410-6.
24. Boboila, C., et al., *Alternative end-joining catalyzes robust IgH locus deletions and translocations in the combined absence of ligase 4 and Ku70.* Proc Natl Acad Sci U S A, 2010. **107**(7): p. 3034-9.
25. Boboila, C., F.W. Alt, and B. Schwer, *Chapter One - Classical and Alternative End-Joining Pathways for Repair of Lymphocyte-Specific and General DNA Double-Strand Breaks*, in *Advances in Immunology*, W.A. Frederick, Editor. 2012, Academic Press. p. 1-49.
26. Nishana, M. and S.C. Raghavan, *Role of recombination activating genes in the generation of antigen receptor diversity and beyond.* Immunology, 2012. **137**(4): p. 271-81.
27. Helmink, B.A. and B.P. Sleckman, *The response to and repair of RAG-mediated DNA double-strand breaks.* Annu Rev Immunol, 2012. **30**: p. 175-202.
28. Buck, D., et al., *Cernunnos, a novel nonhomologous end-joining factor, is mutated in human immunodeficiency with microcephaly.* Cell, 2006. **124**(2): p. 287-99.
29. Frank, K.M., et al., *DNA ligase IV deficiency in mice leads to defective neurogenesis and embryonic lethality via the p53 pathway.* Mol Cell, 2000. **5**(6): p. 993-1002.
30. Gao, Y., et al., *A critical role for DNA end-joining proteins in both lymphogenesis and neurogenesis.* Cell, 1998. **95**(7): p. 891-902.
31. Gu, Y., et al., *Growth Retardation and Leaky SCID Phenotype of Ku70-Deficient Mice.* Immunity, 1997. **7**(5): p. 653-665.
32. Li, Z., et al., *The XRCC4 gene encodes a novel protein involved in DNA double-strand break repair and V(D)J recombination.* Cell, 1995. **83**(7): p. 1079-89.
33. Nussenzweig, A., et al., *Requirement for Ku80 in growth and immunoglobulin V(D)J recombination.* Nature, 1996. **382**(6591): p. 551-5.
34. Chaudhuri, J., et al., *Evolution of the immunoglobulin heavy chain class switch recombination mechanism.* Adv Immunol, 2007. **94**: p. 157-214.
35. Honjo, T., M. Muramatsu, and S. Fagarasan, *AID: how does it aid antibody diversity?* Immunity, 2004. **20**(6): p. 659-68.
36. Chaudhuri, J. and F.W. Alt, *Class-switch recombination: interplay of transcription, DNA deamination and DNA repair.* Nat Rev Immunol, 2004. **4**(7): p. 541-552.
37. Manis, J.P., et al., *Ku70 Is Required for Late B Cell Development and Immunoglobulin Heavy Chain Class Switching.* J. Exp. Med., 1998. **187**(12): p. 2081-2089.

38. Yan, C.T., et al., *IgH class switching and translocations use a robust non- classical end-joining pathway.* Nature, 2007. **449**: p. 478- 482.
39. Maul, R.W. and P.J. Gearhart, *AID and somatic hypermutation.* Adv Immunol, 2010. **105**: p. 159-91.
40. Maul, R.W. and P.J. Gearhart, *Controlling somatic hypermutation in immunoglobulin variable and switch regions.* Immunol Res, 2010. **47**(1-3): p. 113-22.
41. Goossens, T., U. Klein, and R. Kuppers, *Frequent occurrence of deletions and duplications during somatic hypermutation: implications for oncogene translocations and heavy chain disease.* Proc Natl Acad Sci U S A, 1998. **95**(5): p. 2463-8.
42. Bross, L., et al., *DNA double-strand breaks in immunoglobulin genes undergoing somatic hypermutation.* Immunity, 2000. **13**(5): p. 589-97.
43. Sale, J.E. and M.S. Neuberger, *TdT-accessible breaks are scattered over the immunoglobulin V domain in a constitutively hypermutating B cell line.* Immunity, 1998. **9**(6): p. 859-69.
44. Bemark, M., et al., *Somatic hypermutation in the absence of DNA-dependent protein kinase catalytic subunit (DNA-PK(cs)) or recombination-activating gene (RAG)1 activity.* J Exp Med, 2000. **192**(10): p. 1509-14.
45. Stracker, T.H. and J.H. Petrini, *The MRE11 complex: starting from the ends.* Nat Rev Mol Cell Biol, 2011. **12**(2): p. 90-103.
46. Lee, J.H., et al., *Regulation of Mre11/Rad50 by Nbs1: effects on nucleotide-dependent DNA binding and association with ataxia-telangiectasia-like disorder mutant complexes.* J Biol Chem, 2003. **278**(46): p. 45171-81.
47. Furuse, M., et al., *Distinct roles of two separable in vitro activities of yeast Mre11 in mitotic and meiotic recombination.* EMBO J, 1998. **17**(21): p. 6412-25.
48. Moreau, S., J.R. Ferguson, and L.S. Symington, *The Nuclease Activity of Mre11 Is Required for Meiosis but Not for Mating Type Switching, End Joining, or Telomere Maintenance.* Mol. Cell. Biol., 1999. **19**(1): p. 556-566.
49. Paull, T.T. and M. Gellert, *The 3′ to 5′ Exonuclease Activity of Mre11 Facilitates Repair of DNA Double-Strand Breaks.* Molecular Cell, 1998. **1**(7): p. 969-979.
50. Trujillo, K.M., et al., *Nuclease activities in a complex of human recombination and DNA repair factors Rad50, Mre11, and p95.* J Biol Chem, 1998. **273**(34): p. 21447-50.
51. Stracker, T.H., et al., *The Mre11 complex and the metabolism of chromosome breaks: the importance of communicating and holding things together.* DNA Repair, 2004. **3**(8-9): p. 845-854.
52. Arthur, L.M., et al., *Structural and functional analysis of Mre11-3.* Nucl. Acids Res., 2004. **32**(6): p. 1886-1893.
53. Williams, R.S., et al., *Mre11 Dimers Coordinate DNA End Bridging and Nuclease Processing in Double-Strand-Break Repair.* Cell, 2008. **135**: p. 97- 109.
54. Llorente, B. and L.S. Symington, *The Mre11 nuclease is not required for 5′ to 3′ resection at multiple HO-induced double-strand breaks.* Mol Cell Biol, 2004. **24**(21): p. 9682-94.
55. de Jager, M., et al., *DNA end-binding specificity of human Rad50/Mre11 is influenced by ATP.* Nucleic Acids Res, 2002. **30**(20): p. 4425-31.
56. de Jager, M., et al., *Differential arrangements of conserved building blocks among homologs of the Rad50/Mre11 DNA repair protein complex.* J Mol Biol, 2004. **339**(4): p. 937-49.

57. Becker, E., et al., *Detection of a tandem BRCT in Nbs1 and Xrs2 with functional implications in the DNA damage response.* Bioinformatics, 2006. **22**(11): p. 1289-92.
58. Xu, C., et al., *Structure of a second BRCT domain identified in the nijmegen breakage syndrome protein Nbs1 and its function in an MDC1-dependent localization of Nbs1 to DNA damage sites.* J Mol Biol, 2008. **381**(2): p. 361-72.
59. Williams, G.J., S.P. Lees-Miller, and J.A. Tainer, *Mre11-Rad50-Nbs1 conformations and the control of sensing, signaling, and effector responses at DNA double-strand breaks.* DNA Repair (Amst), 2010. **9**(12): p. 1299-306.
60. Williams, R.S., J.S. Williams, and J.A. Tainer, *Mre11-Rad50-Nbs1 is a keystone complex connecting DNA repair machinery, double-strand break signaling, and the chromatin template.* Biochem Cell Biol, 2007. **85**(4): p. 509-20.
61. Hopfner, K.P., C.D. Putnam, and J.A. Tainer, *DNA double-strand break repair from head to tail.* Curr Opin Struct Biol, 2002. **12**(1): p. 115-22.
62. Moreno-Herrero, F., et al., *Mesoscale conformational changes in the DNA-repair complex Rad50/Mre11/Nbs1 upon binding DNA.* Nature, 2005. **437**(7057): p. 440-3.
63. Dinkelmann, M., et al., *Multiple functions of MRN in end-joining pathways during isotype class switching.* Nat Struct Mol Biol, 2009. **16**(8): p. 808-813.
64. Xie, A., A. Kwok, and R. Scully, *Role of mammalian Mre11 in classical and alternative nonhomologous end joining.* Nat Struct Mol Biol, 2009. **16**(8): p. 814-8.
65. Rass, E., et al., *Role of Mre11 in chromosomal nonhomologous end joining in mammalian cells.* Nat Struct Mol Biol, 2009. **16**(8): p. 819-24.
66. Lee, J.H. and T.T. Paull, *Activation and regulation of ATM kinase activity in response to DNA double-strand breaks.* Oncogene, 2007. **26**(56): p. 7741-8.
67. Waltes, R., et al., *Human RAD50 deficiency in a Nijmegen breakage syndrome-like disorder.* Am J Hum Genet, 2009. **84**(5): p. 605-16.
68. Uchisaka, N., et al., *Two brothers with ataxia-telangiectasia-like disorder with lung adenocarcinoma.* J Pediatr, 2009. **155**(3): p. 435-8.
69. Carney, J.P., et al., *The hMre11/hRad50 protein complex and Nijmegen breakage syndrome: linkage of double-strand break repair to the cellular DNA damage response.* Cell, 1998. **93**(3): p. 477-86.
70. Xu, Y., et al., *Targeted disruption of ATM leads to growth retardation, chromosomal fragmentation during meiosis, immune defects, and thymic lymphoma.* Genes Dev, 1996. **10**(19): p. 2411-22.
71. Buis, J., et al., *Mre11 nuclease activity has essential roles in DNA repair and genomic stability distinct from ATM activation.* Cell, 2008. **135**(1): p. 85-96.
72. Zhu, J., et al., *Targeted disruption of the Nijmegen breakage syndrome gene NBS1 leads to early embryonic lethality in mice.* Curr Biol, 2001. **11**(2): p. 105-9.
73. Luo, G., et al., *Disruption of mRad50 causes embryonic stem cell lethality, abnormal embryonic development, and sensitivity to ionizing radiation.* Proc Natl Acad Sci U S A, 1999. **96**(13): p. 7376-81.
74. Tsujimoto, Y., et al., *The t(14;18) Chromosome Translocations Involved in B-Cell Neoplasms Result from Mistakes in VDJ Joining.* Science, 1985. **229**(4720): p. 1390-1393.
75. Taub, R., et al., *Translocation of the c-myc gene into the immunoglobulin heavy chain locus in human Burkitt lymphoma and murine plasmacytoma cells.* Proc Natl Acad Sci U S A, 1982. **79**(24): p. 7837-41.

76. McKeithan, T.W., et al., *BCL3 rearrangements and t(14;19) in chronic lymphocytic leukemia and other B-cell malignancies: a molecular and cytogenetic study.* Genes Chromosomes Cancer, 1997. **20**(1): p. 64-72.
77. Iida, S., et al., *The t(9;14)(p13;q32) chromosomal translocation associated with lymphoplasmacytoid lymphoma involves the PAX-5 gene.* Blood, 1996. **88**(11): p. 4110-7.
78. Ramiro, A.R., et al., *AID Is Required for c-myc/IgH Chromosome Translocations In Vivo.* Cell, 2004. **118**(4): p. 431-438.
79. Vogelstein, B. and K.W. Kinzler, *The multistep nature of cancer.* Trends Genet, 1993. **9**(4): p. 138-41.
80. Adams, J.M., et al., *The c-myc oncogene driven by immunoglobulin enhancers induces lymphoid malignancy in transgenic mice.* Nature, 1985. **318**(6046): p. 533-8.
81. Gostissa, M., et al., *Long-range oncogenic activation of Igh-c-myc translocations by the Igh 3' regulatory region.* Nature, 2009. **462**(7274): p. 803-7.
82. McKinnon, P.J. and K.W. Caldecott, *DNA strand break repair and human genetic disease.* Annu Rev Genomics Hum Genet, 2007. **8**: p. 37-55.
83. Wyman, C. and R. Kanaar, *DNA Double-Strand Break Repair: All's Well that Ends Well.* Annual Review of Genetics, 2006. **40**(1): p. 363-383.
84. Audebert, M., B. Salles, and P. Calsou, *Involvement of poly(ADP-ribose) polymerase-1 and XRCC1/DNA ligase III in an alternative route for DNA double-strand breaks rejoining.* J Biol Chem, 2004. **279**(53): p. 55117-26.
85. Corneo, B., et al., *Rag mutations reveal robust alternative end joining.* Nature, 2007. **449**(7161): p. 483-6.
86. Soulas-Sprauel, P., et al., *Role for DNA repair factor XRCC4 in immunoglobulin class switch recombination.* The Journal of Experimental Medicine, 2007. **204**(7): p. 1717-1727.
87. Wang, H., et al., *DNA ligase III as a candidate component of backup pathways of nonhomologous end joining.* Cancer Res, 2005. **65**(10): p. 4020-30.
88. Soulas-Sprauel, P., et al., *V(D)J and immunoglobulin class switch recombinations: a paradigm to study the regulation of DNA end-joining.* Oncogene, 2007. **26**(56): p. 7780-7791.
89. Liu, M., et al., *Two levels of protection for the B cell genome during somatic hypermutation.* Nature, 2008. **451**(7180): p. 841-5.
90. Berkovich, E., R.J. Monnat, Jr., and M.B. Kastan, *Roles of ATM and NBS1 in chromatin structure modulation and DNA double-strand break repair.* Nat Cell Biol, 2007. **9**(6): p. 683-90.
91. Lisby, M., et al., *Choreography of the DNA damage response: spatiotemporal relationships among checkpoint and repair proteins.* Cell, 2004. **118**(6): p. 699-713.
92. Shroff, R., et al., *Distribution and dynamics of chromatin modification induced by a defined DNA double-strand break.* Curr Biol, 2004. **14**(19): p. 1703-11.
93. Lavin, M.F., *ATM and the Mre11 complex combine to recognize and signal DNA double-strand breaks.* Oncogene, 2007. **26**(56): p. 7749-7758.
94. Lee, J.H. and T.T. Paull, *Activation and regulation of ATM kinase activity in response to DNA double- strand breaks.* Oncogene, 2007. **26**: p. 7741- 7748.
95. Shiloh, Y., *ATM and related protein kinases: safeguarding genome integrity.* Nat Rev Cancer, 2003. **3**(3): p. 155-68.

96. Stavnezer, J., J.E. Guikema, and C.E. Schrader, *Mechanism and regulation of class switch recombination.* Annu Rev Immunol, 2008. **26**: p. 261-92.
97. Han, L. and K. Yu, *Altered kinetics of nonhomologous end joining and class switch recombination in ligase IV-deficient B cells.* J Exp Med, 2008. **205**(12): p. 2745-53.
98. Chaudhuri, J., et al., *Transcription-targeted DNA deamination by the AID antibody diversification enzyme.* Nature, 2003. **422**(6933): p. 726-30.
99. Begum, N.A., et al., *Requirement of non-canonical activity of uracil DNA glycosylase for class switch recombination.* J Biol Chem, 2007. **282**(1): p. 731-42.
100. Rickert, R., J. Roes, and K. Rajewsky, *B lymphocyte-specific, Cre-mediated mutagenesis in mice.* Nucl. Acids Res., 1997. **25**(6): p. 1317-1318.
101. Lumsden, J.M., et al., *Immunoglobulin class switch recombination is impaired in Atm-deficient mice.* J Exp Med, 2004. **200**(9): p. 1111-21.
102. Reina-San-Martin, B., et al., *ATM Is Required for Efficient Recombination between Immunoglobulin Switch Regions.* J. Exp. Med., 2004. **200**(9): p. 1103-1110.
103. Kracker, S., et al., *Nibrin functions in Ig class-switch recombination.* Proc Natl Acad Sci U S A, 2005. **102**(5): p. 1584-9.
104. Reina-San-Martin, B., et al., *Genomic instability, endoreduplication, and diminished Ig class-switch recombination in B cells lacking Nbs1.* Proc Natl Acad Sci U S A, 2005. **102**(5): p. 1590-5.
105. Kraus, M., et al., *Survival of resting mature B lymphocytes depends on BCR signaling via the Igalpha/beta heterodimer.* Cell, 2004. **117**(6): p. 787-800.
106. Franco, S., et al., *H2AX prevents DNA breaks from progressing to chromosome breaks and translocations.* Mol Cell, 2006. **21**(2): p. 201-14.
107. Rogakou, E.P., et al., *DNA double-stranded breaks induce histone H2AX phosphorylation on serine 139.* J Biol Chem, 1998. **273**(10): p. 5858-68.
108. Lou, Z., et al., *MDC1 maintains genomic stability by participating in the amplification of ATM-dependent DNA damage signals.* Mol Cell, 2006. **21**(2): p. 187-200.
109. Manis, J.P., et al., *53BP1 links DNA damage-response pathways to immunoglobulin heavy chain class-switch recombination.* Nat Immunol, 2004. **5**(5): p. 481-7.
110. Reina-San-Martin, B., et al., *H2AX is required for recombination between immunoglobulin switch regions but not for intra-switch region recombination or somatic hypermutation.* J Exp Med, 2003. **197**(12): p. 1767-78.
111. Ward, I.M., et al., *53BP1 is required for class switch recombination.* J Cell Biol, 2004. **165**(4): p. 459-64.
112. Cahill, D. and J.P. Carney, *Dimerization of the Rad50 protein is independent of the conserved hook domain.* Mutagenesis, 2007. **22**(4): p. 269-74.
113. Hopfner, K.-P., et al., *The Rad50 zinc-hook is a structure joining Mre11 complexes in DNA recombination and repair.* Nature, 2002. **418**(6897): p. 562-566.
114. Wiltzius, J.J., et al., *The Rad50 hook domain is a critical determinant of Mre11 complex functions.* Nat Struct Mol Biol, 2005. **12**(5): p. 403-7.
115. Xu, Z., et al., *Immunoglobulin class-switch DNA recombination: induction, targeting and beyond.* Nat Rev Immunol, 2012. **12**(7): p. 517-31.
116. Bressan, D.A., B.K. Baxter, and J.H. Petrini, *The Mre11-Rad50-Xrs2 protein complex facilitates homologous recombination-based double-strand break repair in Saccharomyces cerevisiae.* Mol Cell Biol, 1999. **19**(11): p. 7681-7.

117. Tauchi, H., et al., *Nbs1 is essential for DNA repair by homologous recombination in higher vertebrate cells.* Nature, 2002. **420**(6911): p. 93-8.
118. Lengsfeld, B.M., et al., *Sae2 is an endonuclease that processes hairpin DNA cooperatively with the Mre11/Rad50/Xrs2 complex.* Mol Cell, 2007. **28**(4): p. 638-51.
119. Sartori, A.A., et al., *Human CtIP promotes DNA end resection.* Nature, 2007. **450**(7169): p. 509-14.
120. Mimitou, E.P. and L.S. Symington, *Sae2, Exo1 and Sgs1 collaborate in DNA double-strand break processing.* Nature, 2008. **455**(7214): p. 770-4.
121. Paull, T.T. and M. Gellert, *A mechanistic basis for Mre11-directed DNA joining at microhomologies.* Proc Natl Acad Sci U S A, 2000. **97**(12): p. 6409-14.
122. Deriano, L., et al., *Roles for NBS1 in alternative nonhomologous end-joining of V(D)J recombination intermediates.* Mol Cell, 2009. **34**(1): p. 13-25.
123. Helmink, B.A., et al., *MRN complex function in the repair of chromosomal Rag-mediated DNA double-strand breaks.* J Exp Med, 2009. **206**(3): p. 669-79.
124. Deng, Y., et al., *Multiple roles for MRE11 at uncapped telomeres.* Nature, 2009. **460**(7257): p. 914-8.
125. Difilippantonio, S., et al., *53BP1 facilitates long-range DNA end-joining during V(D)J recombination.* Nature, 2008. **456**(7221): p. 529-33.
126. Dimitrova, N., et al., *53BP1 promotes non-homologous end joining of telomeres by increasing chromatin mobility.* Nature, 2008. **456**(7221): p. 524-8.
127. Heyer, W.D., K.T. Ehmsen, and J. Liu, *Regulation of homologous recombination in eukaryotes.* Annu Rev Genet, 2010. **44**: p. 113-39.
128. Grawunder, U., et al., *Requirement for an interaction of XRCC4 with DNA ligase IV for wild-type V(D)J recombination and DNA double-strand break repair in vivo.* J Biol Chem, 1998. **273**(38): p. 24708-14.
129. Weinstock, D.M., et al., *Modeling oncogenic translocations: distinct roles for double-strand break repair pathways in translocation formation in mammalian cells.* DNA Repair (Amst), 2006. **5**(9-10): p. 1065-74.
130. Zhang, Y. and J.D. Rowley, *Chromatin structural elements and chromosomal translocations in leukemia.* DNA Repair (Amst), 2006. **5**(9-10): p. 1282-97.
131. Jung, D. and F.W. Alt, *Unraveling V(D)J recombination; insights into gene regulation.* Cell, 2004. **116**(2): p. 299-311.
132. Manis, J.P., M. Tian, and F.W. Alt, *Mechanism and control of class-switch recombination.* Trends in Immunology, 2002. **23**(1): p. 31-39.
133. Muramatsu, M., et al., *Class Switch Recombination and Hypermutation Require Activation-Induced Cytidine Deaminase (AID), a Potential RNA Editing Enzyme.* Cell, 2000. **102**(5): p. 553-563.
134. Cogne M, B.B., *Molecular Biology of B Cells*, ed. A.F. Honjo T, Neuberger MS. 2004: Academic, London.
135. Taccioli, G.E., et al., *Impairment of V(D)J recombination in double-strand break repair mutants.* Science, 1993. **260**(5105): p. 207-10.
136. Hopkins, B.B. and T.T. Paull, *The P. furiosus Mre11/Rad50 Complex Promotes 5' Strand Resection at a DNA Double- Strand Break.* Cell, 2008. **135**: p. 250-260.
137. Difilippantonio, M.J., et al., *DNA repair protein Ku80 suppresses chromosomal aberrations and malignant transformation.* Nature, 2000. **404**(6777): p. 510-4.

138. Gao, Y., et al., *Interplay of p53 and DNA-repair protein XRCC4 in tumorigenesis, genomic stability and development.* Nature, 2000. **404**(6780): p. 897-900.
139. Rooney, S., et al., *Artemis and p53 cooperate to suppress oncogenic N-myc amplification in progenitor B cells.* Proc Natl Acad Sci U S A, 2004. **101**(8): p. 2410-5.
140. Wang, J.H., et al., *Oncogenic transformation in the absence of Xrcc4 targets peripheral B cells that have undergone editing and switching.* J Exp Med, 2008. **205**(13): p. 3079-90.
141. Dickerson, S.K., et al., *AID Mediates Hypermutation by Deaminating Single Stranded DNA.* The Journal of Experimental Medicine, 2003. **197**(10): p. 1291-1296.
142. Kovalchuk, A.L., J.R. Muller, and S. Janz, *Deletional remodeling of c-myc-deregulating chromosomal translocations.* Oncogene, 1997. **15**(19): p. 2369-77.
143. Chiarle, R., et al., *Genome-wide Translocation Sequencing Reveals Mechanisms of Chromosome Breaks and Rearrangements in B Cells.* Cell, 2011. **147**(1): p. 107-119.
144. Ramiro, A.R., et al., *Role of genomic instability and p53 in AID-induced c-mycâ€“Igh translocations.* Nature, 2006. **440**(7080): p. 105-109.
145. Buis, J., et al., *Mre11 regulates CtIP-dependent double-strand break repair by interaction with CDK2.* Nat Struct Mol Biol, 2012. **19**(2): p. 246-52.
146. Germani, A., et al., *SIAH-1 interacts with CtIP and promotes its degradation by the proteasome pathway.* Oncogene, 2003. **22**(55): p. 8845-51.
147. Satyanarayana, A. and P. Kaldis, *Mammalian cell-cycle regulation: several Cdks, numerous cyclins and diverse compensatory mechanisms.* Oncogene, 2009. **28**(33): p. 2925-39.
148. Campaner, S., et al., *Cdk2 suppresses cellular senescence induced by the c-myc oncogene.* Nat Cell Biol, 2010. **12**(1): p. 54-9; sup pp 1-14.
149. Hydbring, P., et al., *Phosphorylation by Cdk2 is required for Myc to repress Ras-induced senescence in cotransformation.* Proc Natl Acad Sci U S A, 2010. **107**(1): p. 58-63.
150. Jazayeri, A., et al., *ATM- and cell cycle-dependent regulation of ATR in response to DNA double-strand breaks.* Nat Cell Biol, 2006. **8**(1): p. 37-45.
151. Nussenzweig, A. and M.C. Nussenzweig, *Origin of chromosomal translocations in lymphoid cancer.* Cell, 2010. **141**(1): p. 27-38.
152. Gostissa, M., F.W. Alt, and R. Chiarle, *Mechanisms that promote and suppress chromosomal translocations in lymphocytes.* Annu Rev Immunol, 2011. **29**: p. 319-50.
153. Cory, S., *Activation of cellular oncogenes in hemopoietic cells by chromosome translocation.* Adv Cancer Res, 1986. **47**: p. 189-234.
154. Potter, M., *Neoplastic development in plasma cells.* Immunol Rev, 2003. **194**: p. 177-95.
155. Janz, S., *Myc translocations in B cell and plasma cell neoplasms.* DNA Repair (Amst), 2006. **5**(9-10): p. 1213-24.
156. Gostissa, M., et al., *Chromosomal location targets different MYC family gene members for oncogenic translocations.* Proceedings of the National Academy of Sciences, 2009. **106**(7): p. 2265-2270.
157. Kovalchuk, A.L., et al., *AID-deficient Bcl-xL transgenic mice develop delayed atypical plasma cell tumors with unusual Ig/Myc chromosomal rearrangements.* The Journal of Experimental Medicine, 2007. **204**(12): p. 2989-3001.
158. Rooney, S., et al., *Artemis and p53 cooperate to suppress oncogenic N-myc amplification in progenitor B cells.* Proceedings of the National Academy of Sciences of the United States of America, 2004. **101**(8): p. 2410-2415.

159. Revy, P., et al., *Activation-Induced Cytidine Deaminase (AID) Deficiency Causes the Autosomal Recessive Form of the Hyper-IgM Syndrome (HIGM2).* Cell, 2000. **102**(5): p. 565-575.
160. Dorsett, Y., et al., *A role for AID in chromosome translocations between c-myc and the IgH variable region.* The Journal of Experimental Medicine, 2007. **204**(9): p. 2225-2232.
161. Robbiani, D.F., et al., *AID Is Required for the Chromosomal Breaks in c-myc that Lead to c-myc/IgH Translocations.* Cell, 2008. **135**(6): p. 1028-1038.
162. Dunnick, W.A., et al., *Germline Transcription and Switch Recombination of a Transgene Containing the Entire H Chain Constant Region Locus: Effect of a Mutation in a STAT6 Binding Site in the γ1 Promoter.* The Journal of Immunology, 2004. **173**(9): p. 5531-5539.
163. Pelanda, R., et al., *Receptor editing in a transgenic mouse model: site, efficiency, and role in B cell tolerance and antibody diversification.* Immunity, 1997. **7**(6): p. 765-75.
164. Grillot, D.A., et al., *bcl-x exhibits regulated expression during B cell development and activation and modulates lymphocyte survival in transgenic mice.* J Exp Med, 1996. **183**(2): p. 381-91.
165. Bishop, G.A., W.D. Warren, and M.T. Berton, *Signaling via major histocompatibility complex class II molecules and antigen receptors enhances the B cell response to gp39/CD40 ligand.* European Journal of Immunology, 1995. **25**(5): p. 1230-1238.
166. Janz, S., et al., *Detection of recombinations between c-myc and immunoglobulin switch alpha in murine plasma cell tumors and preneoplastic lesions by polymerase chain reaction.* Proceedings of the National Academy of Sciences, 1993. **90**(15): p. 7361-7365.
167. Ramiro, A.R., et al., *Role of genomic instability and p53 in AID-induced c-myc-Igh translocations.* Nature, 2006. **440**(7080): p. 105-9.
168. Dunnick, W.A., et al., *Switch recombination and somatic hypermutation are controlled by the heavy chain 3′ enhancer region.* The Journal of Experimental Medicine, 2009. **206**(12): p. 2613-2623.
169. Liyanage, M., et al., *Multicolour spectral karyotyping of mouse chromosomes.* Nat Genet, 1996. **14**(3): p. 312-5.
170. Webb, E., J.M. Adams, and S. Cory, *Variant (6 ; 15) translocation in a murine plasmacytoma occurs near an immunoglobulin kappa gene but far from the myc oncogene.* Nature, 1984. **312**(5996): p. 777-9.
171. Siwarski, D., et al., *Structure and expression of the c-Myc/Pvt 1 megagene locus.* Curr Top Microbiol Immunol, 1997. **224**: p. 67-72.
172. Yamane, A., et al., *Deep-sequencing identification of the genomic targets of the cytidine deaminase AID and its cofactor RPA in B lymphocytes.* Nat Immunol, 2011. **12**(1): p. 62-9.
173. Huppi, K., et al., *Genomic instability and mouse microRNAs.* Toxicol Mech Methods, 2011. **21**(4): p. 325-33.
174. Klein, Isaac A., et al., *Translocation-Capture Sequencing Reveals the Extent and Nature of Chromosomal Rearrangements in B Lymphocytes.* Cell, 2011. **147**(1): p. 95-106.
175. Hakim, O., et al., *DNA damage defines sites of recurrent chromosomal translocations in B lymphocytes.* Nature, 2012. **484**(7392): p. 69-74.
176. Hasham, M.G., et al., *Widespread genomic breaks generated by activation-induced cytidine deaminase are prevented by homologous recombination.* Nat Immunol, 2010. **11**(9): p. 820-6.

177. Zhang, Y., et al., *Spatial Organization of the Mouse Genome and Its Role in Recurrent Chromosomal Translocations.* Cell, 2012. **148**(5): p. 908-921.
178. Meaburn, K.J., T. Misteli, and E. Soutoglou, *Spatial genome organization in the formation of chromosomal translocations.* Semin Cancer Biol, 2007. **17**(1): p. 80-90.
179. Parada, L.A., et al., *Conservation of relative chromosome positioning in normal and cancer cells.* Curr Biol, 2002. **12**(19): p. 1692-7.
180. Roix, J.J., et al., *Spatial proximity of translocation-prone gene loci in human lymphomas.* Nat Genet, 2003. **34**(3): p. 287-91.
181. Osborne, C.S., et al., *Myc dynamically and preferentially relocates to a transcription factory occupied by Igh.* PLoS Biol, 2007. **5**(8): p. e192.
182. Madisen, L. and M. Groudine, *Identification of a locus control region in the immunoglobulin heavy-chain locus that deregulates c-myc expression in plasmacytoma and Burkitt's lymphoma cells.* Genes Dev, 1994. **8**(18): p. 2212-26.
183. Truffinet, V., et al., *The 3' IgH locus control region is sufficient to deregulate a c-myc transgene and promote mature B cell malignancies with a predominant Burkitt-like phenotype.* J Immunol, 2007. **179**(9): p. 6033-42.
184. Duan, H., C.A. Heckman, and L.M. Boxer, *The immunoglobulin heavy-chain gene 3' enhancers deregulate bcl-2 promoter usage in t(14;18) lymphoma cells.* Oncogene, 2007. **26**(18): p. 2635-41.
185. Huppi, K. and D. Siwarski, *Chimeric transcripts with an open reading frame are generated as a result of translocation to the Pvt-1 region in mouse B-cell tumors.* Int J Cancer, 1994. **59**(6): p. 848-51.
186. Zha, S., C. Boboila, and F.W. Alt, *Mre11: roles in DNA repair beyond homologous recombination.* Nat Struct Mol Biol, 2009. **16**(8): p. 798-800.
187. Schiestl, R.H., J. Zhu, and T.D. Petes, *Effect of mutations in genes affecting homologous recombination on restriction enzyme-mediated and illegitimate recombination in Saccharomyces cerevisiae.* Mol Cell Biol, 1994. **14**(7): p. 4493-500.
188. Dudasova, Z., A. Dudas, and M. Chovanec, *Non-homologous end-joining factors of Saccharomyces cerevisiae.* FEMS Microbiol Rev, 2004. **28**(5): p. 581-601.
189. Dery, U., et al., *A glycine-arginine domain in control of the human MRE11 DNA repair protein.* Mol Cell Biol, 2008. **28**(9): p. 3058-69.
190. Yu, Z., et al., *The MRE11 GAR motif regulates DNA double-strand break processing and ATR activation.* Cell Res, 2012. **22**(2): p. 305-20.
191. Wilson, P.C., et al., *Somatic hypermutation introduces insertions and deletions into immunoglobulin V genes.* J Exp Med, 1998. **187**(1): p. 59-70.
192. Wu, H.Y. and M. Kaartinen, *The somatic hypermutation activity of a follicular lymphoma links to large insertions and deletions of immunoglobulin genes.* Scand J Immunol, 1995. **42**(1): p. 52-9.
193. Robinson, K., et al., *c-Myc accelerates S-phase and requires WRN to avoid replication stress.* PLoS One, 2009. **4**(6): p. e5951.
194. Schoppy, D.W., et al., *Oncogenic stress sensitizes murine cancers to hypomorphic suppression of ATR.* J Clin Invest, 2012. **122**(1): p. 241-52.
195. Cole, K.A., et al., *RNAi screen of the protein kinome identifies checkpoint kinase 1 (CHK1) as a therapeutic target in neuroblastoma.* Proc Natl Acad Sci U S A, 2011. **108**(8): p. 3336-41.

196. Murga, M., et al., *Exploiting oncogene-induced replicative stress for the selective killing of Myc-driven tumors.* Nat Struct Mol Biol, 2011. **18**(12): p. 1331-5.
197. Lowe, S.W., E. Cepero, and G. Evan, *Intrinsic tumour suppression.* Nature, 2004. **432**(7015): p. 307-15.
198. Amati, B., K. Alevizopoulos, and J. Vlach, *Myc and the cell cycle.* Front Biosci, 1998. **3**: p. d250-68.
199. Campaner, S., et al., *Myc, Cdk2 and cellular senescence: Old players, new game.* Cell Cycle, 2010. **9**(18): p. 3655-61.